Universidade Federal do Rio de Janeiro

Escola de Química

Engenharia de Processos Químicos e Bioquímicos

Synthesis of iodine 123-labeled polymeric microspheres for the use of SPECT images in the embolization procedure

Luciana Carvalheira

Rio de Janeiro

2019

Luciana Carvalheira

Synthesis of iodine 123-labeled polymeric microspheres for the use of SPECT images in the embolization procedure

Doctorate thesis submitted to the Faculty of the Chemical and Biochemical Process Engineering of Federal University of Rio de Janeiro in partial fulfillment of the requirements for the Degree of Doctor of Science.

Advisors:

Márcio Nele de Souza, D.Sc.
Jose Carlos Costa da Silva Pinto, D.Sc.

Rio de Janeiro

2019

FOLHA DE APROVAÇÃO

Luciana Carvalheira

Obtenção de microesferas poliméricas marcadas com iodo 123 para utilização de imagens SPECT no procedimento de embolização

Tese de Doutorado apresentada ao Programa de Pós-Graduação em Engenharia de Processos Químicos e Bioquímicos, Escola de Química, da Universidade Federal do Rio de Janeiro, como requisito final à obtenção do título de Doutora em Engenharia de Processos Químicos e Bioquímicos.

_____

Marcio Nele de Souza, Dr., EQ/UFRJ

_____

José Carlos Costa da Silva Pinto, Dr., PEQ/COPPE/UFRJ

_____

Marilza Batista Corrêa, Dra., FIOCRUZ

_____

Fernando Gomes de Souza Júnior, Dr., IMA/UFRJ

_____

Delson Braz, Dr., PEN/COPPE/UFRJ

_____

Amaro Gomes Barreto Júnior, Dr., EQ/UFRJ

Rio de Janeiro

2019

Carvalheira, Luciana

C331o Obtenção de microesferas poliméricas marcadas com iodo 123 para utilização de imagens SPECT no procedimento de embolização / Luciana Carvalheira. - Rio de Janeiro, 2019.
146 f.

Orientador: Marcio Nele de Souza.
Coorientador: José Carlos Costa da Silva Pinto.
Tese (doutorado) - Universidade Federal do Rio de Janeiro, Instituto Alberto Luiz Coimbra de Pós Graduação e Pesquisa de Engenharia, Programa de Pós Graduação em Engenharia Química, 2019.

1. Microesferas poliméricas. 2. Embolização vascular. 3. Iodo 123 e SPECT. 4. Acetato de vinila. 5. 4-vinilfenol. I. Souza, Marcio Nele de, orient. II. Pinto, José Carlos Costa da Silva, coorient. III. Título.

To my love Jackson Britto, for being
with me in one more journey.

ACKNOWLEDGEMENTS

First of all, I would like to thank the Universe for allowing me one more realization. Also, I would like to thank my beloved mom Edith, dad Wanderley, brother Eduardo, sister-in-law Nubia, and nephew Pietro that arrived in the middle of this journey. In addition, I cannot describe how my love Jackson Britto supported me during this project, taking care of me and being patient with me. My spiritual godson Vicente, thanks for all the joy you gave me. To your mom Vinicia, your dad Alexander and your grandmother Mariza, thanks for all the support and prayers.

For good times and bad times, that's what friends are for and you did it great my beloved friends Gleici, Luciano, Michelle, Alfredo, Marilza, José, Ana Paula. Thank you all. To my friends from Arts, Music and Samba I address here all my gratitude to you Luiza, Monica, Elika, Nelsinho, Nara, Lucimar, Hideo, Yuki, Andreia, Rubia, Dani Ramalho, Ricciuto, Hugo, Carlos, Clayton, Thiago, Michele e Michele. During this journey, a magnetic friendship arose and I am so glad for being with you Marcel, Lizandra, Luna, and Adriana.

Teachers and professors were always by my side to help me achieving my goals. I am glad for having encountered these understanding professors Nele and Zé that gave me the real chance to accomplish this journey.

To all my colleagues from the Nuclear Engineering Institute that supported me I would like to express my gratitude, specially to Cleiton, Glauco, D. Claudia, Zelmo, Josivaldo, Suita, Fabio Staude, Rogerio, Francisco, Eraldo, and Rosa. I am also thankful for the new professional partnerships constructed with Viviane, Ademir, and Alessandro along this journey.

I would also like to express my gratitude for all the characterizations provided by the competent staff of EngePol, EngeCol, LAPIN/IMA/UFRJ and IQ/UFRJ.

Temos que espalhar o saber com muita liberdade, precisamos sentirmos à vontade quando falamos do que sabemos. Como os semeadores de trigo: eles não têm medo algum em abrir as mãos, e lançar, até com certa força. O saber precisa ser espalhado como se espalha o trigo. Há muita imperfeição no ser humano, nossa cultura é o que somos: há uma série de distúrbios em cada pessoa, problemáticas variavelmente graves, mas todas significativas, que criam o que cada um é. Esta humana "humanice" é que forma a novidade. Novidade que forma nossa bagagem de descobertas. E não há outro pão comestível para crescer como humanos se não o que é feito pela autenticidade do nosso ser, do nosso saber. Pão que se faz com aquele trigo, que não se vê na hora de semear. Por isso precisa espalhar o que sabemos, o que somos, sabor e saber, pois haverá muita semente perdida, mas também haverá outras que frutificarão, e portanto haverá trigo, haverá farinha e haverá pão.

Não devemos ter medo de falar do que sabemos.

Sergio Ricciuto Conte

ABSTRACT

CARVALHEIRA, Luciana. **Synthesis of iodine 123-labeled polymeric microspheres for the use of SPECT images in the embolization procedure**. Rio de Janeiro, 2019. Thesis (Doctor in Chemical and Biochemical Process Engineering) - School of Chemistry, Federal University of Rio de Janeiro, Rio de Janeiro, 2019.

Vascular embolization is a clinical procedure widely used in the treatment of hypervascularized tumors. In this technique, dispersed polymer microspheres are injected through a catheter and reach the main blood vessel of the tumor, promoting an immediate obstruction. Consequently, the tumor region tends to atrophy or even die due to restricted nutrient supply. The vascular embolization procedure can be monitored by the Angiography technique; however, the images provided by this technique are not able to show the exact location of the blockade or the location of the particles. In this case, obtaining SPECT images may be an alternative, since this technique produces images of higher resolution, which would allow more precise tracking of the distribution of these particles in the body. The iodine 123 is a radioisotope widely used to obtain SPECT images and presents high *in vivo* stability when the radioiodine insertion occurs in aromatic rings. Therefore, the strategy used in this work was to obtain polymeric microspheres from the suspension polymerization of 4-vinylphenol with vinyl acetate for subsequent radioiodination of the same. This phenolic compound presents polymerization unsaturation and aromatic ring activated for radioiodination, which was performed using the iodo-beads oxidizing agent. Prior to radioiodination, different percentages of 4-vinylphenol (0.10, 0.25 and 0.50 % w/w) were studied in order to select the composition that presented the most compatible characteristics for the use as an embolization agent. Mass polymerization, suspension polymerization, kinetic assays and the characterization of the synthesized polymeric materials were performed. The results showed that the desired copolymer was successfully obtained in the form of microspheres. Among the contents of 4-vynilphenol studied, microparticles synthesized with 0.10 % w/w of this comonomer exhibited the best properties to be used as an embolization agent and underwent radioiodination. Labeling results indicated a significant insertion of radioiodine in both PVAc and P(VAc-co-4VPh) backbone.

Keywords: embolization; microspheres; vinyl acetate; 4-vinylphenol; iodo-beads; iodine 123 and SPECT.

RESUMO

CARVALHEIRA, Luciana. **Obtenção de microesferas poliméricas marcadas com iodo 123 para utilização de imagens SPECT no procedimento de embolização**. Rio de Janeiro, 2019. Tese (Doutorado em Engenharia de Processos Químicos e Bioquímicos) - Escola de Química, Universidade Federal do Rio de Janeiro, Rio de Janeiro, 2019.

A embolização vascular é um procedimento clínico bastante utilizado no tratamento de tumores hipervascularizados. Nessa técnica, microesferas poliméricas dispersas são injetadas através de um cateter e alcançam o principal vaso sanguíneo do tumor, promovendo uma obstrução imediata. Consequentemente, a região tumoral tende a atrofiar ou até mesmo morrer, devido ao restrito fornecimento de nutrientes. O procedimento de embolização vascular pode ser monitorado pela técnica de Angiografia; no entanto, as imagens fornecidas por essa técnica não são capazes de mostrar o local exato do bloqueio nem a localização das partículas. Nesse caso, a obtenção de imagens SPECT pode constituir uma alternativa, pois essa técnica produz imagens de resolução superior, que permitiriam acompanhar, com maior precisão, a distribuição dessas partículas no organismo. O radioisótopo iodo 123 é largamente utilizado para a obtenção de imagens SPECT e apresenta alta estabilidade *in vivo*, quando a inserção do iodo ocorre em anéis aromáticos. Portanto, a estratégia utilizada neste trabalho consistiu em obter microesferas poliméricas a partir da polimerização em suspensão do 4-vinilfenol com o acetato de vinila para posterior radioiodação das mesmas. Este composto fenólico possui insaturação para polimerização e anel aromático ativado para radioiodação, que foi realizada utilizando-se o agente oxidante *iodo-beads*. Previamente à radioiodação, diferentes porcentagens de 4-vinilfenol (0,10; 0,25 e 0,50 % m/m) foram estudadas de forma a selecionar a composição que apresentasse as características mais compatíveis ao uso como agente de embolização. Ensaios de polimerização em massa, polimerização em suspensão, ensaios de cinética e a caracterização dos materiais poliméricos sintetizados foram realizados. Os resultados mostraram que o copolímero desejado foi obtido com sucesso na forma de microesferas. Dentre os percentuais de 4-vinilfenol estudados, as micropartículas sintetizadas com 0,10 % m/m deste comonômero apresentaram as melhores características para serem usadas como agente de embolização e, portanto, foram submetidas à radioiodação. Os resultados da marcação indicaram uma inserção significativa de radioiodo nas matrizes poliméricas de PVAc e P(VAc-co-4VF).

Palavras-chave: embolização; microesferas; acetato de vinila; 4-vinilfenol; iodo-beads; iodo 123 e SPECT.

GLOSSARY

Activity	Physical parameter that expresses the disintegration rate, represented in Becquerel unit (Bq).
Angiography	X-ray technique used to evaluate arteries, veins and organs. During the procedure, the interventional radiologist inserts a catheter into an artery or vein from an access point (groin or arm). The substance, called a contrast agent (radiopaque material), is injected through the catheter to obtain blood vessel X-ray images.
Beam	Set of particles or electromagnetic radiation collimated in the same direction.
Becquerel	In the International System, it is the unit of measurement of radioactivity.
Carrier-free	Expression used to indicate the absence of non-radioactive isotopes of the same chemical element as the radioisotope present in the radioactive sample.
Cyclotron	Particle accelerator in which charged particles repeatedly pass through an electric acceleration field while helically moving outward in the center of the machine. The particles are held in this path by a strong magnetic field.
Decay	Spontaneous transformation of a nuclide to a more stable energy state or to another different nuclide.
Detector NaI(Tl)	The thallium-fortified sodium iodide detector (NaI(Tl)), which is the inorganic scintillator type, is a radioactivity detector that has low energy resolution because it is not able to differentiate gamma ray peaks whose differences in energy are around 10 keV. However, it is very sensitive as it has 80 to 90 % efficiency for the energy range of interest.

Dose	Amount of energy absorbed per unit mass of irradiated material.
Eletronvolt (eV)	It is the work required to move an electron against a potential difference of one Volt.
Fluoroscopy	A technique in which an x-ray beam passes through the body and the real-time image is shown on a flat, digitally intensified fluorescent screen, which reduces the amount of ionizing radiation required when compared to the angiography technique. A contrast agent (radiopaque material) can be administered by injection into the bloodstream or through catheters into internal organs, allowing the body to visualize this material and the movement of body parts.
Interventional Radiology	Medical practice area which covers invasive medical procedures usually performed through needles and/or catheters in which the interventional radiologist (specialist in diagnostic imaging and intervention) uses imaging techniques to guide the procedure without the need for cuts, surgical procedures or use of video-surgery cameras. The imaging techniques used are: Angiography, Computed Tomography, Fluoroscopy, Magnetic Resonance and Ultrasound.
Iodo-beads™	They are water-insoluble non-porous polystyrene spheres with a diameter of 23 mm, functionalized with chloramine-B oxidant. They are used in the radioiodination of substances sensitive to severe oxidation conditions, where the direct insertion of the radioiodine occurs into the phenol function of tyrosine residues present in these molecules. The reaction is stopped by removing the beads from the reaction medium. Iodo-beads™ is the commercial name of this substance that will be referred in this text as iodo-beads.
Iodogen®	This oxidant agent is commonly used for the radioiodination of proteins and is provided in a defined amount (500 µg) for only one usage.

Ionizing radiation	Any radiation that removes or displaces electrons from atoms or molecules, producing ions.
Labeling	Insertion of a radioactive atom or ion into a molecule.
Liposome	They are spherical and uni, bi or multilamellar lipid nanoparticles with surfactant lipid membranes and aqueous interior, with the ability to encapsulate hydrophilic or hydrophobic substances.
Nuclide	General term applied to all atomic forms of elements.
PET	Positron Emission Tomography or PET is an imaging technique used in Nuclear Medicine in which gamma-type ionizing radiation from positron annihilation is detected and computed to provide imaging of organs and tissues. To obtain these images, a substance called as radiopharmaceutical is injected into the patient and a device called as gamma camera is used to detect the gamma radiation released from the disintegration of the positron emitted by the radiopharmaceutical.
Radioisotope	Radioactive isotope; unstable isotope of an element that decays spontaneously emitting ionizing radiation.
Radionuclide	Radioactive nuclide.
Radiopaque material	Ionizing radiation absorbing substance.
Scintigraphy	Clinical investigation method consisting of intravenous injection or ingestion of radiopharmaceuticals for imaging organs or tissues using a scintillator type radioactivity detector.

Specific activity	It is the relationship between the activity of a radioisotope by mass of the labeled compound. It is expressed in activity per unit of mass or volume.
SPECT	Single Photon Emission Computed Tomography or SPECT is an imaging technique used in Nuclear Medicine in which gamma-type ionizing radiation is detected and computed to provide images of organs and tissues. To obtain these images, a substance called a radiopharmaceutical is injected into the patient and a device called a gamma camera is used to detect the gamma radiation emitted by the radiopharmaceutical.

Content

Chapter 1 17
INTRODUCTION 17
1.1 Motivation 20
1.2 General objectives 20
1.3 Specific objectives 21
1.4 Thesis organization 21
References 21
Chapter 2 24
LITERATURE REVIEW 24
2.1 Embolization agents 24
2.1.1 Gelatin sponges 25
2.1.2 Trisacrylic sponge 26
2.1.3 PVA particles 28
2.1.4 The poly(vinyl acetate) 30
2.1 Images on Nuclear Medicine 32
2.2 SPECT and iodine 123 34
2.3 Nuclear Medicine and Radiopharmaceuticals 37
2.4 Radiopharmaceuticals and particles 39
2.5 Radioiodines and particles 43
2.6 The 4-vinylphenol 52
2.7 Bulk polymerization 54
2.8 Suspension polymerization 55
2.8.1 Suspending agent 56
2.8.2 Initiator 57
2.8.3 Mechanical agitation 58
2.8.4 Gel and vitreous effects 58
2.8.5 Retarding and inhibition effects 59
2.9 Radioiodination 60
2.9.1 The iodo-beads 64
2.9.2 Iodo-beads applications 68
2.10 Special cares with radioactivity 74
2.11 Final remarks 76
References 78
Chapter 3 87

BULK POLYMERIZATION 87
3.1 Introduction 87
3.2 Methodology 89
3.2.1 Chemicals 89
3.2.2 Comonomer load study 89
3.2.3 Conversion study 90
3.2.4 Characterization 90
3.3 Results and discussion 91
3.3.1 Comonomer load study 91
3.3.2 Conversion study 92
3.3.3 Molar mass distribution 93
3.3.4 Infrared spectroscopy 94
3.3.5 ^{1}H-NMR analysis 95
3.3.6 Thermal analysis 98
3.4 Conclusions 100
3.5 Complementary remarks 100
References 105
Chapter 4 108
SUSPENSION POLYMERIZATION 108
4.1 Introduction 108
4.2 Methodology 111
4.2.1 Chemicals 111
4.2.2 Suspension polymerization 112
4.2.3 Conversion study with different contents of 4VPh 112
4.2.4 Polymers characterization 113
4.2.5 Radioiodination 114
4.3 Results and discussion 115
4.3.1 Reaction kinetics 115
4.3.2 PVAc and P(VAc-co-4VPh) characterization 119
4.3.3 Microparticles labeling 132
4.3.4 Stability of labelled microparticles 134
4.4 Conclusions 135
4.5 Complementary remarks 136
References 140
Chapter 5 145

FINAL REMARKS 145
FUTURE WORKS 146

CHAPTER 1

INTRODUCTION

Minimally invasive therapies (MIT) are a class of treatments whose action is restricted to the area of interest and that have the benefit of reducing aggression to tissues involved in surgical intervention, preserving healthy tissue in the surrounding area, and the very low side effects. Vascular embolization is a type of MIT widely used in the treatment of hypervascularized tumors and arteriovenous malformations to reduce tumor size, facilitate removal or define a safer treatment for tumor malformation (1,2).

Embolization consists of injecting solid particles dispersed in a liquid medium and with the help of a catheter (0.053-0.069 cm internal diameter, 100-150 cm length) into blood vessels that are located near the tumor region, promoting obstruction of the bloodstream that nourishes this region. In this way, the supply of essential nutrients to the injured area is disrupted and the tumor region tends to atrophy and eventually die. This technique has been successfully used for various treatments, such as removal of vascular tumors, meningiomas (benign brain tumor), uterine fibroids, and stopping bleeding. For example, an embolization procedure for the therapy of uterine fibroids lasts a maximum of, approximately, 3 h. More recently, several applications associated with the treatment of prostate tumors have been reported (1-5).

Uterine artery embolization, for example, is a safe and effective alternative to hysterectomy for the treatment of symptomatic uterine fibroids. In the United States, fibroids account for about 30% of the more than 600,000 hysterectomies performed annually. The cost of hospitalizations due to symptoms caused by fibroids and hysterectomies is estimated at approximately two billion dollars. The annual cost for each woman who experiences lost productivity is approximately $ 1,692. Compared to hysterectomy, embolization of the uterine arteries requires shorter hospital stays

and allows for faster recovery. Therefore, it is a cheaper procedure than hysterectomy (7). According to Carnevale (8), there are no statistics on how many women undergo hysterectomy in Brazil, because the numbers are inaccurate, but it is known that the minority is aware of the option for the alternative procedure.

The embolization procedure is a technique of Interventional Radiology that uses biocompatible and non-toxic particles. Normally, in this devascularization procedure, poly(vinyl alcohol) (PVA) polymeric microparticles have been used as embolization agents due to their high compressibility and elasticity, hydrophilic character, and chemical stability in the blood. These characteristics allow the particles to move through the catheter with the aid of physiological solution, without formation of aggregates or sedimentation, changes in particle morphology or blood pH. PVA is usually obtained by partial saponification of poly(vinyl acetate) (PVAc) particles or precipitation of PVA in alcohol (9-11).

PVAc particles are obtained by suspension polymerization reaction using a free radical initiator. The most commonly used initiators are benzoyl peroxide (BPO) - which is inexpensive and used at temperatures above 50 °C - and azo-compounds such as azobisisobutyronitrile (AIBN), which are important when narrowing the size distribution of particles and minimize the content of branches (12). Unlike BPO, AIBN can be used at room temperature to promote polymerization, which can prevent excessive coalescence, aid droplet stabilization, and avoid branch-to-polymer chain transfer reactions (12,13). Suspension polymerization allows operation at low viscosities, resulting in spherical particles with regular morphology, which is an important feature to avoid catheter occlusion (14,15).

Preoperative planning of the vascular embolization procedure uses imaging techniques such as magnetic resonance imaging (MR), computed tomography (CT) and ultrasound. These techniques provide mapping of the arterial blood supply route, surrounding tissues and veins. During the embolization procedure, the radiologist uses the angiography or fluoroscopy technique (X-ray images) to estimate

devascularization, as only pathological exams are able to show the exact blockage location and the microsphere location. The embolization procedure may take from 30 minutes to several hours, depending on the condition of the tumor to be treated. Although it is a well-established procedure, embolization has weaknesses that are circumvented according to the interventionist radiologist's subjectivity and experience. Defining the end point of the embolization procedure is an example (15-17).

To circumvent this limitation, radiopaque polymeric microspheres, which are non-transparent X-ray contrast agents, have been developed. These particles contain a heavy element attached to the polymer structure, providing not only radiopacity to the particles, but also greater rigidity and less elasticity when compared to non-radiopaque particles. However, these changes in the physical and mechanical properties of microspheres may result in the formation of aggregates or particle sedimentation during injection, which may lead to a catheter obstruction (15).

Single Photon Emission Computed Tomography (SPECT) technique is an imaging technology used in Nuclear Medicine, where the resulting images correspond to functional imaging of an organ of interest. Functional imaging (or physiological imaging) is a medical imaging technique of detecting or measuring changes in metabolism, blood flow, regional chemical composition, and absorption (18). Non-invasively, SPECT utilizes a gamma-type radioactivity detection system to provide images of the interior of the human body. These images are constructed from a tomographic mapping of the target organ containing the patient-administered radiopharmaceutical (18-20). The SPECT technique is very sensitive and widely used in Brazil (21,22). SPECT provides higher quality images than the techniques normally used in the vascular embolization procedure, allowing to monitor, in real time, the distribution of particles in the veins and the tumor, the homogeneity of this distribution and the end of this procedure, with better resolution images.

1.1 Motivation

As shown, the importance of imaging as a component for the evaluation and safety of patients undergoing vascular embolization is notorious. Therefore, the improvement of this component is a necessity that motivated the development of this thesis. With this in mind, in the present work, the need to insert the radioisotope iodine 123 (^{123}I) into PVAc microspheres was identified. With the insertion of this radioisotope on this polymeric matrix, a new embolization agent can be obtained and the SPECT technique can be applied.

The strategy used in this work is to use the 4-vinylphenol (4VPh) molecule, whose structure presents an unsaturation that can undergo copolymerization with VAc, in addition to an activated aromatic ring for iodination. The insertion of ^{123}I into this aromatic ring ensures that this radioisotope is covalently attached to the polymer. Thus, the risk of *in vivo* deiodination is reduced, preserving the patient from unnecessary radiation exposure and improving the quality of the images obtained. Obtaining this new embolization agent can have a major technological impact, as the use of the SPECT technique can add greater precision, safety and efficacy to the vascular embolization procedure.

1.2 General objectives

This work focused on to obtain radioactive polymeric microspheres by copolymerizing 4VPh with VAc and subsequently the labeling with ^{123}I so that this radioactive material can allow SPECT imaging during the vascular embolization procedure.

1.3 Specific objectives

The specific objectives of this work are:

- to perform the copolymerization between VAc and 4VPh;
- to obtain this copolymer as microspheres particles;
- to evaluate the effect of different contents of 4VPh on the microsphere's properties;
- to label the microspheres with ^{123}I.

1.4 Thesis organization

This work contains a glossary to familiarize the reader with some specific terms of the Nuclear and Biology fields and is divided into five chapters. Chapter II presents a literature review comprising embolization agents, imaging on Nuclear Medicine, radiopharmaceuticals, the description of bulk and suspension polymerization, and radioiodination of molecules with iodo-beads. Chapter III and IV present bulk and suspension polymerization systems, respectively, used in this work to perform the copolymerization between 4VPh and VAc. Chapter IV also contains the proposed approach to microparticles radioiodination. Moreover, Chapter III is based on a scientific paper already published resulting from part of this thesis work (23). Chapter IV presents the continuation of the previous Chapter and is based on an accepted scientific paper that is under review. Finally, Chapter V covers the final remarks of this thesis and lists suggestions of complementing works and developments.

References

[1] Basso, G. G. Síntese e Caracterização de Partículas Esféricas de Poli(Álcool Vinílico) e Poli(Acetato Vinílico) para Utilização em Embolização. 2011. 103 p. Dissertação (Mestrado em Biofísica Molecular) - Universidade Estadual Paulista "Júlio de Mesquita Filho", São José do Rio Preto, 2011.

[2] Embolution. Soluções médicas por emboloterapia. Available in <http://www.embolution.com.br>. Access in 10 feb 2017.

[3] Latchaw, R. E., Gold, L. H. A. Polyvinyl foam embolization of vascular and neoplastic lesions of the head, neck and spine. Radiology, v. 131, n. 3, p. 669-679, 1979.

[4] Yu, H., Isaacson, A. J., Burke, C. T. Review of Current Literature for Prostatic Artery Embolization. Seminars in Interventional Radiology, v. 33, pp.231-235, 2016.

[5] Embolic therapies products. Available in <https://www.cookmedical.com/data/resources/PI-NAM-13063-EN-201404_M3.pdf>. Acces in 03 jan 2019.

[6] Latchae, Gold, 1979; Basso, 2011; Yu, Isaacson, Burke, 2016; Embolution, 2017; Embolic therapies products, 2019.

[7] Pinto, R. A. P. Tratamento das pacientes sintomáticas portadoras de miomas uterinos através da associação das técnicas de embolização dos miomas e ligadura endovascular das artérias uterinas. 2007. 85p. Tese (Doutorado em Ciências) – Faculdade de Medicina, Universidade de São Paulo, São Paulo, 2007.

[8] Carnevale, F. C. Embolização dos miomas uterinos sintomáticos. Indicação baseada em evidências científicas. Radiologia Brasileira, v.40, n.5 p.V-VI, 2007.

[9] Tadavarthy, S. M., Moller, J. H., Amplatz, K. Polyvinyl-alcohol (Ivalon) - New embolic material. American Journal of Roentgenology, v. 125, n. 3, p. 609-616, 1975.

[10] Linfante, I., Wakhloo, A. K. Brain aneurysms and arteriovenous malformations: Advancements and emerging treatments in endovascular embolization. Stroke - Journal of the American Heart Association, v. 38, n. 4, p. 1411-1417, 2007.

[11] Mauro, M. A., Murphy K. P. J., Thomson, K. R., Vembrux A. C., Morgan R. A. Image-Guided Interventions: Expert Radiology Series. 2nd ed. United States of America: Elsevier. 2014.

[12] Machado, F., Lima, E. L., Pinto, J. C. Uma Revisão Sobre os Processos de Polimerização em Suspensão. Polímeros: Ciência e Tecnologia, v.17, n.2, pp.166-179, 2007.

[13] Lee, S. G., Kim, J. P., Kwon, I. C., Shin, D. S., Han, S. S., Lyoo, W. S. Preparation of poly(vinyl acetate) microspheres with narrow particle size distributions by low temperature suspension polymerization of vinyl acetate. Journal of Applied Polymer Science, v.101, pp.4064-4070, 2006.

[14] Odian, G. Principles of Polymerization. 4th ed. United States of America: Wiley Interscience. 2004.

[15] Laurent, A., Microspheres and nonspherical particles for embolization. Techniques in Vascular and Interventional Radiology, n. 10, pp. 248-256, 2007.

[16] Owen, R. J. T., Embolization of musculoskeletal tumors. Radiologic Clinics of North America, n.46, pp.535-543, 2008.

[17] Radiology info for patients - Catheter embolization. Available in <https://www.radiologyinfo.org/en/info.cfm?pg=cathembol> Acces in 3rd nov 2017.

[18] Bushberg, J. T., Seibert, J. A., Leidholt Jr. E. M., Boone, J. M. The essential Physics of Medical Imaging 2nd ed. United States of America: Lippincott Williams & Wilkins, 2002.

[19] Mattos, F. R. SPECT (Single photon emission tomography): Gama Câmara, Reconstrução Tomográfica e Características Funcionais. 2009. 46p. Bacharelado (Graduação em Física Médica) – Instituto de Biociências, Universidade Estadual Paulista, Botucatu, 2009.

[20] Bhargava, P., He, G., Samarghandi, A., Delpassand, E. S. Pictorial review of SPECT/CT imaging applications in clinical nuclear medicine. American Journal of Nuclear Medicine and Molecular Imaging, v.2, i.2, pp.221–231, 2012.

[21] Mariani G., Brussel L., Kuwert T., Kim E. E., Flotats A., Israel O., Dondi M., Watanabe N. A review on the clinical uses of SPECT/CT. European Journal of Nuclear Medicine and Molecular Imaging, v.37, n.10, p.1959-1985, 2010.

[22] Pozzo, L., Coura Filho, G., Osso Junior, J. A. Squair, P. L. O SUS na Medicina Nuclear do Brasil: avaliação e comparação dos dados fornecidos pelo Datasus e CNEN. Radiologia Brasileira, v.47, n.3, pp.141-148, 2014.

[23] Carvalheira, L., Martins, M. G., Pinto, J. C., Nele, M. Synthesis of The Copolymer P(VAc-Co-4VP) For Developing A New SPECT Radioactive Tracer IOSR Journal of Applied Chemistry. v.11, i.2, 45-51, 2018.

CHAPTER 2

LITERATURE REVIEW

2.1 Embolization agents

The material used as embolization agent must be inert, biocompatible, non-absorbable by the tissues, have a deformable surface, compatibility between the injected material particle size and catheter diameter, as well as chemical and mechanical stability during sterilization and during use. Calcium alginate gel, metal springs, disposable flasks, silicone rubber, carbon microspheres, dextran, cellulose, hydroxyapatite and polymer particles are some examples of materials used as an embolization agent. When the embolization agent is a particle, the most spherical morphology is desired to prevent aggregation and to facilitate its movement along the catheter (1,2).

During occlusion, embolization agents may also act as prolonged drug delivery vehicles in tumors, a process called chemoembolization. When the embolization agent contains a corpuscular ionizing radiation emitting radioisotope, the technique is then called radioembolization, internal selective radiotherapy, or internal brachytherapy, where corpuscular ionizing radiation causes unwanted cell death. Yttrium 90 (^{90}Y) glass microspheres, for example, have been widely used in liver cancer therapy (1-7). It is important to report that the new embolization agent developed in the present work does not present radioisotope emitting corpuscular ionizing radiation; therefore, it cannot be classified as a radioembolization agent.

The main embolization agents used are gelatin sponges, trisacrylic gelatin microspheres and PVA particles. Embolization agents may be temporary or

permanent and the selection of the most appropriate agent depends on the vascular territory to be embolized, the permanence and the degree of occlusion (1,2).

2.1.1 Gelatin sponges

Gelatin sponge (or absorbable gelatin) is a hemostatic material[1] that causes mechanical obstruction, slowing blood flow and accelerating clot formation. The sponges are water insoluble, prepared from purified pig skin gelatin (denatured collagen). Collagen is a protein with triple-helix conformation that turns to gelatin when heated assuming superposed chains configuration. Denatured collagen is converted into sponge due to nitrogen bubbling during polymerization. With this process, a porous device capable of absorbing up to 45 times their weight in the blood is obtained. The absorptive capacity of gelatin depends on the size of the piece, increasing proportionally with the increasing of the sponge size. Gelatin particles were first used in 1945 to control bleeding during a neurosurgical procedure (8,9).

This temporary embolization agent - marketed under the name Gelfoam® - provides temporary vessel occlusion as it can be completely absorbed into the body, allowing recanalization within a few weeks, which is an advantage in case of hemoptysis or trauma, for example. In the United States, this material is used for the treatment of fibroids in women who wish to preserve fertility. Gelfoam® can be found in powder form, containing particles of 40-60 μm in diameter, or as blades, whose pieces of various sizes can be cut from thin films (10).

Some of the advantages of using gelatin sponge are the low cost, ease and versatility. However, gelatins have irregular morphology and tendency to fragmentation, with risk of ischemia due to particle size. Infections were also observed and associated with the possible trapping of air bubbles. In addition, biodegradability may cause recanalization of embolized arteries and consequently, the need for further embolization (1).

[1] A material is homeostatic when it does not cause changes in the natural conditions of a biological system.

Conroy et al. (11) were the first to develop radioactive embolization agents in order to locate them in the body by means of SPECT images during and after embolization. By using SPECT images, it was possible to reduce the chances of clogging different blood vessels than desired, observe the degree of blood vessel occlusion, migration, and flow of material to other parts of the body (11). The authors reported, for example, that stomach, duodenum, liver, kidney and legs were inadvertently infarcted due to embolization of other areas. In this study, the technetium 99m (^{99m}Tc) Gelfoam® sponge was labeled under aseptic conditions. For this, dried Gelfoam® was cut to desired size and suspended in sterile water. Then, tin chloride and technetium pertechnetate were added, the solution was buffered and the supernatant removed, resulting in 50-80 % labeling. The results obtained in two patients showed the efficiency of the proposed approach. In one case, continuous injection of the embolizing agent into the splenic artery could have resulted in the flow of this material to other major branches of the aorta. In the other case, on two separate occasions, immediate knowledge of the migration of the embolizing agent to the lungs caused a change in the procedure to prevent a pulmonary infarction. The authors did not report the activity of the radioactive embolizing agent used, nor details about the conditions of Gelfoam® sponge labeling.

2.1.2 Trisacrylic sponge

Improvement of the properties of the gelatinous sponge has resulted in precisely sized trisacrylic gelatin microspheres. Such particles are formed by a trisacrylic polymer matrix (Figure 2.1) impregnated and coated with gelatin from purified pig skin, which is not absorbed by the body (10).

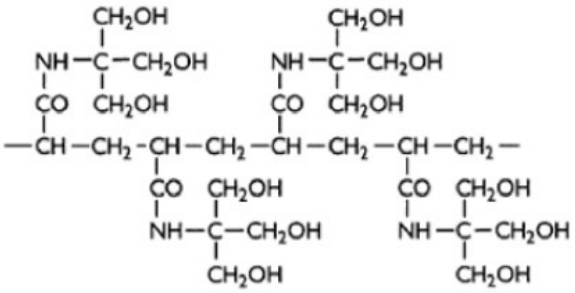

Figure 2.1: Structure of the trisacrylic gelatin polymer matrix. Adapted from Vijayalakshmi (12).

Commercially, these materials are known as Embospheres® and are available in six particle size ranges, ranging from 40 to 1200 µm in diameter, dispersed in 2 mL of saline solution. In addition, gold particles are added to color and give visibility to the particles. Over a period of 48 h to four weeks, the particles cause vascular occlusion when they are housed in vessels, causing a histological reaction similar to those of PVA particles, but without showing signs of degradation (13).

This permanent embolization agent circumvented some of the disadvantages observed in Gelfoam®. Being hydrophilic, Embospheres® particles flow easily through the catheter, improving occlusion effectiveness. These particles are also malleable and when temporarily compressed from 20 to 30 % of their initial diameter allow displacement through the catheter with a diameter smaller than the maximum particle diameter. In addition, fragmentation and aggregation of these particles is uncommon. The non-occurrence of aggregation allows the penetration of particles into smaller diameter blood vessels, incompatible with PVA particles of the same size (1,13).

The disadvantages of this product are associated with the need for intermittent stirring to prevent sedimentation and the allergic potential of porcine gelatin present in the composition. In addition, the same size of Embospheres® similar particles results in deeper penetration compared to PVA particles, which may lead to ischemia in some vascular beds, such as the colon. The difference in effective particle size when using PVA or Embospheres® can be significant (1).

2.1.3 PVA particles

PVA is the most commonly used permanent embolization agent because it is biocompatible and has appropriate mechanical and chemical properties. This polymer has elastic properties when in contact with blood. Because it is hydrophilic, the swelling of particles occurs when in contact with water present in the blood serum. This feature allows compatibility with commercially available catheters, which have a smaller diameter than those of the particles (13).

PVA particles cannot be obtained by direct polymerization because of the instability of vinyl alcohol monomer. When this alcohol is produced, it rapidly rearranges and forms the predominant equilibrium acetaldehyde-tautomer (Figure 2.2). Therefore, it is necessary to saponify a poly(vinyl ester) such as poly(vinyl pivalate) or PVAc to obtain PVA (14).

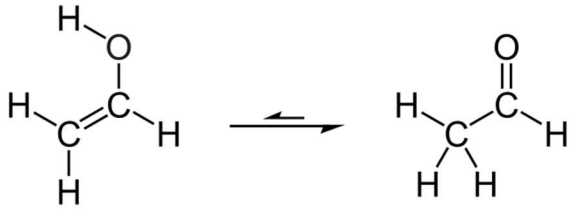

Figure 2.2: Vinyl alcohol and acetaldehyde tautomerism.

PVA particles obtained by precipitation in alcohol may have irregular morphology, favoring agglomeration and, consequently, hindering the flow through the catheter. In addition, porosity may promote recanalization of the embolized vessel after some time. This damage was minimized by the development of a process of synthesis of controlled spherical core shell poly(vinyl alcohol and vinyl acetate) particle structure, whose structure reduces water absorption and spherical morphology reduces aggregation tendency (13).

The first medical application of PVA was reported by Grindlay and Claggett (15), where this material was used to fill the thoracic cavity after surgical removal of a lung. Currently, sulfonated PVA microspheres are used in the chemoembolization of hepatocellular carcinoma, wherein the particles are soaked with the desired chemotherapeutic agent prior to use. PVA particles are widely used in embolization of liver tumors, kidney, uterine fibroids and bronchial lesions (2).

Jack et al. (16) labeled PVA microparticles (about 500 μm in diameter) in colloidal sulfur and ^{99m}Tc mixture by contacting the particles and the colloid for 10 min at 100 °C. The obtained material was washed, centrifuged and the activity of the supernatant and particles was measured in a radioactivity detector. The yield of PVA microparticles labeling was 28 %. Preoperative embolization of a meningioma was performed in a 56 years old patient to reduce blood loss, accompanied by the left carotid injection of 20 mg of these sterile-prepared (295 μCi) labeled microparticles. SPECT images obtained from the neck and head revealed that the particles were located inside and around this tumor. The authors' expectation regarding the use of this easily prepared material was to allow the angiographist, preoperatively, to select the appropriate particle size to be used for embolization through a rapid response to physiological distribution of the material. According to the authors, this technique would be ideal for the evaluation of pre-embolization of a high-flow vascularization malformation due to the problems encountered with the use of PVA during embolization.

Despite the success of the material developed by Jack et al. (16), it is not commercially available. It is also possible to infer that this type of material would not arouse commercial interest in Brazil, since ^{99m}Tc is obtained from molybdenum 99, its precursor, that is an imported material in this country. The alternative use of ^{123}I in this type of application becomes an economically attractive option, since it is produced in Brazil. In addition, from a technical point of view, ^{99m}Tc has a physical half-life of 6 h, which implies a faster or greater dose of embolization procedures

conducted with this nuclide when compared to ^{123}I, whose physical half-life is approximately twice. greater (17).

2.1.4 The poly(vinyl acetate)

VAc homopolymers and copolymers are widely used as components of coatings, paints, sealants and binders. PVAc homopolymer is commonly known for its adhesive properties and is present in wood glue and school glue. PVAc (Figure 2.3) is a synthetic rubbery polymer of molecular formula $(C_4H_6O_2)_n$, belonging to the family of vinyl polyesters (14, 18).

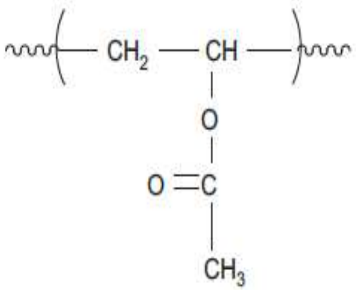

Figure 2.3: Schematic molecular structure of PVAc. Adapted from Moulay (19).

The most commercially important chemical reaction in which VAc is used as a feedstock is free radical polymerization. This monomer can be polymerized by mass, suspension, solution and emulsion methods. In addition, it forms commercially important copolymers with maleic anhydride, crotonic acid, styrene and ethylene, for example (18,20,21). Global market analysis shows that PVAc has accounted for the largest contribution of VAc monomer demand over the past few years. PVAc is one of the major polymers used in the adhesive industry and PVA was the second largest VAc monomer market in 2013 (22).

In the medical field, PVAc is used as a raw material for PVA, which is used as an embolization agent. Polymer particles can be produced in two stages, where PVAc is first obtained by suspension polymerization of VAc and then PVA is synthesized by partial hydrolysis of the produced polymer (saponification) (Figure 2.4). In this way,

spherical poly (vinyl acetate-co-vinyl alcohol) particles with core shell structure can be obtained, reducing possible complications during the embolization procedure (23).

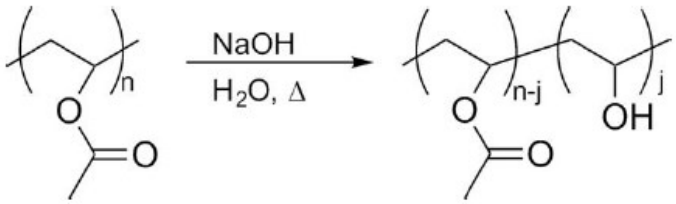

PVAc Partially-hydrolyzed PVAc

Figure 2.4: Hydrolysis reaction used to obtain partially-hydrolyzed PVAc. Adapted from Oliveira et al. (23).

In addition, obtaining PVA/PVAc microparticles containing iron oxide III nanoparticles was studied (Figure 2.5). The addition of magnetic properties to this polymeric matrix allows the simultaneous use of embolization and hyperthermia, which is the temperature increase caused in the tumor region by the application of magnetic nanoparticles submitted to an alternating magnetic field (13,23,24).

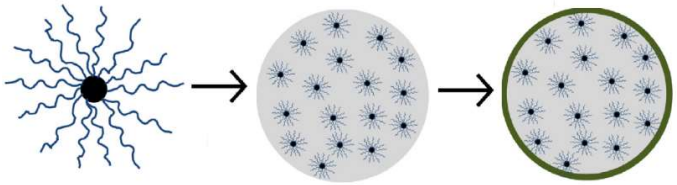

(a) (b) (c)

Figure 2.5: Oleic acid coated iron oxide III nanoparticle (a), PVAc microparticle containing nanoparticles (b), and PVAc/PVAc microparticle containing nanoparticle after hydrolysis (c). This nanoparticle allows the simultaneous use of hyperthermia and embolization techniques. Adapted from Ferreira et al. (24).

PVAc homopolymer has thermoplastic properties suitable for hot melt extrusion processing for particle production and controlled release drug application (25). PVAc copolymers may also be used as controlled release agents. Doxorubicin and

amoxicillin drugs were incorporated into poly(vinyl acetate-co-methyl methacrylate) microspheres via suspension polymerization for this purpose (26,27). Poly(ethylene-co-vinyl acetate) copolymer may also be used for controlled release of the drug metropolol (28).

2.1 Images on Nuclear Medicine

Single Photon Emission Tomography or SPECT and Positron Emission Tomography (PET) are the most commonly imaging techniques used in Nuclear Medicine for the study of biochemical dysfunctions present in the early stages of disease, their mechanisms and associations with pathological states (29). These imaging techniques can be combined with other imaging techniques such as Magnetic Ressonance (MR) or Computed Tomography (CT). MR is used in Radiology to obtain anatomical images of organs by means of strong magnetic fields. CT technique uses an X-ray beam to generate tomographic images, allowing the visualization of high resolution morphological and anatomical structures. Simultaneous acquisition of functional and anatomical information improves the accuracy of localization and quantification of the radioactive substance in the target organ (30-32).

The SPECT uses a gamma emitting radioisotope whose decay should preferably be by electron capture followed by gamma emission with energy of the order of 100 to 300 keV. These characteristics provide a reduction in the ionizing radiation dose for the patient. PET is based on the coincident detection of two light photons, both with 511 keV energy, emitted diametrically opposite, after the positron (β^+) annihilation. Annihilation happens when the β^+ stemmed from a positron emitting radioisotope collides with an electron (31,32). Table 2.1 presents the main radioisotopes used in Nuclear Medicine.

Table 2.1: Main radioisotopes used in SPECT and PET. Adapted from Chery, Sorensen and Phelps (32).

SPECT radioisotope	^{99m}Tc	^{123}I	^{111}In	^{201}Tl	^{67}Ga	^{131}I
Physical half-life	6 h	13 h	68 h	73 h	78 h	8 d
Gamma energy (keV)*	140	159	172	70-80	185	364
PET radioisotope	^{15}O	^{13}N	^{11}C	^{68}Ga	^{18}F	^{124}I
Physical half-life	2 min	10 min	20 min	68 min	110 min	4 d

* There are other energies. These are the most relevant for SPECT imaging.

In both techniques, light photons are detected with the aid of scintillation chambers that are formed by thallium-fortified sodium iodide (NaI(Tl)) radioactivity detectors. The equipment used for imaging is known as gamma chamber or Anger scintillation chamber (Figure 2.6).

Figure 2.6: Example of PET/CT (a) and SPECT equipment (b). Adapted from Thirteen Of Clubs (34).

In this equipment, radioactivity emissions are collected at various angles through detectors positioned around the patient, which allows cross-sectional images of the distribution of the radioisotope in the target organ. The generated signals are transmitted to a computer program that performs the composition and the treatment of the obtained images (33).

The sensitivity of these techniques is in the range of $6 \cdot 10^8$ to $6 \cdot 10^{11}$ molecules per milliliter of tissue, whereas in the MR technique it is approximately $6 \cdot 10^{17}$ molecules per milliliter of tissue. In 2008, more than 30 million of imaging procedures in Nuclear Medicine were performed worldwide (31,32).

2.2 SPECT and iodine 123

The diagnosis obtained by SPECT - also known as Scintigraphy - is suitable for the visualization of very limited and small organs, such as the heart and the brain. Radioisotopes such as ^{99m}Tc, ^{67}Ga and ^{111}In are used in this widespread imaging technique that finds new applications every day. These radioisotopes decay by the electron capture mode, what implies in less dose for the patient due to the absence or small amount of particles release. In addition, the energy of their peaks falls in the range of the SPECT energy window. Moreover, these radionuclides are commercially available in a sterile, pyrogen-free, and carrier-free state. The radiochemistry of ^{99m}Tc is driven by its reduced chemical species that combine with a variety of chelating agents. ^{67}Ga is supplied as gallium chloride that can be complexed with citric acid to form gallium citrate, which is its most used radiopharmaceutical compound. Also, ^{111}In is chelated to DTPA (diethylenetriaminepentaacetic acid) to form the radiopharmaceutical ^{111}In-DTPA (35,36).

Although the PET technique offers higher resolution images and better selectivity, its use has not yet become widespread outside dedicated clinical centers. SPECT is considered to be the most practical approach for routine diagnostic use in Nuclear Medicine. As radiopharmaceuticals containing gamma emitters were worldwide developed and produced, an additional advantage for SPECT is that numerous regional and local research institutions, medical centers, and hospitals have the gamma camera and the radioisotope required to use this technique. In addition, SPECT technique is cheaper than PET to perform imaging (37,38).

Currently, the combination of SPECT and CT, known as SPECT/CT, is also used. The composition between SPECT images and those ones obtained with CT results in a high diagnostic value, as it provides information on the phenotypic functional changes associated with the development of the disease. Therefore, SPECT/CT integrated imaging systems are gaining popularity (33,39).

Although ^{99m}Tc, ^{67}Ga and ^{111}In are frequently used in SPECT imaging, ^{123}I is widely used in the SPECT technique because of its outstanding nuclear properties and availability at high radionuclide purity, which is defined as the fraction, expressed as a percentage, of total radioactivity as the radionuclide of interest present in the final product (36). The ^{123}I is considered a pure gamma emitter as it emits 159 keV gamma rays with 83 % abundance what is quite suitable for the SPECT energy window (100-300 keV). This radioisotope has a physical half-life of 13.2 h, what provides satisfactory investigations of metabolism processes and biodistribution studies (41). ^{123}I decay occurs by electronic capture, where the proton captures an electron of layers near the nucleus, neutralizing the charge and giving rise to a neutron (33). The product formed is the stable element tellurium (Te) 123 which is present in very low quantity (between 10^{-18} and 10^{-14} g) and is therefore, surely below the lethal dose of 20 mg $\cdot$ kg^{-1} (42). Besides, the chemical properties of this radioiodine follow its non-radioactive correspondent that is extremely versatile. Radioiodination approach will be further presented in section 2.9.

^{123}I can be obtained in cyclotron by direct method, in which different isotopes of antimony (Sb) and tellurium are irradiated according to the following reactions:

$$^{121}\text{Sb}\ (\alpha, 2n)\ ^{123}\text{I}$$

$$^{123}\text{Te}\ (p, n)\ ^{123}\text{I}$$

$$^{122}\text{Te}\ (d, n)\ ^{123}\text{I}$$

$$^{124}\text{Te}\ (p, 2n)\ ^{123}\text{I}$$

Where α corresponds to the alpha particle, n corresponds to the neutron particle, d corresponds to the deuteron particle, and p corresponds to the proton particle. However, these methods result in the significant presence of radionuclide impurities. Medium and high energy cyclotrons (from 20 to 70 MeV) are used in the indirect method, which allows obtaining ^{123}I with high radionuclide purity from the xenon 123 (^{123}Xe) decay, according to the following reactions (43):

$$^{122}Te\ (^{3}He, 2n)\ ^{123}Xe \rightarrow\ ^{123}I$$

$$^{122}Te\ (\alpha, 3n)\ ^{123}Xe \rightarrow\ ^{123}I$$

$$^{123}Te\ (^{3}He, 3n)\ ^{123}Xe \rightarrow\ ^{123}I$$

$$^{127}I\ (p, 5n)\ ^{123}Xe \rightarrow\ ^{123}I$$

At the Nuclear Engineering Institute (IEN), located in Rio de Janeiro, Brazil, the ^{123}I radioisotope is obtained indirectly using the Cyclotron CV-28 particle accelerator (with 24 MeV proton beam and 20 μA current) associated with the KIPROS (Karlsruhe Iodine Production System) system, which comprises a set of mechanical, electronic and chemical systems controlled by a computer software. With this production methodology, the ^{123}I produced is considered ultra-pure because it results in a higher degree of radionuclide purity when compared to other methods. This radioisotope is formed by the nuclear reactions presented in Figure 2.7 (17):

$$^{124}Xe\ (p,pn)\ ^{123}Xe \xrightarrow[2.08\ h]{\beta^+}\ ^{123}I \qquad (a)$$

$$^{124}Xe\ (p,2n)\ ^{123}Cs \xrightarrow[5.9\ min]{\beta^+}\ ^{123}Xe \xrightarrow[2.08\ h]{\beta^+}\ ^{123}I \qquad (b)$$

Figure 2.7: ^{123}I obtaining reactions where (b) is majority.

^{123}I produced as sodium iodide ($Na^{123}I$) is widely used in thyroid scintigraphy to study the function of this gland. In Brazil, this exam is covered by the 'Sistema Único de Saúde' (SUS). There are approximately 400 scintigraphy chambers in use in the country's Nuclear Medicine Services (44). The ^{123}I radioisotope is best suited for *in*

vivo diagnostic use because of its physical half-life, which allows for longer diagnostic procedures, and the energy of released photons, which results in a low dose for the patient and medical staff involved, besides not emitting particles due to the characteristic mode of decay (40,45). Figure 2.8 shows an example of SPECT image obtained with ^{123}I. This figure shows planar images of the heart obtained with the ^{123}I-labeled iobenguane radiopharmaceutical produced by the IEN. The orange areas show uptake of this radiopharmaceutical by the organ.

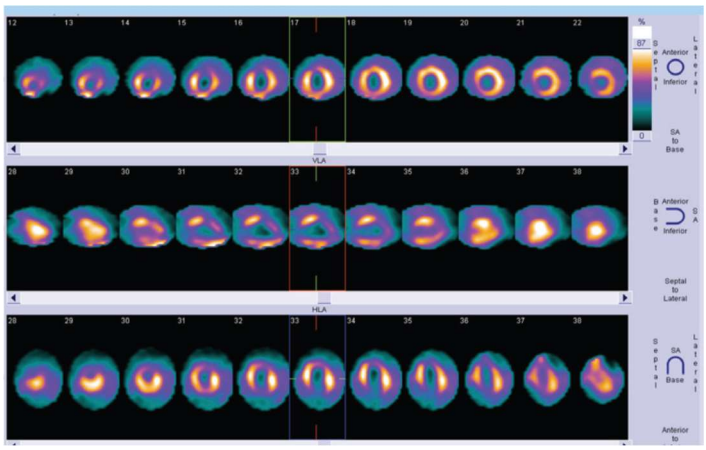

Figure 2.8: Example of SPECT image. Adapted from Miranda et al. (46).

2.3 Nuclear Medicine and Radiopharmaceuticals

Nuclear Medicine was defined in 1972 by the World Health Organization as a branch of Medicine that covers all applications employing radioactive materials in diagnosis, therapy, and medical research, except for the use of sealed ionizing radiation sources in radiotherapy. It is a specialty that covers areas such as Cardiology, Endocrinology, Oncology and Neurology. Imaging techniques used in Nuclear Medicine enable the obtaining of very sensitive functional images, which allow the study of physiological processes *in vivo*, noninvasively, through the use of radiopharmaceuticals (33,47).

Radiopharmaceuticals are diagnostic or therapeutic pharmaceutical preparations containing one or more radionuclides. They also include non-radioactive labeling components and radionuclides, including components extracted from radionuclide generators (48). Successful use of a radiopharmaceutical is closely linked to the

biochemical characteristics that allow for uptake or metabolism by the organ of interest. Radiopharmaceuticals do not usually exhibit pharmacological action and usually do not induce responses to toxicity; however, administration requires compliance with the production and administration requirements of conventional drugs, as well as those specific to the nuclear area, as they are radioactive substances (40).

Diagnosis by radiopharmaceuticals allows dynamic and static imaging besides metabolic function testing. This type of diagnosis can provide useful information about early or advanced cancer, as well as enabling the prognosis of response to a treatment that may be continued, modified or abandoned. Radioisotopes ideal for diagnostic use should emit gamma radiation without the emission of corpuscular ionizing radiation (31-33,40).

Radiopharmaceutical therapy frequently aims to promote tumor cell death. In this case, the ideal radioisotopes should emit very ionizing and little penetrating corpuscular radiation (range less than 100 μm), which deposit energy exclusively in the organ of interest. For this, radionuclides are used whose decay form occurs by the emission of alpha, beta or electron capture particles followed by the emission of Auger electrons. For the application to be effective, the radionuclide physical half-life must be long (from a few hours to 70 days) and the relationship between corpuscular and associated gamma radiation must be high (31-33,40).

In the process of imaging for diagnostic or therapeutic purposes, the effective half-life (T_e) of a radiopharmaceutical should be known so that the duration of the examination or treatment is compatible with the time required for study or treatment of the organ of interest. This parameter is also important for calculating the optimal dose of radiopharmaceutical to be administered and monitoring the amount of exposure to ionizing radiation. Physical half-life ($T_{½}$) is the time required for half a population of atoms of a radionuclide to decay into another nuclear form. The biological half-life (T_b) is the time required for an organism to remove by biological elimination half the amount of a substance administered. T_e is a combination of these

characteristics, i.e., it is the time required for a radionuclide in an organism to decrease its activity in half as a combined result of biological elimination and radioactive decay, as shown in the following equation (40,48):

$$T_e = \frac{T_{1/2} \times T_b}{T_{1/2} + T_b}$$

2.4 Radiopharmaceuticals and particles

Many particulate radiopharmaceuticals are used for diagnostic or therapy purposes. In diagnosis, the first particles used were red and white blood cells, which were taken from a patient, labeled with ^{111}In or ^{51}Cr and then injected again. ^{51}Cr-labeled red blood cells are used for measuring the mass of these cells, determining blood flow and spleen imaging (49). ^{99m}Tc and ^{111}In-labeled polymer micelles are used in the diagnosis of lymphatic ducts and sentinel lymph nodes (50). Monoclonal antibodies are labeled with ^{99m}Tc to detect infections and inflammations. Peptides are labeled with ^{111}In for primary detection and metastasis of neuroendocrine tumors (40). Nanoparticles composed of polymers, lipids, carbon and metals are also used in diagnostics with radioisotopes ^{67}Ga, ^{64}Cu and ^{18}F, for example. A new class of ^{64}Cu and ^{18}F-labeled nanoparticles are called Quantum dots (semiconductor nanocrystals), which are used for combined PET and infrared tumor imaging (51). Other diagnostic applications using radioactive particles are presented in Table 2.2.

Table 2.2: Applications of particulate radiopharmaceuticals for diagnosis. Adapted from Shanthi (49) and Polyak & Ross (52).

Radioisotope	Material	Application
^{111}In, ^{51}Cr	Red Blood Cells	Blood circulation studies
^{111}In	Liposome	Liver and spleen scintigraphy
^{111}In	Platelets	Deep Vein Thrombosis
^{99m}Tc	Sulfur colloid	
^{141}Ce, ^{57}Co, ^{114m}In, ^{85}Sr, ^{51}Cr	Polystyrene microspheres	Blood flow measurements
^{3}H, ^{14}C	Poly(acrylic acid) microspheres	Investigation of biodistribution and location of drug-loaded microspheres
^{141}Ce	Polystyrene microspheres	
^{99m}Tc	Carbon particles	Lung scintigraphy
	Albumin macroaggregate	Liver and spleen imaging, lung scintigraphy and radioembolization [2]
	Sulfur and antimony sulfide colloid	Bone marrow images

[2] The ^{99m}Tc-labeled albumin macroaggregate is used for ^{90}Y liver radioembolization in investigative pretreatment of perfusion studies – known as scout dose - as the image quality is superior to that obtained with ^{90}Y Bremsstrahlung photons.

In therapy, beta particle-emitting radioisotopes, such as ^{166}Ho, ^{90}Y and ^{186}Re or ^{188}Re, are used to deliver ionizing radiation to a defined area of the tumor by means of carriers such as gel, liposomes, albumins, microparticles and nanoparticles. These transporters become radioactive by two general methods: (1) macromolecules are labeled by direct addition of radioisotopes, (2) micro and nanoparticles are charged with the isotope in their non-radioactive state for subsequent neutron irradiation (3,53,54). In addition, metal radioisotopes are reduced in aqueous medium for incorporation into the polymer and radioisotope oxides are encapsulated in the polymer structure (55-57). Some applications of these particles in therapy are presented in Table 2.3.

Table 2.3: Applications of particulate radiopharmaceuticals for therapy. Adapted from Shanthi (49).

Radioisotope	**Material**	**Application**
^{90}Y, ^{186}Re, ^{188}Re	Glassy microspheres	Liver and spleen radioembolization
^{35}S	Colloidal sulfur	Arthritis radiosynovectomy
^{90}Y	Resin Microspheres	
^{169}Er	Citrate complex	
^{90}Y	Poly(lactic acid) microspheres	Local radiotherapy
^{211}At	Albumin microspheres	
^{212}Pb	Sulfur colloid	
^{32}P	Chromium phosphate	Intracavity treatment
^{90}Y	Silicate	

In the field of Nuclear Medicine, radionanoparticles have three main applications: drug development, imaging and therapy. For the first purpose, the choice of the radioisotope depends on characteristics such as nanoparticle type, ease of preparation and stability of the labeled particle, as well as availability, cost and type of the radioisotope decay. Once obtained, these particles are mainly used in biodistribution studies. Nanoparticle molecular imaging has evolved a great deal over the last decade, and one of the most interesting aspects is the potential for use as multimodality imaging agents by combining different properties into a single particle type. In this way, PET and MR images can be obtained, for example. Improvements in the characteristics and synthesis of these nanoparticles have made possible to obtain multifunctional particles capable of offering multiple therapies and thus, combating diseases such as cancer through the internal and localized application of ionizing radiation (52,58,59).

Examples of radionanoparticles used as radiopharmaceuticals for imaging are polyethylene glycol (PEG) coated liposomes containing ^{111}In-DTPA (^{111}In-labeled diethylenetriaminopentaacetic acid). These particles had their biodistribution and pharmacokinetics studied and the results showed the localization in endothelial reticulum tumors, besides presenting significant absorption in this organelle. PET/MR and PET/CT imaging studies were also performed with ^{18}F-labeled iron oxide nanoparticles. Folate and ^{64}Cu nanoparticles were used for tumor imaging, while organometallic nanoparticles containing germanium and ^{99m}Tc were used for spleen imaging (40,59).

The insertion of radioisotopes in particles has stimulated much research and the filing of numerous national and international patents in the field of Radiopharmacy. From 2000 to 2013, more than 4,500 patents were filed and more than $ 50 billion were invested, showing the tremendous interest in developing micro and nanoscale radiopharmaceuticals for diagnosis and therapy (60). Unfortunately, much of what is developed does not become a marketable drug, because after product development, clinical trials (*in vitro* and *in vivo*) must be performed, in addition to the registration

of the drug. These steps are costly and can last up to 10 years (60,61). As an example, silica nanoparticles containing a fluorophore and iodine 124 is undergoing clinical trials, but is not recruiting for human tests. In addition, a liposome labeled with rhenium 188 (^{188}Re-*N*,*N*-bis (2-mercaptoethyl)-*N'*,*N'*-diethylethylenediamine pegylated liposome), has passed its study completion date and the status has not been verified in more than two years, according to Clinical Trials.gov database[3] (62).

2.5 Radioiodines and particles

Some radioiodines attached to nanoparticles, microparticles and macromolecules are used or may have potential for use as radiopharmaceuticals. Radioisotope ^{125}I emits Auger electrons and radioisotope ^{131}I emits beta (β^-) particles. These types of ionizing radiation are used in therapy; therefore, materials developed with these radioisotopes can be used as radiopharmaceuticals for organ therapy with which they have affinity. Iodine 124 is a positron emitter and is used for diagnosis; therefore materials containing it can be used for these same applications. Table 2.4 presents some nuclear properties of the most commonly used radioiodines in Nuclear Medicine. Radioiodines are used as sodium radioiodide in alkaline medium. Therefore, when the chemical species in which the radioiodine is not presented, it is understood to be in the form of sodium radioiodide.

[3] ClinicalTrials.gov is a database of privately and publicly funded clinical studies conducted around the world.

Table 2.4: Main radioiodines used in nuclear medicine and some of its nuclear properties. Adapted from Saha (40).

Radioiodine	^{120}I	^{122}I	^{123}I	^{124}I	^{125}I	^{131}I
Physical half-life	1,4 h	3,6 min	13,2 h	4,18 d	59,4 d	8,02 d
Decay mode	β^+	β^+	EC	β^+	AE	β^-
γ (keV)*	601	564	159	603	35,5	364
Use	PET	PET	SPECT	PET	Therapy	Therapy

* Most abundant gamma ray energy. EC = electronic capture. AE = Auger electron.

The methodologies used to determine the yield obtained in radioiodation employ: (i) ionization chamber or inorganic NaI (Tl) scintillator type radioactivity detector to, after centrifugation, measure both the decantate and supernatant activities; (ii) ionization chamber, NaI (Tl) or radiochromatography system to measure the activity of the strip/plate used in thin layer chromatography; (iii) NaI(Tl) detector associated with high performance liquid chromatography (HPLC) system or size exclusion chromatography (Figure 2.9).

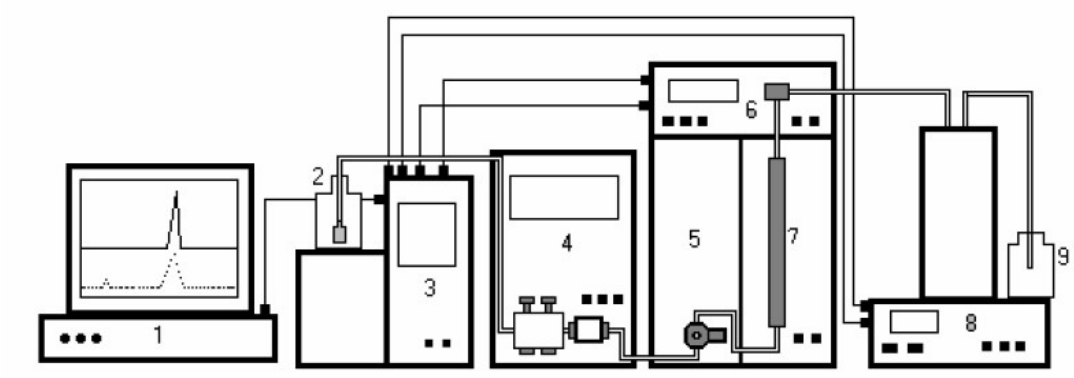

Figure 2.9: Illustrative example of a HPLC system coupled to NaI(Tl) absorbance and radioactivity detectors. 1 = computer. 2 = mobile phase reservoir. 3 = signal integrator. 4 = pump. 5 = oven. 6 = UV detector. 7 = chromatographic column. 8 = NaI(Tl) detector. 9 = radioactive waste reservoir. Adapted from Carvalheira (17).

Another important step related to radioiodination of molecules for *in vivo* applications is the biodistribution study. Studying the biodistribution of a radioactive substance in a living organism includes mapping and measuring the distribution of substance activity in tissues, organs, plasma clearance, urinary and fecal excretion after administration. This study can be performed by measuring the activity in each organ, excrement or fluid, by means of radioactivity detector after dissection or by obtaining SPECT or PET images.

Gordon (63) described the preparation of ^{131}I-labeled polyvinylpyrrolidone (PVP) particles (Figure 2.10), with an average molar mass between 30,000 and 40,000 Da for investigations of human plasma protein metabolism. The polymer (1 g) was dissolved in 0.4 mol · L^{-1} sulfuric acid (10 mL) with subsequent addition of 0.1 mol · L^{-1} sodium nitrite (1 mL), keeping the mixture in an ice bath for 15 min. The desired amount of ^{131}I was then added and the mixture was immediately heated to 100 °C. After 30 min., the mixture was cooled, made alkaline with 1 mol ·L^{-1} sodium carbonate (2 mL) and approximately 100 mg of sodium hydrosulfite was added to consume the excess of nitrous acid. The mixture was first dialyzed in pH 9.0 buffered potassium iodide solution with sodium carbonate and bicarbonate, and then in water for 24 hours. The yield obtained was 20-25 %. The author did not perform the *in vitro* or *in vivo* assays, but believes that his work has made a great contribution when compared to previous ones, in which ^{131}I-labeled PVP particles were not chemically stable enough, which made it impossible to use in plasma metabolism studies.

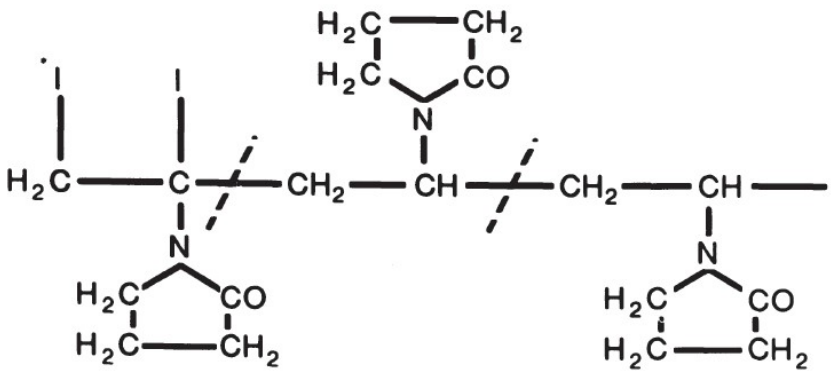

Figure 2.10: Structure of the radioiodine-labeled polyvinylpyrrolidone (left, *I represents the ^{131}I). Adapted from Dewanjee (64).

Mitchell, Harden, and O'Rourke (65) developed a procedure that measures the absorption of ^{131}I-labeled triiodothyronine thyroid hormone from *in vitro* testing using a resin sponge. The sponge, consisting of a mixture of polyurethane foam and finely divided anion exchange resin (Amberlite IRA-400), showed satisfactory absorption of the hormone contained in the serum. After preparation of the sponge, it was necessary to wait 1 to 4 hours to insert the serum, half an hour to wait for the balance to be changed and another hour of stirring. In the end, supernatant and sponge were separated and the activity of both fractions were measured in a radioactivity detector. Significant differences in absorption of radioiodinated hormone present in serum and sponge were observed in patients with hyperthyroidism and or uncomplicated pregnancy compared to normal subjects. The authors indicate that these results demonstrate the usefulness of this assay for identifying certain thyroid abnormalities. Despite the positive results, this method is not used for triiodothyronine hormone evaluation, since other methods that do not use ionizing radiation are effective and reliable for the determination of this substance.

Picard et al. (66) embolized 45 extra-cerebral lesions using ^{131}I-labeled gelatin sponges. Unfortunately, this article was not found. Berenstein and Russel (1981) cite it, but do not present the procedures used for the synthesis of this compound. Therefore, more details about the radioiodination of this material were not obtained. However, it can be inferred that, at the time of publication, radioiodination occurred through some methodology based on potassium iodide, hydrogen peroxide, chloramine-T or Bolton-Hunter reagent, which were the most popular at that time.

Lang and Sullivan (67) presented the results obtained in interstitial radiotherapy of the kidney using ^{I25}I seed embolization. Interstitial radiotherapy can reduce the dose to which the patient should be exposed and the tumor burden without causing damage to adjacent healthy tissues. Seed embolization is the embolization performed with seeds of ^{125}I in the form of a silver compound sealed in a 5 mm long by 1 mm diameter titanium capsule. In this study, the authors used a 5.8 cm length and

0.038 cm diameter catheter to transport the seeds to the kidney. The authors stated at the time that this procedure seemed to be the most effective method for treating renal cell carcinoma, but this therapy is not frequently reported in the literature related to renal brachytherapy procedures.

Dewanjee (64) labeled PS-DVB (poly(styrene-co-divinylbenzene) with ^{125}I (1 mCi or $3.7 \cdot 10^7$ Bq) using Iodogen® (1,3,4,6-tetrachloro-3α,6α-diphenylglucoluril), which is an oxidant agent commercially available as a vial coated with a film of 500 μg of this oxidant for single use in the radioiodination of proteins and peptides. In this oxidation, the radioiodide is transformed into a radioelectrophile, which attacks the benzene ring, by means of electrophilic aromatic substitution reaction (Figure 2.11). To avoid a possible radiolysis, i.e., the breakage of covalent bond between the radioiodine and the benzene ring, the particles were coated with medical grade silicone oil (0.1 mL) and the mixture was evaporated (90 °C) to dryness. The free radioiodide was removed by centrifugation and the yield of this labeling ranged from 50% to 60%. *In vitro* blood plasma studies performed at room temperature showed 5 % deiodination after 24 hours of incubation. Accordingly, the author concluded that the stability of the carbon-radioiodine bond suggests that these particles can be used for measuring peripheral blood flow, along with other metal radionuclide-labeled microspheres.

(a) (b)

Figure 2.11: Scheme of PS-DVB radioiodination by the Iodogen® method (a). The bottle has the walls lined with the oxidant. The reaction occurred at room temperature. Adapted from Dewanjee (64). Chemical structure of Iodogen®.

Saha (40) argued that while human serum albumin can be labeled with any radioiodine, ^{125}I human serum albumin (^{125}I-RISA) is the most commonly used radiopharmaceutical for lung or heart plasma volume studies in that the intention is to keep the radiopharmaceutical in the bloodstream long enough to determine this plasma volume. At the desired interval, a blood sample is taken and its activity measured in a radioactivity detector. This compound is prepared by radioiodination of albumin using the Iodogen® method or the chloramine-T method at 10 °C in alkaline medium. Chloramine-T (*N*,*N*-dichloro-p-toluenesulfonic acid) is an oxidant of the *N*-chloroamide family used in the electrophilic radioiodination of aromatic compounds at room temperature at neutral or basic pH. In both methods, residual free iodide is removed by anion exchange resin, followed by membrane filtration for product sterilization. The author did not report the yield obtained, the radioiodine activity used or details about the radioiodination procedure.

Saha (40) also reported the use of ^{131}I and ^{125}I in the labeling of antibodies, which are heterogeneous and non-specific in tumor detection. However, a technology called hybridoma was introduced and allowed the production of homogeneous and highly specific monoclonal antibodies for a particular antigen. Antibodies are immunoglobulins produced *in vivo* in response to an antigen and specifically bind to it, forming an antigen-antibody complex. Antibodies have polypeptide chains and can therefore be labeled with radioiodines. The general antibody radioiodination protocol uses 100 to 500 mg of the antibody dissolved in phosphate buffer solution (pH 7.0). This solution and ^{131}I (1-5 mCi or 37-185 MBq) are added to the vial containing Iodogen®. After 12-15 min of reaction at room temperature, the radioiodinated antibody is separated from the remaining radioiodide by dialysis or gel permeation chromatography. The labeling yield obtained is 60-80 %. The radiopharmaceutical ^{131}I-Tositumomab, for example, is a commercially available radioiodinated antibody under the name Bexxar®. This radiopharmaceutical is used to treat non-Hodgkin's lymphoma. The ^{131}I-Tositumomab antibody binds to the CD20 antigen, which is expressed by this lymphoma, inducing cytotoxicity and apoptosis, mainly due to beta radiation released from this radioiodine.

Kumar et al. (68) labeled organically modified silica nanoparticles (diameter ~ 20 nm) with ^{124}I. These silica nanoparticles are functionalized with PEG (2-[methoxy(polyethylenoxy)propyl]trimethoxy silane) polymer and amino groups. In addition, these particles are conjugated to a near infrared dye. In the particles labeling, Bolton-Hunter (*N*-succinimidyl 3-(4-hydroxy, 5-iodophenyl) propionate) reagent was used. First, Bolton-Hunter reagent was labeled with ^{124}I (370 MBq) using Chloramine-T. Then, the obtained compound was conjugated to the amino group present on the nanoparticle surface, where the amino group loses one hydrogen atom and bounds to the carbonyl group. *N*-hydroxysuccinimide is the leaving group that accepts the lost hydrogen (Figure 2.12). *In vivo* studies of this material showed uptake by cells of the reticuloendothelial system and that almost 100 % of the nanoparticles were effectively eliminated from the animal by hepatobiliary excretion without any sign of organ toxicity. Therefore, the authors report that these results provide preliminary answers to some of the major biological questions raised about the use and safety of silica-based nanoparticles for diagnostic and therapeutic applications.

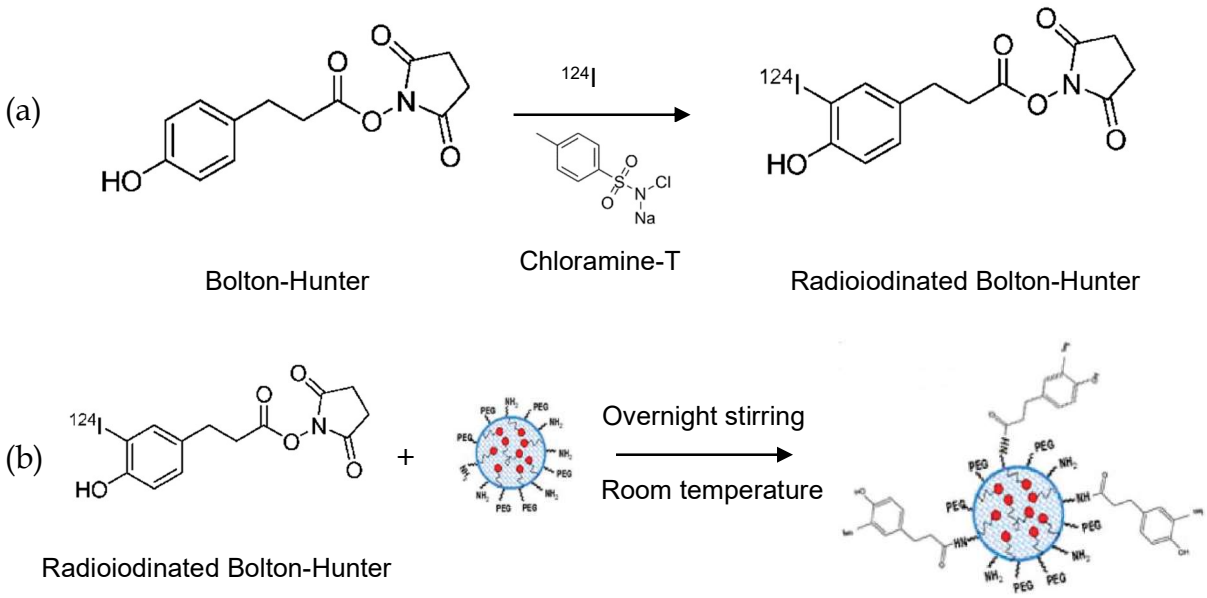

Figure 2.12: (a) Radioiodination of Bolton-Hunter reagent using Chloramine-T. (b) Conjugation of the radioiodinated reagent with the amino group in the particle. Adapted from Kumar et al. (68).

Shao et al. (69) described, for the first time, the incorporation of radioiodine in gold nanoparticles, since iodine has a high affinity for the golden surface and is strongly bonded to it. These particles were coated with hexadecyltrimethylammonium bromide or with this substance added of poly(ethylene glycol) containing terminal thiol grouping. For the incorporation of ^{125}I as sodium iodide (11.1 MBq or 300 µCi), 0.1 mL of gold nanoparticle suspension (1012 particles per milliliters) was used. After labeling, the obtained material was centrifuged and separated from the supernatant. Activity in both samples was measured and labeling yields ranged from 60 to 99 %, with a minimum specific activity of 3700 GBq · µmol^{-1}. These particles were used to determine biodistribution patterns in mouses by SPECT imaging within six days after intravenous administration of the material.

Fritz et al. (70) deposited a patent regarding the synthesis of microspheres whose core was formed by poly(methyl methacrylate), coated with poly(bis2,2,2-trifluoroethoxyphosphazane) or derivatives for application in embolization. The synthesis occurred via suspension polymerization with peroxide-based initiators and water. In this patent, the authors indicated the possibility of insertion of ^{123}I or ^{131}I in the polymeric matrix, which could then be used as a component for obtaining SPECT images. However, the authors do not describe details about the procedure to be used for the insertion reaction.

Kaiho (71) reported the use of ^{125}I seeds as a medical device used for many years to treat prostate cancer by internal radiation (brachytherapy). Usually, for this treatment 60 to 80 seeds (^{125}I on a silver compound sealed in a titanium capsule measuring 5 mm in length and 1 mm in diameter) are implanted in the patient's prostate using a special needle. With this type of therapy, in addition to dispensing a laparotomy, the patient can leave the hospital in 2 or 3 days and return to work shortly after. Less adverse reactions and the maintenance of sexual function are also great advantages of this brachytherapy. This type of treatment is widely used and problems such as the migration of these seeds to other parts of the body are reported in the literature.

Tang et al. (72) encapsulated the poly(4-vinylphenol) (PVPh) polymer with poly(ethylene glycol) (PEG) and later labeled the obtained nanoparticles (10 mg · mL^{-1}) with ^{125}I (250 µCi or 9.25 · 10^6 Bq in 2 mL phosphate buffer), using chloramine-T oxidant (17.6 mmol in 2 mL phosphate buffer) for 30 min under stirring (Figure 2.13). The radioiodine, by means of aromatic electrophilic substitution reaction, is inserted in the ortho position to the phenol group of the encapsulated polymer. The remaining radioiodide was removed by ultracentrifugation and the yield obtained was at least 90 %. The authors also added that the specific activity obtained (0.1 µCi ·$µg^{-1}$ or 3.7 · 10^3 Bq ·$µg^{-1}$) was sufficient to perform biodistribution studies, which showed that these particles remained intact for about 96 h in the body, presented long duration in the blood circulation and gradual release of organs such as liver and spleen. Further details on the procedure used in the biodistribution studies were not reported. The authors stated that these particles act as a starting point for the expansion of segmentation and biodistribution studies, which are extremely important for the evaluation of the location in the body of nanoparticles used as localized drug release agents.

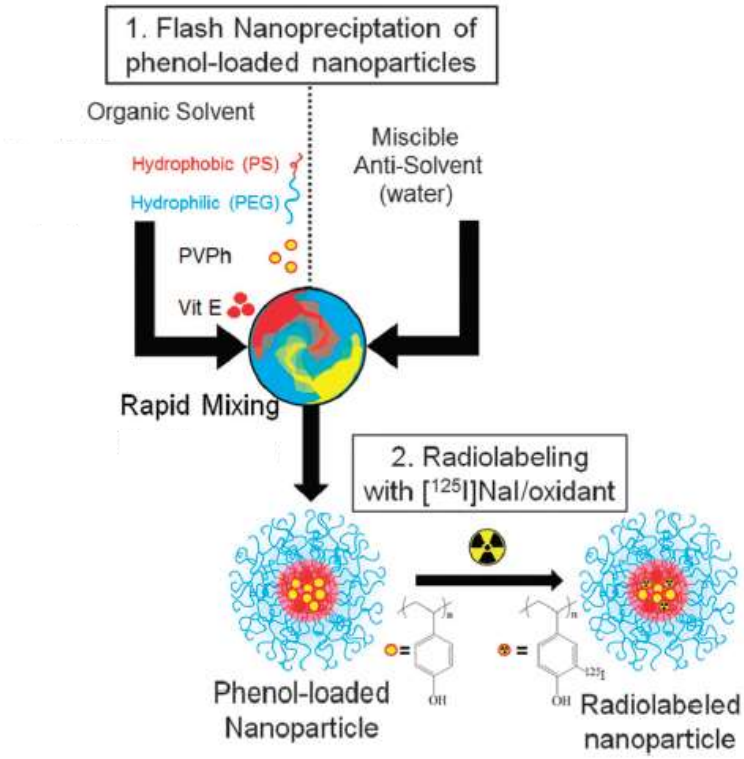

Figure 2.13: Reaction scheme for chloramine-T nanoparticle labeling. Adapted from Tang et al. (72).

In this section, the literature review of radioiodinated particles showed that few works comprising this issue have been developed since 1958. Radioiodinated polymeric particles for embolization purpose were mentioned in just one work, as a possibility (Fritz et al., 2015). This indicates a lack of studies regarding this issue that this thesis intended to cover. The methods used in the particles radioiodination is based on an oxidant agent usage. Chloramine-T, Iodogen® and Iodo-beads were the agent cited. The first one is the cheapest reactant, the second one is limited for just one batch and the last one, provides high labeling yields. The chloramine-T drawback is the need of adding a reducing agent to the reaction media after radioiodination completion. *In vitro* and *in vivo* studies are key assays to indicate the successful biological performance of the designed radioiodinated particles, but are not covered in this thesis. Dewanjee (64) and Tang et al. (72), for example, presented some biological performance results of the synthesized material. With respect to Radiological Protection, the works cited herein used low activities of radioiodines, as expected for preserving researchers from excessive exposure to ionizing radiation. Among the works presented in this section, the work performed by Tang et al. (72) discusses a successful approach using radioiodinated poly(4-vinylphenol) polymer in *in vivo* studies, with low deiodination of this material in the body. These good results arouse interest in the use of this material in other polymeric matrices. Some characteristics of this material, such as high *in vivo* stability, simplified radioiodination procedure, and high labeling yield are extremely interesting and can add unique values to the functionality of polymeric materials used as embolization agents, such as PVAc.

2.6 The 4-vinylphenol

The comonomer to be used for suspension polymerization with VAc must meet specific requirements to ensure the success of obtaining a new radioactive embolization agent that allows the use of the SPECT technique. This comonomer should be non-toxic, poorly water-soluble, have vinyl group available for free radical polymerization with VAc, and an aromatic ring containing electron-donor grouping

(activating grouping) to facilitate the iodination via aromatic electrophilic substitution, because iodinated aromatic compounds present greater chemical stability *in vivo* (45). In addition to unsubstituted vinyl monomers, free radical polymerization is possible for vinyl monomers mono- or disubstituted by the following functional groups and heteroatoms: $-C_6H_5$, $-OCOCH_3$, -COOR, -Cl or -Br (73). Among these substituents, the aromatic ring is recommended, but to enable iodination it must be monosubstituted by any of the following strongly activating groups: $-NH_2$, -NHR, $-NR_2$, -O, -OR, $-OCH_3$ or -OH (74). Different substituted vinyl benzene compounds may meet these requirements; however, the 4-vinylphenol (4VPh) molecule is the simplest and therefore has been selected for VAc copolymerization and subsequent radioiodination (Figure 2.14).

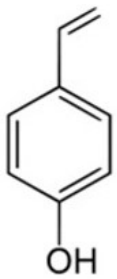

Figure 2.14: Chemical structure of 4-vinyl phenol (IUPAC Nomenclature: 4-ethenylphenol).

As seen in Figure 2.14, the vinyl unsaturation of 4-vinylphenol resembles styrene, which forms copolymer with VAc (75). Phenols and their substituted derivatives are easily iodinated by electrophilic substitution, resulting in the insertion of iodine in the ortho position relative to the hydroxyl group (76-78). A disadvantage with respect to the presence of phenols in polymerizations is their known retarding effect; that is, phenols slow down polymerizations, but do not prevent them from occurring (79,80). Naturally, 4VPh occurs in cider, wine, and berries, for example, and is used as a flavoring in the food industry (81). This substance has a water solubility of 8.4 $mg \cdot mL^{-1}$ at 25 °C, pKa equal to 9.56, melting point of 68-69 °C, boiling point of 189 °C at 760 mm Hg, and vapor pressure of 0.168000 mm Hg at 25.00 °C (82). Its polymers and copolymers have several applications, for example, use as

microphotoresistant materials, thermosetting or chelating resins, surface treatment agents and additives (83).

Poly(4-vinylphenol) homopolymer (P4VPh) can be obtained using 4VPh and AIBN at 60 °C for 16 h (84), or with AIBN at 60 °C for 24 h (83). For example, mixing 50 % of 4VPh (1:1 THF) with 1 % AIBN (based on the monomer) at 70 °C for 20 h results in an average molar mass P4VPh of 22,000 Da at 66 % conversion (83). 4VPh copolymerizes with methyl metacrylate (1:1 ratio) and AIBN at 60 °C for 45 h, resulting in 100 % of conversion. Cationic polymerization of 4VPh using methylene chloride as solvent and boron trifluoride etherate ($BF_3O(C_2H_5)_2$) as initiator at 12 °C for 5 min results in an average molar mass homopolymer of 126,000 Da with 95% conversion (83).

The literature presents controversies regarding the reactivity of the 4VPh monomer. According to Sovish (84), both homo and copolymerization of 4VPh are not spontaneous. However, Kaneko, Noguchi and Oka (85) state that it is very difficult to store this monomer as it polymerizes rapidly at room temperature.

2.7 Bulk polymerization

By definition, it is a type of polymerization wherein the reaction medium contains no solvent or diluent and the initiator is added directly to the monomer. In this type of polymerization, the reaction is initiated by the activation of the initiator, usually by heating. The main advantage of this type of polymerization is the obtaining of high purity final product. However, temperature control of a mass polymerization system presents great difficulty, as the reaction is very exothermic and results in high viscosities. Localized generation of hot spots can result in degradation and discoloration of the final material, which may still have a wide molecular weight distribution. Heat dissipation and viscosity problems are circumvented, for example, by performing low conversion polymerization by separating and recycling unreacted monomer. Acrylic sheets are commercially obtained by this system (73,86).

2.8 Suspension polymerization

Suspension polymerization occurs when one or more dispersed droplet monomers are polymerized into a continuous, generally aqueous, dispersing phase. The combination of vigorous shaking and the use of one or more suspending agents keeps the droplets suspended and prevents agglomeration. In this heterogeneous reaction process, there is also the participation of a soluble initiator in the monomer. BPO and AIBN are examples of the most commonly used initiators. Suspending agents, which prevent the coalescence of suspended organic droplets in the continuous phase, may be a water-soluble polymer, such as PVA, or water-insoluble inorganic compounds, such as calcium phosphate (87,88).

Similarly, suspension polymerization is a mass polymerization that occurs within the suspended monomer droplet; that is, each drop consists of a mass polymerization microreactor. This polymerization process can be described as a three-step process. First, the organic and aqueous phases are mixed and both agitation and suspending action stabilize the dispersion of droplets containing the monomer. Then a dynamic equilibrium known as coalescence-breakage is developed. This equilibrium is a function of the shaking characteristics. Near the agitator there is a zone of high shear stress, where particle breakage predominates, while distant from the impeller predominates coalescence. The relative rates of breakage and coalescence determine the final particle size. Finally, these phenomena cease when the droplets reach such high viscosity that they become solid polymer particles of constant size, reaching the particle identification point (87,88).

During suspension polymerization reactions, other compounds or fillers may be introduced to modify the material properties. A simple way to promote incorporation of these materials is to dissolve or suspend the additional material in the monomer charge. X-ray contrasts and modifiers are examples of additional loads used in bone cement manufacturing (89,90).

The final product is obtained as spherical particles of relatively homogeneous size and shape. As the particles formed are relatively large (characteristic diameters typically in the range of 20 to 2000 μm), separation of the final product occurs by sedimentation and filtration. This size range also allows the recovery of particles obtained by aqueous or gaseous stream, resulting in low separation costs. At the end of suspension polymerization, it is also possible to perform vacuum expansion of the obtained particles to produce lower density particles suitable for applications such as thermal and mechanical insulation (styrofoam) (87,88).

The suspension polymerization process has the following advantages (10):

• Ease of heat removal and formation of low viscosity heterogeneous mixtures due to the low viscosity of the dispersed phase;
• Low levels of impurities and product separation costs due to the use of few components in the recipe and high particle settling speed;
• Ease in controlling the final average particle size;
• The particle size ranges that can be produced are wide, allowing for a wide variety of applications.

The main disadvantages of this process are as follows (10):

• Fouling and loss due to material build-up on the reactor walls, which impairs the thermal performance of the process;
• Water, which is the dispersing agent, occupies 50 to 60 % of the reactor's usable volume, resulting in reduced productivity compared to mass polymerization.

2.8.1 Suspending agent

The suspending agent or stabilizing agent acts directly on the morphology and particle size distribution. This substance acts at the water monomer interface, reducing surface tension and promoting the dispersion of monomer drops. Thus, the thin layer produced prevents uncontrolled coalescence. The suspending agent affects

the balance breaking coalescence by shifting the particle size to smaller values. Normally, the amount of stabilizers used corresponds to 0.1 % of the total amount of water used, although larger amounts may be used (87).

Partially water-soluble polymers, water-insoluble inorganic compounds and mixtures thereof are the main types of suspending agent used. In the first type, the most common examples are PVA, hydroxypropyl cellulose and sodium polystyrene sulfonate. The most commonly used inorganic compounds are hydroxyapatite, barium sulphate, kaolin, magnesium carbonate and magnesium hydroxide. These inorganic salts are cheaper than polymeric suspending agents, have less environmental impact and are easily removed by washing the reaction medium (88).

2.8.2 Initiator

Polymerization of vinyl monomers generally occurs through the free radical mechanism. These radicals can be generated by various mechanisms, with the aid of thermal, photochemical or oxirreduction methods. The initiator is a chemical specie sensitive to these methods, which generates free radicals when decomposed (73). Among these methods, thermal decomposition is the most employed because it is easily accessible and inexpensive. Use requires adjusting the temperature of the reaction medium to the half-life of the selected initiator. In this case, the half-life concept is defined as the time required for 50 % of the initiator mass to decompose at the specified temperature. The most commonly used initiators are benzoyl peroxide (BPO), which has low cost, and azocompounds, important when minimizing the content of branches (73).

Free radicals are very reactive and unspecific species; therefore, they remain stable for a very short time in the solvent, monomer or polymer. If there is resistance to diffusion of these species in the reaction medium, the combination or termination of these radicals may occur even before they start the monomers. This resistance reduces the efficiency of the initiator, characterizing the cage effect (73).

In suspension polymerization, the initiator employed is soluble in the organic phase (oil soluble initiator). Usually, the initiator feed into the system is accomplished by dissolving the monomer charge. The amount used is typically in the range of 0.1 to 0.5 % of monomer mass (73).

2.8.3 Mechanical agitation

Mechanical agitation causes various effects on the reaction medium. Increased stirring speed improves contact between mixture components and heat transfer. However, this increase raises the breakage rate of the droplets and decreases the protective layer formed by the suspending agent. Thus, at slower speeds, average sizes are larger because of lower breakage rates; at very high speeds, average sizes may be larger because of higher coalescence rates induced by increased particle collision rates (10,73).

2.8.4 Gel and vitreous effects

Increased viscosity of the organic reaction medium leads to decreased mobility of the polymer chains and consequent drop in termination rates. This phenomenon is known as the gel effect, Trommsdorf effect or Norrish-Smith effect. As a consequence, it is possible to observe the acceleration of the reaction rate when the conversion reaches 20 to 40 %, in which the reaction rate is usually reduced by the consumption of reagents. The gel effect causes an increase in the concentration of radicals and, consequently, in reaction rates, and may also hinder the thermal control of the process. In addition, it can increase the amplitude of particle size and molar mass distributions (10,73).

The vitreous effect, quite common in radical polymerization, occurs when propagation rates are affected by diffusional resistances. Therefore, this effect is expressive at high conversions, at which point the monomers have very low mobility. As the conversion increases, the fraction of the polymer phase also

increases and the medium gradually changes to the solid (vitreous) state. Naturally, the glass transition temperature (Tg) increases with increasing monomer conversion. When the Tg of the obtained polymeric mixture exceeds the reaction temperature, the molecular mobility of the medium is reduced, significantly decreasing the reaction rate and polymerization may cease. On the other hand, when the polymerization is performed at a temperature lower than Tg of the obtained material, there is a sudden decrease in the reaction propagation constant due to the lower mobility of monomers in the dispersed phase (10).

2.8.5 Retarding and inhibition effects

Some substances may inhibit polymerization by reacting with the radicals produced and eliminating or reducing the action of these intermediates. Substances that completely stop polymerization until consumed are called inhibitors. Those that reduce the polymerization rate by deactivating the propagating radicals are known as retarders. This reduction results in lower molar mass polymers. Impurities present in the monomer may also act as inhibitors or retarders (79). Some examples of substances that retard VAc polymerization are phenols, hydroquinone, nitrobenzenes and aniline (80). Phenols, for example, are considered as poor polymerization inhibitors and even act as accelerants in the ATRP (Atom transfer radical polymerization) of methyl methacrylate (91).

Retarders are species that deactivate the propagating radicals. Initiator-derived and propagating radicals show similar selectivity in their reactions and the distinction between inhibitors and retarders becomes a matter of concentration. A nitroxide, for example, would be considered an inhibitor when used in high concentration and a retarder, when at very low concentration. Moreover, inhibitors can be understood as a specie that is able to rapidly and efficiently scavenge propagating and/or initiator-derived radicals and consequently, to prevent polymer chain formation. A retarder is defined as a specie that slows rather than prevents polymerization. Ideally, inhibition and retardation phenomena can be divided in six steps: initiation,

inhibition, propagation, disproportionation, combination, retardation, and termination. In theory, after the initial reaction with inhibitor or retarder, these are the possible further pathways: i) slow reinitiation with reference to propagation following chain transfer; ii) slow propagation with reference to normal propagation following addition; iii) further reaction of the initially formed species as an inhibitor or retarder; iv) reversal of the reaction associated with inhibition or retardation. However, mechanism for inhibition is more complex than suggested in this sequence (91).

2.9 Radioiodination

Iodination is extensively used to obtain compounds of medical and biological interest. Iodination of a molecule is governed mainly by the oxidation state of iodine. In oxidized form, iodine binds strongly to various molecules, while in reduced form it does not. Normally, iodine is commercially available as sodium iodide (NaI), where iodide (I^-) is oxidized to iodonium (I^+) by various oxidizing agents. Hydrated iodonium ion (H_2OI^+) and hypoiodous acid (HOI) are believed to be the chemical species involved in electrophilic iodination processes. Iodination may occur by aromatic electrophilic substitution of hydrogen in the molecule of interest or by nucleophilic substitution when the iodide ion displaces an atom or a group from the substrate. Since the physicochemical properties of non-radioactive iodine and their radioisotopes are not distinct, these mechanisms also apply to radioiodination. The literature related to radioiodination does not mention the radioiodine as a radical species despite this radical is also as an electrophile (45,71).

Of the carbon-halogen bonds, the C-I bond is the weakest and susceptible to enzymatic cleavage. There are rare cases of patients with iodide hypersensitivity, even in strokes; Therefore, the presence of the free ion in the body should be avoided (92). Regarding the stability of iodine binding in molecules; amino and sulfhydryl groups bind to iodine, but these reactions are reversible (64,93). Aliphatic unsaturated fatty acids - for example oleic acid -, and neutral fats (triolein, for

example) may be partially iodinated; However, the presence of iodine saturates the double bond in these molecules, altering the chemical and biological properties (36,45). On the other hand, iodinated and iodo-vinyl aromatic compounds exhibit greater chemical stability *in vivo*, since iodine binds tightly and irreversibly to these compounds (94).

Nuclear Medicine is the area that most uses radioiodinated compounds. Molecules such as peptides, proteins and radioiodinated antibodies have been used in a wide range of applications for many years (95). Among the available radioisotopes, radioiodines have the highest synthetic versatility, as they can be used in the labeling of hydrophilic and lipophilic compounds by direct or indirect methods. Direct methods are those in which the hydrogen atom is replaced by a radioiodine atom. Indirect methods replace non-radioactive iodine, other atoms, or clusters in the molecule of interest with a radioiodine (64). It is desirable that the method used results in products with high specific activity. The unlabeled substrate present in formulations with low specific activity compromises radiopharmaceutical absorption in the tissue or organ of interest, due to the competition of both species by the same cellular mechanisms (36,45).

Labeling of molecules occurs through a conventional chemical reaction, such as synthesis, electro and nucleophilic substitutions, addition to double bonds, complexation and biosynthesis, for example (92,95). Labeling reactions follow physicochemical laws, but occur in sub-stoichiometric quantities. Generally, the concentration of radioisotope in the reaction medium is 10^6 to 10^9 times lower than that of the molecule to be labeled (36,93). Radioiodination is a type of labeling and the main methods used are: triiodide, iodine monochloride, isotopic exchange, chloramine-T, Iodogen® (1,3,4,6-tetrachlor-3α, 6α-diphenylglycoluril), iodo-beads, electrolytic, enzymatic, demetalation and conjugation. Generally, it is broken off from radioiodine in anionic form (radioiodide). After radioiodination, residual free radioiodide can be removed by precipitation, centrifugation, anion exchange, gel filtration or dialysis (45,71).

Among the existing methods for radioiodination of macromolecules such as peptides, proteins and antibodies, the following methodologies can be used: (i) directly, by the oxidation of the radioiodide by chloramine-T, Iodogen® or iodo-beads and subsequent electrophilic aromatic substitution in an activated aromatic ring (e.g. containing the hydroxyl group); (ii) indirectly, by the binding of a chemically active radioiodinated substance (Bolton-Hunter or *N*-succinimidyl-3-(4-hydroxy,5-iodophenyl)-propionate reagent) to a functional group present in the molecule to be labeled - this conjugation reagent forms the corresponding amides with primary amines; (iii) indirectly, by isotopic exchange, if the molecule to be labeled already contains an iodine atom. With respect to nanoparticle radioiodination, Bolton-Hunter reagent is the most commonly used; However, direct radioiodination has also proven to be efficient. Figure 2.15 presents a summary of the most commonly used strategies for radioiodination (94).

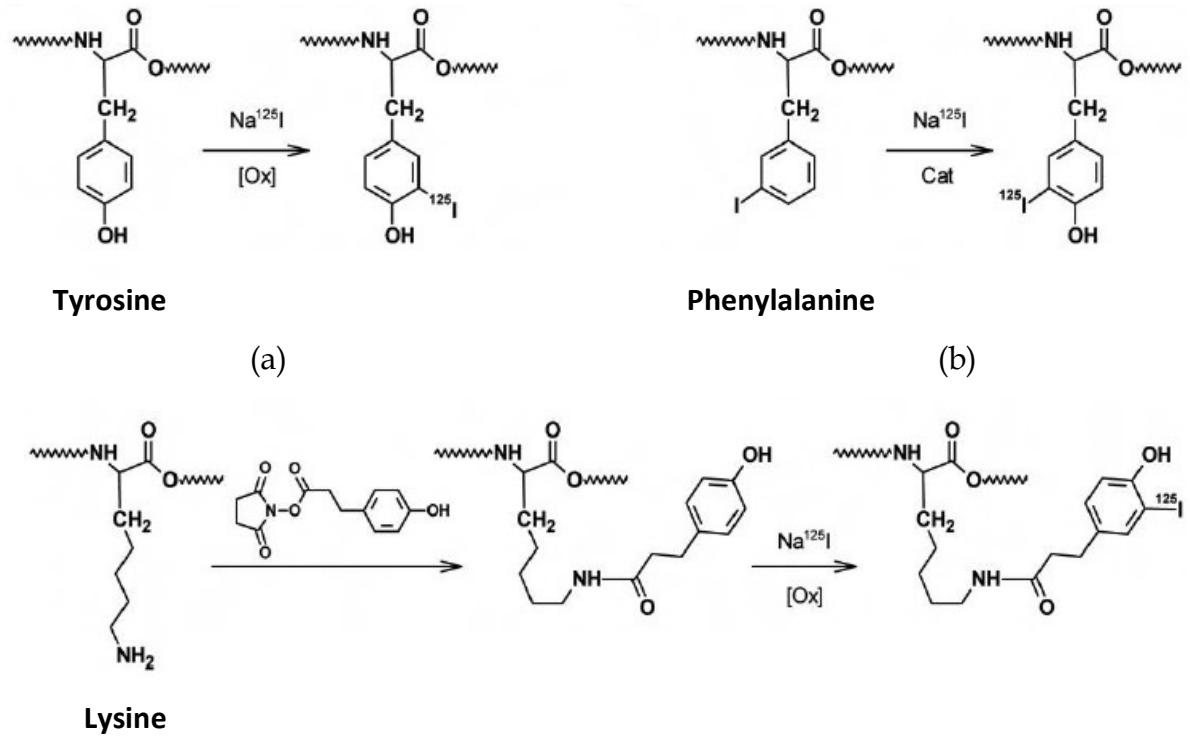

(a) (b) (c)

Figure 2.15: Schematic representation of the main strategies used for protein radioiodination: (a) electrophilic substitution, (b) isotopic exchange and (c) indirect

radioiodination. Ox = oxidant. Cat = catalyst. Adapted from Roig, Gómez Vallejo, Gibson (94).

Coenen, Mertens and Mazière (45) reported that the choice of radioiodination methodology should consider parameters such as the chemical structure of the molecule to be labeled and the reaction conditions, for example. The authors also highlighted the following aspects as relevant to these operations:

- Knowledge of the pharmacological and toxicological properties of the iodinated compound;
- Knowledge of the specific activity for diagnosis or therapy;
- Radioiodine incorporation site;
- Stability *in vivo*;
- Labeling in a few hours and preferably in a single step;
- High labeling yields due to the high cost of radioiodine.

Of course, pharmacological, toxicological and *in vivo* stability studies are performed after the synthesis of a new radiopharmaceutical. However, these studies are not part of the scope of this thesis. In the United States, for example, once a radiopharmaceutical is successfully developed, its clinical efficacy must be evaluated by testing it first in animals and then in humans (36). For use in humans, an Investigative Exemption Claim Notice is required from the US Food and Drug Administration (FDA), which regulates human drug trials. If there are any serious adverse effects in humans due to administration or if the intended biodistribution is not obtained, the radiopharmaceutical is immediately discarded. In Brazil, the National Health Surveillance Agency (ANVISA) follows a very similar process (48).

Furthermore, the determination of the specific activity appropriate for the use of radioiodinated copolymer microspheres obtained herein will not be performed in this thesis either. Saha (36) reported that a combination of parameters must be performed for this determination. Radiopharmaceuticals should have a relatively short effective half-life so that they do not exceed the duration of the study in

question (metabolism or biodistribution, for example). The time to start imaging varies according to the type of study and radiopharmaceutical pharmacokinetics. The faster the radiopharmaceutical buildup, the sooner imaging should begin. However, the duration of imaging depends mainly on the amount of activity administered, the accumulated fraction in the target organ, and the camera gamma window setting.

Dewanjee (64) presented other parameters that should also be considered. Specific activity is related to the calculation of the target organ dose required for imaging. For this, the radiopharmaceutical biodistribution, variations of this parameter with time and excretion of the radiopharmaceutical in urine and feces should be studied in animal models. From these data, the clearance half-life of each organ should be obtained and the critical organ will be the one with the highest dose. The critical organ is expected to be the target organ. Radiation attenuation and scattering corrections as well as approximate radiation doses should be calculated from data obtained with a test object simulating human organs in weight and shape (phantom) and with the clearance data. The total dose in the critical organ should be obtained by considering the integral of radiopharmaceutical activity in that organ over time, the effective half-life (T_e), the organ mass, the fraction of radiation energy absorbed by the critical organ, and the constant of equilibrium dose. This constant represents the average energy released per unit of accumulated radiopharmaceutical activity, is dimensionless and obtained by the Monte Carlo mathematical method. Therefore, the specific activity value of radioiodinated copolymer microspheres should encompass this entire study to be defined and will not be covered in this work.

2.9.1 The iodo-beads

Electrophilic radioiodation is a process whereby a positively charged radioiodine attacks a system with high electron density, such as a double bond or an aromatic ring. Radioiodinated aliphatic substances are almost exclusively labeled by nucleophilic substitution; however, they play a minority role in Nuclear Medicine. Thus, almost all electrophilic radioiodination methods developed so far have focused

on obtaining radioiodoarenes. Mostly, the direct methods of radioiodine-deprotonation and radioiodine-demetallation, which are based on *in situ* oxidation of the radioiodide, are suitable for the radioiodation of substrates in high yield, also providing carrier-free radiopharmaceuticals (45).

This scenario shows that the use of oxidizing agents is extremely relevant for the success of arenes radioiodination. Coenen, Mertens and Mazière (45) report that iodine monohalides such as *N*-chloroamides, *N*-halosuccinimides, Iodogen® and peracids are the major classes of substances used in radioelectrophile formation. Each class has its own characteristics, advantages and disadvantages that should be evaluated during the selection of the oxidizing agent for radioiodination of molecules. Among these substances, the class of *N*-chloroamides comprises the sodium salts of the amides chloramine-T (CAT) or *N*-chlorosulfonic acid, which was the first used, chloramine-B (*N*-chloro-benzenesulfonic acid) and dichloramine-T (*N*,*N*-dichloro-p-toluenesulfonic acid). This class of relatively strong oxidants can lead to the formation of degradation by-products and chlorinated products. Therefore, it is recommended to work at low temperatures and to keep the oxidant concentration as low as possible. To circumvent these limitations, chloramine-T is immobilized on polymeric beads, commercially known as iodo-beads (Figure 2.16).

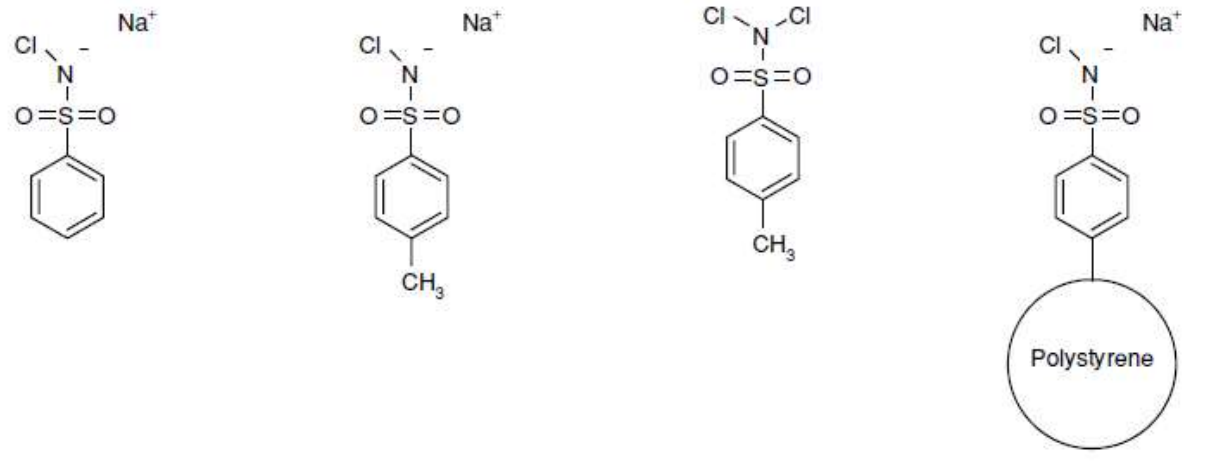

(a) (b) (c) (d)

Figure 2.16: Structures of (a) chloramine-T (CAT), (b) chloramine-B, (c) dichloramine-T and (d) iodo-beads. Adapted from Coenen, Mertens, Mazière (45).

Iodo-beads are presented in the form of water-insoluble, non-porous polystyrene spheres, 23 mm in diameter, functionalized with chloramine-T oxidant (45). The use of iodo-beads delays the release of oxidizing species and thus, the oxidant concentration in the medium is very low. Thus, the rate of the labeling reaction is slower as the appropriate oxidation environment for radioiodination exists only near the surface of the beads and not throughout the reaction medium (37). For these reasons, iodo-beads are used in radioiodination of substances sensitive to severe oxidation conditions, such as proteins and peptides. In these substances, the direct insertion of radioiodine occurs in the phenol moiety of tyrosine residues present in these molecules (Figure 2.17). In the labeling process, iodo-beads transform the radioiodide into a radioactive electrophile, which is inserted in the *ortho* position relative to the phenol group present in the aromatic ring by means of aromatic electrophilic substitution (95). The formation of radioelectrophile by iodo-beads occurs by a mechanism equivalent to CAT, in which the oxidant releases hypochlorous acid that leads the radioiodide to radioiodonium. Proteins and peptides are directly involved in numerous cellular mechanisms and, when labeled, allow the study of the metabolism of various processes *in vivo* (96,97).

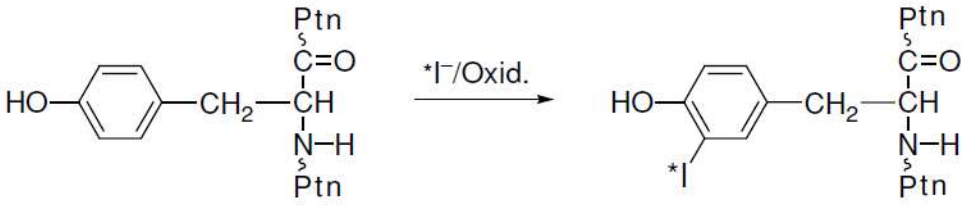

Figure 2.17: Example of phenolic protein radioiodination. * I = radioiodine. Oxid. = oxidizing agent. Adapted from Coenen, Mertens, Mazière (45).

When using iodo-beads, pH must be controlled to preserve proteins and peptides from denaturation and consequently, radioiodinated side-products. According to the literature, the optimum pH is 7 to 9. In addition, as H_2OI^+ and HOI are considered to be the iodinating species, strongly acid or basic medium must be avoided to preserve the solubility of I+ in water that results in such species (36,45).

The advantages found in using iodo-beads are as follows (36,45,98,99):

• The size of the beads is small enough to fit in reaction microvessels, but large enough to be removed from the reaction medium with tweezers;
• They can be used in a reaction medium separate from the substrate to be radioiodinated, thus avoiding possible substrate degradation and consequent impurities;
• The step of eliminating the remaining oxidant by the addition of a reducing agent is not necessary as it is sufficient that the product obtained or the beads can be removed from the reaction medium;
• Normally, only 5 to 6 beads are required for radioiodination of 100 μg of protein or peptide.
• Radioelectrophile formation occurs in phosphate buffer medium for 15 min at room temperature;
• Protein and peptide radioiodination yields reach up to 99%;
• Iodo-beads act in the presence of azides, detergents, urea and high salt concentration;
• Iodo-beads remain stable for at least 6 months when stored in an amber bottle at 4 °C.

Disadvantages include (36,45,98,99):

• Ensure use in the absence of any reducing agents; otherwise there will be competition between the oxidation of the radioiodine and the present reducer;
• The use is limited to the aqueous medium;
• High cost when compared to chloramine-T reagent, older reagent used in the radioelectrophile formation.

2.9.2 Iodo-beads applications

Several direct protein radioiodination methodologies are available in the literature; however, the stoichiometry insertion of radioiodide in tyrosyl, histidyl and cysteinyl groups, for example, is not reproducible (95). This problem is not observed in the radioiodination of tyrosine and histidine phenolic residues, when the reaction occurs at pH 7.4 and in the presence of chloramine-T as oxidant. However, the main disadvantage of this method is related to the intense contact of this reagent with the protein to be labeled, which can result in chlorination, polymerization, macroaggregate formation and methionine oxidation, for example (45).

To circumvent these complications, the iodo-beads oxidant has been developed. Markwell (98) was the first to report the use of this reagent for the ^{125}I labeling of antiporcine insulin antiserum. The author reported that the efficiency of radioiodine incorporation by iodo-beads (99 %) and the recovery of the initial amount of protein (95 % for one unit and 92 % for six units of iodo-beads) were particularly remarkable, because under similar conditions, lactoperoxidase (oxidizing enzyme used in radioiodination) produces a 29 to 46 % incorporation. Furthermore, it states that the antiserum maintained its immunological ability to recognize insulin, even in the face of the high radioelectrophile activity produced by iodo-beads. The advantages reported by this author leave no doubt about the high reliability in the use of this oxidizing agent.

Consequently, further studies on the comparison between the use of CAT and iodo-beads have been performed. Lee and Griffths (99) were the first to experimentally evaluate the use of iodo-beads and CAT in the labeling of human ^{125}I α-fetoprotein. These authors report that while the use of CAT provides apparently 40 % higher yields than with iodo-beads, the latter comprises a simpler, controllable and milder method, which results in a more stable distribution of the product obtained. They also mentioned as a singular and important advantage in the use of this methodology flexibility in the labeling conditions such as time (2-15 min),

reaction medium (0.1 mol · L^{-1} phosphate or tris buffer, pH 5.5-8.5), presence or absence of azide, detergents, urea or high salt, temperature (from 4 °C to room temperature) and obtaining the desired yield. They recommended that iodo-beads may be a reliable alternative and replace CAT for the radioiodination of protein traces (e.g., less than 10 µg), routinely.

Tsomides and Eisen (100) described procedures for stoichiometric insertion of ^{125}I into peptides containing from 8 to 25 tyrosyl and/or histidyl residues. The specific activity obtained was 10 Ci · $mmol^{-1}$ ($3.7 \cdot 10^{11}$ Bq · $mmol^{-1}$) peptide. In this procedure, 4 units of iodo-beads are used in pH 7.0 buffer for tyrosine radioiodation or pH 8.2 for histidine or histidine and tyrosine radioiodination at 2-40 mCi ($7.4 \cdot 10^{7}$-$1.48 \cdot 10^{9}$ Bq) of $Na^{125}I$. The authors stated that the developed protocol can be applied to peptide radioiodination in which a chemically homogeneous product is desired. The use of a reliable and reproducible procedure is extremely important for routine commercial production of radiopharmaceuticals.

Choi et al. (101) prepared albumin-coated magnetic iron oxide and manganese nanoparticles by means of the crosslinking reagents of *N*-3-dimethylaminopropyl-*N*-ethylcarbodiimide and *N*-hydroxysulfosuccinimide. The obtained material was purified, labeled with ^{124}I (37 MBq or 1 mCi) using iodo-beads for 15 min and then centrifuged (Figure 2.18). The minimum yield obtained was 92 %. The authors successfully developed multifunctional nanoparticles for combined PET/MR imaging, in which two different types of lymph nodes were clearly identified and precisely located.

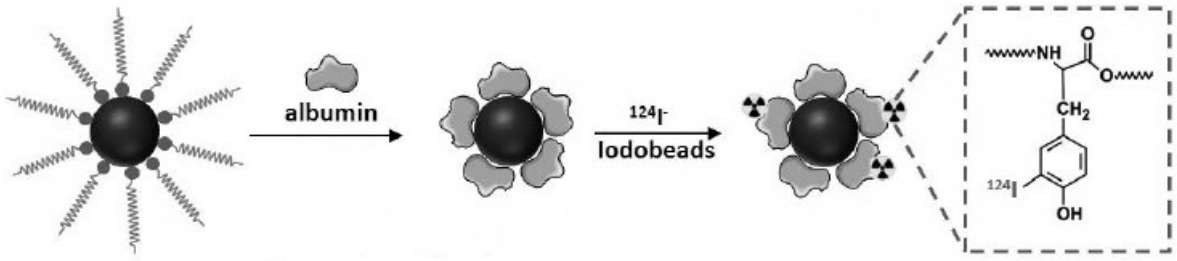

Figure 2.18: Illustrative scheme of radioiodation. Adapted from Roig, Gómez-Vallejo, Gibson (94).

Wager and Jones (37) reported that despite problems reported in the literature on CAT use, their application is still current for radioiodination of substances such as benzamides and iodophenyl metomidate, with yields of 50-95 % for radioiodine incorporation (Figure 2.19). The use of CAT in these reactions has as its main advantage the cost reduction and as the main disadvantage, the large variation in the labeling yield. This variation is, for example, an impediment to the routine and reliable obtaining of these substances for use as radiopharmaceuticals.

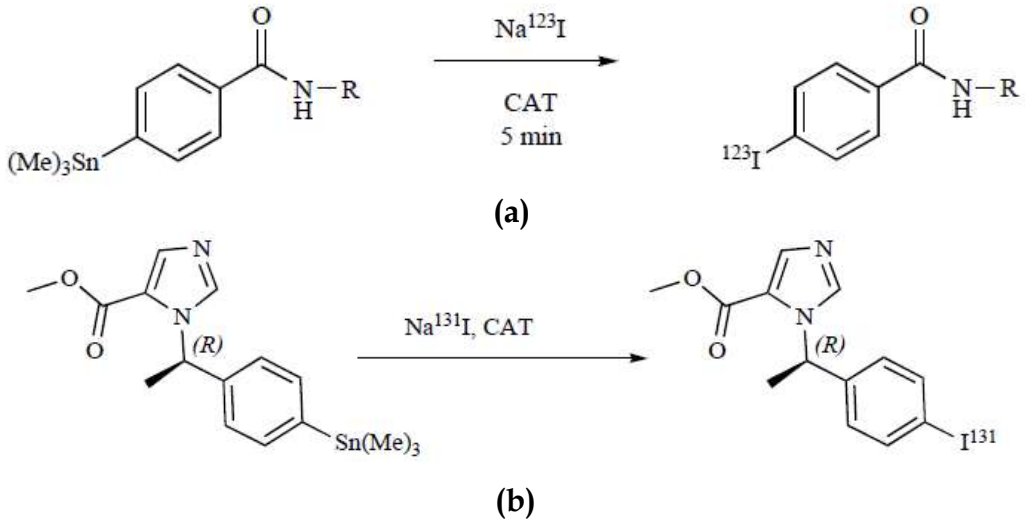

Figure 2.19: Example of benzamide (a) and iodophenyl metomidate radioiodination using CAT at room temperature. Adapted from Wager and Jones (37).

Wager and Jones (37) also mentioned the use of iodo-beads for enantioselective labeling of ^{125}I benzodiazepines (Figure 2.20). This labeling resulted in high specific

activity (2000 Ci · mmol^{-1}), which demonstrates the successful use of this reagent in high yield labels and without the formation of side products for substrates of high isomeric specificity.

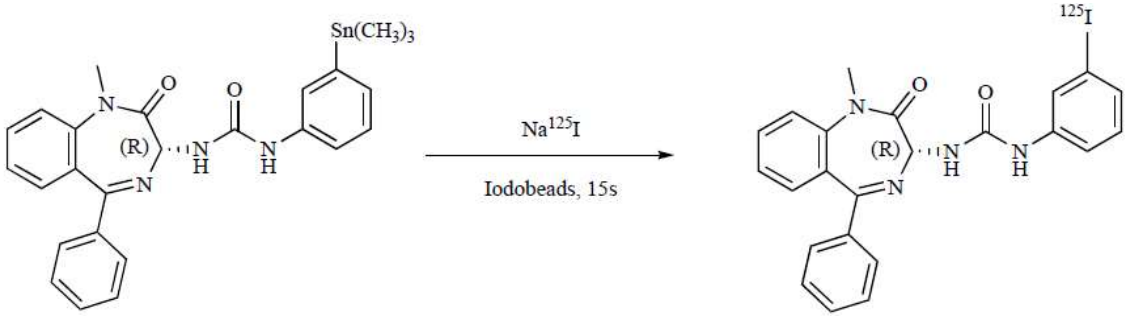

Figure 2.20: Example of benzodiazepine radioiodination using iodo-beads. Adapted from Wager and Jones (37).

Metals such as silver can also be radioiodinated by iodo-beads. Chrastina and Schnitzer (102) synthesized silver nanoparticles from the reduction of silver nitrate, using poly(*N*-vinyl 2-pyrrolidone) as a reducing agent and also as a polymeric matrix for the coating of these particles. They then incorporated ^{125}I into the surface of these silver nanoparticles for biodistribution studies and SPECT imaging. In this work, iodo-beads were used to transform radioiodide into a radioactive electrophile for incorporation of this compound on the particle surface. In this reaction, 1 mCi ($3.7 \cdot 10^7$ Bq) of ^{125}I was oxidized at room temperature for 10 min. The solution was removed and added to the silver nanoparticle dispersion (2.5 mg) in pH 6.0 buffer. The reaction medium was protected from light and the mixture was stirred at 10 rpm for 30 min. The obtained material was purified by size exclusion chromatography. The obtained yield was 80 % and the specific activity obtained was 0.4 0.6 μCi · μg^{-1}. The authors concluded that this material has potential for use in the diagnosis of liver tumors. Poly(*N*-vinyl 2-pyrrolidone) is a weak reducing agent and therefore did not affect the preference of the radioelectrophile for silver.

Khanna et al. (103) used iodo-beads to insert ^{125}I into the protein called fibroblast-1 growth factor. This molecule promotes neovascularization in cells such as fibroblasts and endothelial progenitor cells. With this labeling, the authors studied the release

behavior of this encapsulated substance in poly-L-ornithine coated alginate microcapsules over time by measuring the activity of the labeled protein in a radioactivity detector. Thus, they concluded that these microcapsules can be used for encapsulation and site-specific delivery of this protein. Labeling yield or any other results regarding the use of iodo-beads have not been mentioned.

Blois, Chan and Breeman (104) performed a new comparison between the use of CAT and iodo-beads to label 70 moles of DOTA-TATE, that is a peptide containing tyrosine residue, with ^{125}I. In this study, the reaction kinetics of the iodinated and radioiodinated substrates was investigated as a function of reaction time and reagent concentration in order to optimize peptide radioiodination. The authors observed that the obtained yield (39 %) was very similar for both oxidants. Although the use of iodo-beads with larger amounts of peptide resulted in higher labeling yield, the di-radioiodide peptide was obtained, which is not interesting for *in vivo* studies because biodistribution may be compromised.

The use of iodo-beads in the phenol group radioiodination aroused interest in the use of this oxidant in polymers that contain this function. Simone et al. (96) prepared poly(4-vinylphenol) nanoparticles by solvent diffusion to obtain spherical particles suspended in water. The nanoparticles were radioiodinated (^{124}I or ^{125}I) using iodo-beads reaching 90 % yield. At the end of the reaction, the beads of this oxidizing agent were removed from the reaction medium and the labeled nanoparticles were functionalized with different monoclonal antibodies (Figure 2.21). Residual radioiodide was separated by centrifugation. Then, the activity of the particles and the supernatant were measured in a radioactivity detector. The nanoparticles obtained were successfully used to obtain real-time images of the surface of the endothelial cells in the blood vessels, thus allowing the study of physiological and pathological changes of the vascular system.

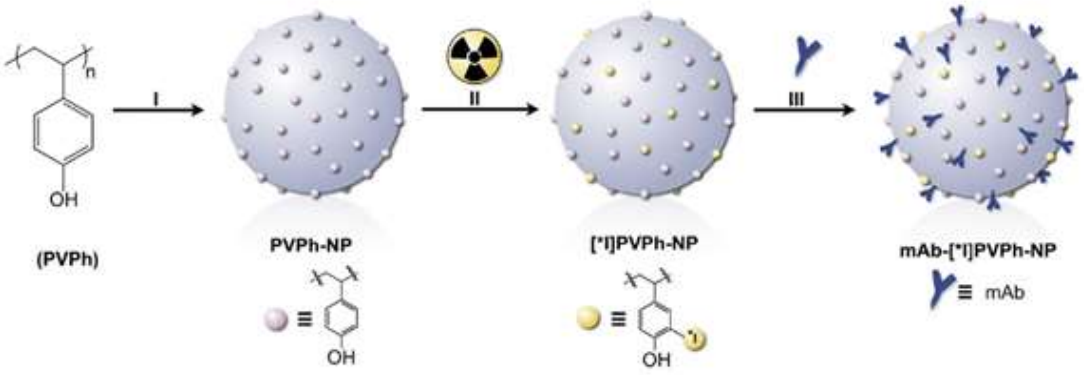

Figure 2.21: Illustrative scheme of obtaining poly(4-vinylphenol) nanoparticles (PVPh-NP) by solvent diffusion (I), subsequent direct labeling (II) with radioiodine (*I) and functionalization of the antibody compound (mAb) by adsorption (III). Adapted from Simone et al. (96).

Lee et al. (97) developed nanoparticles to obtain images with different techniques (980 nm laser luminescence, MR and PET) and to study the angiogenesis of the U87MG (Uppsala 87 Malignant Glioma) tumor cell model. Particles composed of gadolinium, ytterbium and europium hexagonal crystals (NaGdF4: Yb^{+3}/Er^{+3}) are a type of Upconversion nanophosphors (UCNPs) that have magnetic and fluorescent properties. In this research, the authors proceeded from a cyclic dimeric peptide based on RGD (arginine-glycine-aspartic acid chain), conjugated it to UCNP, coated the obtained compound with poly(ethylene glycol) and tagged tyrosine residue with ^{124}I using iodo-beads. The obtained compound was purified by membrane filtration. The labeling reaction lasted 1 h (an atypical duration), yielded 19 % yield, with specific activity of 0.88 GBq, without the formation of aggregates or precipitation of nanoparticles. In addition, the PET images obtained were satisfactory, despite the low labeling yield. According to the authors, the other images were also successfully obtained and, therefore, this compound has great potential for obtaining three different images for the specific diagnosis of cancer.

Another substance had its efficiency compared to iodo-beads. Russell et al. (105) studied the insertion of ^{125}I into Annexin V protein with iodo-beads and Bolton-Hunter reagent, with 21 % and 50 % yield, respectively. This protein

participates in the mechanisms of apoptosis (programmed cell death) and, when labeled, may assist in the *in vivo* monitoring of this process by SPECT images. In addition to the low yield, unlike that observed with Bolton-Hunter reagent, free radioiodide accumulated in the thyroid gland when Annexin V was labeled with iodo-beads. *In vivo* deiodination has exposed this gland to an unnecessary dose. For these reasons, it was clear that iodo-beads did not perform at their best and therefore was not recommended as a radioiodination method for this particular protein.

The iodo-beads radioiodination method does not require the use of reducing agents in the elimination of the remaining oxidant. Also, by using iodo-beads, the separation of the oxidant from the reaction medium is easy, the duration of radioelectrophilic formation is short, and the possibility of achieving high labeling yield is increased. Moreover, labeling reproducibility is achieved and the possibility of formation of secondary products or degradation of the obtained microspheres is remote. These were the main factors that led to the selection of iodo-beads as the oxidizing agent to perform radioiodination studies in this thesis. In addition, the success achieved with this reagent in different radioiodinations reported in the literature ratified this decision. Although there is tremendous flexibility in reaction conditions for iodo-beads radioiodination, the procedure to be used in this thesis will be that recommended by the reagent manufacturer (99).

2.10 Special cares with radioactivity

It is noteworthy that procedures involving the use of ionizing radiation require special care. At the laboratory level, the manipulated activities usually range from $3.7 \cdot 10^5$ Bq to $3.7 \cdot 10^7$ Bq (10 μCi to 1 mCi), for example (17,64). This range of activity not only provides detection measurements with good reliability, but also do not exceed dose limits. Radioactivity detectors used to investigate possible contamination are extremely sensitive to the presence of gamma-type radiation, which aids in the safe conduct of experiments with ^{123}I, for example (Figure 2.22).

Figure 2.22: Example of Geiger detector model 7013 with pancake probe made in Nuclear Engineering Institute.

Lead barrier shield as well as exhaust hoods containing a carbon filter or HEPA (High Efficiency Particulate Arrestance) are also indispensable devices for radioactive material practices, especially when the material handled is liquid and will be subjected to stirring and/or heating (Figure 2.23). The use of personal protective equipment such as cotton coats, gloves and glasses are also extremely necessary. All these precautions were taken during the polymeric microsphere radioiodination experiments.

Figure 2.23: Example of L-shaped apparatus made of lead and lead glass. Adapted from Aurea Medic (106).

Moreover, it is imperative to wear disposable gowns, a pair of gloves (surgical latex gloves), caps, glasses and shoe covers while performing radioiodination experiments. Immediately after each simple procedure, possible contaminations must be

monitored using Geiger-Müller detector over gloves and arms. If positive, the gloves must be wrapped in a polyethylene bag and placed in properly labeled radioactive waste containers to be disposed as soon as possible. Liquid radioactive waste or washing of contaminated glassware and equipment must be storage in a capped polyethylene or glass flask for further disposal. If skin contamination occurs, the area must be washed vigorously with water and soap. The laboratory must contain a stock solution containing sodium thiosulfate 0.1 $mol.L^{-1}$, sodium hydroxide 0.1 $mol.L^{-1}$, and sodium iodide 0.1 $mol.L^{-1}$. In the case of radioiodine solution spilling, this solution must be used to cover the spilled area. Neither acidic solutions nor detergents can be used in radioiodine decontamination. This safety measure prevents oxidation and further spread of radioiodine into the laboratory air (64).

For workers in the nuclear field, the Radiation Protection services establish procedures that promote the safe use of radioactive materials in such a way that exposure levels to ionizing radiation do not exceed the limits of dose recommended by the International Commission on Radiation Protection (ICRP). In Brazil, the National Commission of Nuclear Energy (CNEN) applies more restrictive limits than those stablished by the ICRP. The patient exposure arises from a person as part of a treatment or diagnosis. There is no dose limit for patient exposure, this is determined by medical need, however, it is recommended to use the minimum dose as possible. A text that provides an overview of the concepts of Radiological Protection in a very didactic way is presented by Tauhata et al. (107). Reading this book is highly recommended for beginners in the nuclear field.

2.11 Final remarks

This literature review shows that micrometric polymer particles have been widely applied in Medicine. Polymeric microspheres may contain different substances or elements that give them unique or multiple characteristics. Therefore, this material may be used as embolization agent, chemoembolization agent or radioembolization agent for diagnostic or therapeutic purposes. Drugs, magnetic or radioactive

elements may be inserted into the polymeric matrix of the embolization agent to promote blood vessel embolization and treatments in the occlusion site.

As new studies on these agents are performed, new dimensions in their applications emerge, ratifying the applicability of the material and opening new markets. The stimulus for this development can be attributed to the benefits obtained, for example, with the use of polymeric microspheres for the treatment of brain and uterine tumors, with minimal side effect for the patient and the preservation of the organ's functions subjected to embolization. In addition, as a minimally invasive therapy, embolization is highly attractive as it reduces costs and risks when compared to conventional surgical intervention.

Regarding the images obtained during the embolization procedure, it was shown in this review that the imaging techniques used do not include those used in Nuclear Medicine, which are admittedly more sensitive and of better resolution. Inserting a radioisotope into an embolization agent that enables the use of these imaging techniques may change this scenario. Therefore, the chemical, nuclear and commercial characteristics of ^{123}I are an interesting option, since the presence of this radioiodine in PVAc microspheres would enable SPECT images to be obtained using the Nuclear Medicine Services in Brazil.

Among the available synthesis methodologies, suspension polymerization and the use of iodo-beads for the radioiodination were the selected methodologies to obtain the radioiodinated embolization agent. It is noteworthy that to obtain this innovative material, the 4VPh comonomer was selected because it presents suitable and the simple structural characteristics to be copolymerized with VAc and radioiodinated. Preference has been given to practical methodologies and the use of non-toxic substances, as it is intended to obtain a radioactive material for human application. In this way, the use of other types of more complex polymerization - such as ionic polymerization or polymerization via RAFT (Reversible Addition-Fragmentation chain Transfer) – that require longer time, higher number of steps and toxic reagents

were disregarded as they would imply a higher dose of ionizing radiation to obtain the final product and higher toxicity.

Finally, the results of searches conducted with the Web of Science database showed no reports in the literature about 4VPh polymerization with VAc, 4VPh iodination or radioiodination, and the use of 4VPh in embolization agents. Therefore, the present work presents a high degree of originality. In addition, the importance of developing this thesis is to improve imaging during the embolization procedure, which can be of high value to the interventional radiologist and the patient.

References

[1] Vaidya, S., Tozer, K. R., Chen, J. An Overview of Embolic Agents. Seminars on Interventional Radiology, v. 25, pp.204-215, 2008.

[2] Medsinge, A., Zajko, A., Orons, P., Amesur, N. Santos, E. A Case-Based Approach to Common Embolization Agents Used in Vascular Interventional Radiology American Journal of Roentgenology v.203, pp.699-708, 2014.

[3] Hamoudeh, M., Salim, H., Barbos, D., Paunoiu, C., Fessi, H. Preparation and characterization of radioactive dirhenium decacarbonyl-loaded PLLA nanoparticles for radionuclide intra-tumoral therapy. European Journal of Pharmaceutics and Biopharmaceutics, n. 67, pp. 597–611, 2007.

[4] Memon, K., Lewandowski, R. J., Mulcahy, M. F. , Riaz, A., Ryu, R. K., Sato, K. T., Gupta, R., Nikolaidis, P., Miller, F. H., Yaghmai, V., Gates, V. L., Atassi, B., Newman, S., Omary, R. A., Benson, A. B. 3rd, Salem, R. Radioembolization for Neuroendocrine Liver Metastases: Safety, Imaging, and Long-Term Outcomes. International Journal of Radiation Oncology Biology Physics, v.83, n.3, pp. 887-894, 2012.

[5] Sangro, B., Iñarrairaegui, M., Bilbao, J. I. Radioembolization for hepatocellular carcinoma. Journal of Hepatology v.56, pp.464-473, 2012.

[6] Kritzinger, J., Klass, D., Ho, S., Lim, H., Buczkowiski, A., Yoshida, E., Liu, D. Hepatic embolotherapy in interventional oncology: Technology, techniques, and applications. Clinical Radiology, n. 68, p. 1-15, 2013.

[7] Kennedy, A. Radioembolization of hepatic tumors. Journal of Gastrointestinal Oncology, v.5, n.3, pp.178-189, 2014.

[8] Berenstein, A., Russel, E. Gelation Sponge in Therapeutic Neuroradiology: A Subject Review. Radiology, v. 141, pp. 105-112, 1981.

[9] Pfizer, Folheto de instruções - Gelfoam® hemostático absorvível. Disponível em: <http://www.pfizer.com.br/sites/g/files/g10010996/f/product_attachments/Gelfoam.pdf>. Access in 27 oct 2017.

[10] Santos, D. P. Produção de partículas de poli(acetato de vinila) (PVAc) e poli(acetato de vinila-co-metacrilato de metila) (PVAc-co-PMMA) para imobilização de L-asparaginase, BSA e Lisozima. 2014. 201p. Tese (Doutorado em Engenharia Química) – COPPE, Universidade Federal do Rio de Janeiro, Rio de Janeiro, 2014.

[11] Conroy, R. M., Lyons, K. P., Kuperus, J. H., Juler, G. L., Joy I., Pribram, H. F. W. New Technique for Localization of Therapeutic Emboli Using Radionuclide Labeling American Journal of Roentgenology v. 130, p.523-528, 1978.

[12] Vijayalakshmi, M. A. Biochromatography: Theory and Practice. United States of America: Taylor & Francis. 2003.

[13] Peixoto, L. S., Silva, F. M., Niemeyer, M. A. L., Espinosa, G., Melo, P. A., Nele, M., Pinto, J. C. Synthesis of poly(vinyl alcohol) and/or poly(vinyl acetate) particles with spherical morphology and core-shell structure and its use in vascular embolization. Macromolecular Symposia, v. 243, p. 190-199, 2006.

[14] Sandler, S. R., Karo, W., Bonesteel, J-A., Pearce, E. M. Polymer Synthesis and Characterization United States of America: Academic Press 1998.

[15] Grindlay, J.H., Claggett, O.T. Plastic Sponge Prothesis for Use after Pneumonectomy: Preliminary Report. Mayo Clinic Proceedings, v. 24, pp. 1538-1539, 1949.

[16] Jack, C.R., Dewanjee, M.K., Brown, M.L., Forbes, G., Chowdury, S. Radiolabeled polyvinyl alcohol particles: a potential agent to monitor embolization procedures. International Journal of Radiation and Applied Instrument v.13, pp.235–243, 1986.

[17] Carvalheira, L. Desenvolvimento, otimização e validação parcial de método para determinação de pureza radioquímica da metaiodobenzilguanidina marcada com iodo 123 (123I MIBG). 2008. 157p. Dissertação (Mestrado em Química Analítica) – Instituto de Química, Universidade Federal do Rio de Janeiro, Rio de Janeiro, 2008.

[18] Cordeiro, C. F., Petrocelli, F. P. Vinyl Acetate Polymers Encyclopedia of Chemical Technology v.12, United States of America: John Wiley & Sons. 2002.

[19] Moulay, S. Molecular iodine/polymer complexes. Journal of Polymer Engineering, pp.1 55, DOI 10.1515/polyeng-2012-0122, 2013.

[20] Bartl, H., Muller, E. Methods of Organic Chemistry (Houben-Weyl), Macromolecular Materials, pp. 905–918, 1961.

[21] Oro, D., Machado, R. A. F., SAYER, C., ARAÚJO, P. H. H. Obtenção de poliacetato de vinila via polimerização em emulsão com baixa concentração de emulsificante. In: 8o Congresso Brasileiro de Polímeros, Águas de Lindóia, pp.977-978, 2006.

[22] Cision. Global Vinyl Acetate Monomer (VAM) Market for Polyvinyl Acetate, Polyvinyl Alcohol, Ethylene-Vinyl Acetate, Ethylene-Vinyl Alcohol and Other Applications - Forecasts to 2020. Available in < https://www.prnewswire.com/news-releases/global-vinyl-acetate-monomer-vam-market-for-polyvinyl-acetate-polyvinyl-alcohol-ethylene-vinyl-acetate-ethylene-vinyl-alcohol-and-other-applications---forecasts-to-2020-274937371.html > Access in 3rd nov 2017.

[23] Oliveira, M., Cirilo, L. C. M.; Nele, M.; Pinto, J. C. Synthesis of Spherical Core-Shell Poly(vinyl acetate)/Poly(vinyl alcohol) Particles for Use in Vascular Embolization: Study of Morphological and Molecular Modifications During Shell Formation. Polymer Engineering and Science, pp.2237-2244, 2015.

[24] Ferreira, G. R.; Segura, T.; Jr Souza, F. G.; Umpierre, A. P.; Machado, F. Synthesis of poly(vinyl acetate)-based magnetic polymer microparticles European Polymer Journal v.48, pp.2050-2069, 2012.

[25] Siepmann, J., Siegel, R. A., Rathbone, M. J. Fundamentals and Applications of Controlled Release Drug Delivery United States of America: Elsevier, 2012.

[26] Oliveira, M.; Melo, P. A. Jr., Nele, M., Pinto, J. C., In-Situ Incorporation of Amoxilicillin in PVA/PVAc-co-PMMA Particles during Suspension Polymerizations. Macromolecular Symposia v. 299/300 pp. 34-40, 2011.

[27] Oliveira, M., A. M. O., Melo, P. A. Jr, Pinto, J. C., Suspension Copolymerization of Vinyl Acetate and Methyl Methacrylate in the Presence of Amoxicillin. Macromolecular Reaction Engineering, v. 6, pp. 280-292, 2012.

[28] Dhaenens, K. Ethylene vinyl acetate as matrix for oral sustained release multiple-unit dosage forms produced via hot-melt extrusion. Dissertation (Masters of Industrial Pharmacy) Universiteit Gent, Belgium, 2010.

[29] Imam, S. K., Molecular Nuclear Imaging: The Radiopharmaceuticals (Review). Cancer Biotherapy & Radiopharmaceuticals, v. 20, n. 2, pp. 163-172, 2005.

[30] McRobbie, D. W.; Moore, E. A.; Graves, M. J.; Prince, M. R. MRI From Picture to Proton Second edition, United Kingdom: Cambridge University Press, 2006.

[31] Powsner, R. A.; Powsner, E. R. Essential nuclear medicine physics. 2nd ed. United States of America: Blackwell Publishing. 2006.

[32] Cherry, S.R.; Sorenson, J.A.; Phelps, M.E. Physics in Nuclear Medicine. 4th ed. China: Elsevier Saunders, 2012.

[33] Bushberg, J. T., Seibert, J. A., Leidholt Jr. E. M., Boone, J. M. The essential Physics of Medical Imaging 2nd ed. United States of America: Lippincott Williams & Wilkins, 2002.

[34] Thirteen Of Clubs. Available in <Visualhunt.com/CC BY-S>. Accessed in May 2017.

[35] Zimmermann, R. Nuclear medicine. France: EDP Sciences, 2007.

[36] Saha, G. B. Fundamentals of Nuclear Pharmacy. 5th ed. United States of America: Springer. 2004.

[37] Mariani, G., Bruselli, L., Kuwert, T., Kim, E. E., Flotats, A., Israel, O., Dondi, M., WATANABE N. A review on the clinical uses of SPECT/CT. European Journal of Nuclear Medicine and Molecular Imaging, v.37, n.10, p.1959-1985, 2010.

[38] Wager, K. M., Jones, G.B. Radio-Iodination Methods for the Production of SPECT Imaging Agents. Current Radiopharmaceuticals. v.3, p.37-45, 2010.

[39] Mattos, F. R. SPECT (Single photon emission tomography): Gama Câmara, Reconstrução Tomográfica e Características Funcionais. 2009. 46p. Bacharelado (Graduação em Física Médica) – Instituto de Biociências, Universidade Estadual Paulista, Botucatu, 2009.

[40] Gomes, C. M., Abrunhosa, A. J., Ramos, P., Pauwels, E. K. J. Molecular imaging with SPECT as a tool for drug development. Advanced Drug Delivery Reviews, n. 63, pp.547–554, 2011.

[41] Eckerman, K. F.; Endo, A. MIRD: Radionuclide data and decay schemes. 2nd ed. Reston: The Society of Nuclear Medicine, 2007.

[42] Martel, B. Chemical Risk Analysis: A practical Handbook. United Kingdom: Kogan Page Science, 2004.

[43] Catanoso, M. F. Purificação de 123I e 131I para marcação de biomoléculas. 2011. 99p. Dissertação (Mestrado em Tecnologia Nuclear) IPEN, São Paulo, 2011.

[44] Pozzo L., Coura Filho G., Osso Junior J.A., Squair P. L. O SUS na Medicina Nuclear do Brasil: avaliação e comparação dos dados fornecidos pelo Datasus e CNEN. Radiologia Brasileira, v.47, n.3, pp.141-148, 2014.

[45] Coenen, H. H., Mertens, J., Mazière, B. Radioiodination reactions for pharmaceuticals: Compendium for effective synthesis strategies United States of America: Springer, 2006.

[46] Miranda, S. M., Mesquita, E. T., Dohmann, H. F. R., Azevedo, J. C., Barbirato, G. B., Freire, F. L., Ribeiro, M. L., Nóbrega, A. C. L., Coimbra, A., Mesquita, C. T. Efeito do carvedilol a curto prazo na atividade simpática cardíaca pela cintilografia com 123I-MIBG. Arquivos Brasileiros de Cardiologia, v.94, n.3, pp. 328-332, 2010.

[47] World Health Organization, The medical uses of ionizing radiation and radioisotopes. Technical Report Series, n. 492, Geneva: World Health Organization, 1972. Available in <http://whqlibdoc.who.int/trs/WHO_TRS_492.pdf>. Access in 19 aug 2017.

[48] Agência Nacional de Vigilância Sanitária, Farmacopeia Brasileira. 5 ed. v. I e II, Brasília, Agência Nacional Vigilância Sanitária, 2010.

[49] Shanti, C. N., Gupta, Mahato, A. K. Traditional and emerging applications of microspheres: A Review. International Journal of Pharmacy Technology Research. v. 2, n.1, pp.675-681, 2010.

[50] Grallert, S. R. M., Rangel-Yagui, C. D., Pasqualoto, K. F. M., Tavares, L. C. Polymeric micelles and molecular modeling applied to the development of radiopharmaceuticals. Brazilian Journal of Pharmaceuticals Sciences, v.48, n.1, pp.1-16, 2012.

[51] de Barros, A. B., Tsourkas, A., Saboury, B., Cardoso, V. N., Alavi, A. Emerging role of radiolabeled nanoparticles as an effective diagnostic technique. EJNMMI research, v.2, i.1, p.39, 2012.

[52] Poliak, A.; Ross, T.L. Nanoparticles for SPECT and PET Imaging: Towards Personalized Medicine and Theranostics. Current Medicinal Chemistry, n.25, p.4328-4353, 2018.

[53] Costa, R. F., Azevedo, M. B. M., Nascimento, N., Sene, F. F., Martinelli, J. R., Osso, J. A. production of microspheres labeled with Holmium-166 for liver cancer therapy: The preliminary experience at IPEN-CNEN/SP, In: International Nuclear Conference – INAC, Rio de Janeiro, RJ, 2009.

[54] Uliel, L. et al. From the Angio Suite to the gamma-Camera: Vascular Mapping and Tc 99m-MAA Hepatic Perfusion Imaging Before Liver Radioembolization - A Comprehensive Pictorial Review. Journal of Nuclear Medicine, v. 53, n. 11, p. 1736-1747, 2012.

[55] Song, J., Suh, C.H., Park, Y.B., Lee, S.H., Yoo, N.C., Lee, J.D., Kim, K. H., Lee, S. K., A phase I/IIa study on intra-articular injection of holmium-166-chitosan complex for the treatment of knee synovitis of rheumatoid arthritis. European Journal of Nuclear Medicine, n. 28, pp. 489–497, 2001.

[56] Parka, Y. J., Leea, J. Y., Chang, Y. S., Jeon, J. M., Chung, J. K., Lee, M. C., Park, K. B., Leea, S. J. Radioisotope carrying polyethylene oxide polycaprolactone copolymer micelles for targetable bone imaging. Biomaterials, n. 23, pp. 873-879, 2002.

[57] Luzzi, D. E., Smith, B. W., 2007, Nanoradiopharmaceuticals and methods of use. United State Patent Application Publication US 2007/0031327 A1, 2007.

[58] Koziorowskia, J., Stanciub, A.E., Gómez-Vallejoc, V., Llopd, J. Radiolabeled Nanoparticles for Cancer Diagnosis and Therapy. Anti-Cancer Agents in Medicinal Chemistry, n.17, p.333-354, 2017.

[59] Sheets, N. C., Wang, A. Z. Radioisotopes and Nanomedicine, Radioisotopes - Applications in Bio-Medical Science. Available in <http://www.intechopen.com/books/radioisotopes-applications-in-bio-medical-science/radioisotopes-andnanomedicine> Acces in 3 nov 2017.

[60] Wasserman, V. M. A., Orlando. M. M. C., Zubillaga, M., Sousa-Batista, A. J., AL-Qahtani, M., Santos-Oliveira, R. Nanoradiopharmaceuticals for Nanomedicine: Building the Future. Recent Patents on Nanomedicine, v.4, n.2, pp.90-94, 2014.

[61] Anselmo, A. C., Mitragotri, S. Nanoparticles in the clinic. Bioengineering & Translational Medicine, v. 1, p.10-29, 2016.

[62] Clinical trials. Available in < https://clinicaltrials.gov/ct2/home> Access in 20th aug 2019.

[63] Gordon Jr., R. S. The preparation of radioactive polyvinylpyrrolidone for medical use. Journal of Polymer Science Part A: Polymer Chemistry, v.31, i.122, pp.191-192, 1958.

[64] Dewanjee, M. K. Radioiodination: Theory, Practice and Biomedical Applications United States of America: Springer Science + Business Media LLC 1992.

[65] Mitchell, M.L., Harden, A.B., O'Rourke, M.E. The in vitro resin sponge uptake of triiodothyronine-I131 from serum in thyroid disease and in pregnancy. Journal of Clinical Endocrinology and Metabolism, pp.1474-1483, 1960.

[66] Picard, L., Robert, J., Andre J.M., et al. Embolization with iodine 131-marked sponge: Technique, indications and results. Journal of Neuroradiology , v. 3, pp.53-74, 1976.

[67] Lang, E. K., Sullivan, J. Management of Primary and Metastatic Renal Cell Carcinoma by Transcatheter Embolization With lodine I25 Cancer, v.62, pp.274-282, 1988.

[68] Kumar, R., Roy, I., Ohulchanskky, T. Y., Vathy, L. A., Bergey, E. J., Sajjad, M., Prasad, P. N. In vivo biodistribution and clearance studies using multimodal organically modified silica nanoparticles. American Chemical Society Nano, v.4, i.2, pp. 699-708, 2010.

[69] Shao, X., Zhang, H., Rajian, J. R., Chamberland, D. L., Sherman, P. S., Quesada, C. A., Koch, A. E., Kotov, N. A., Wang, X. 125I-Labeled gold nanorods for targeted imaging of inflammation. American Chemical Society Nano, v.5, i.11, pp.8967–8973, 2011.

[70] Fritz, U., Fritz O., Gordy, T. A., Wojcik, R., Blümmel, J., Küller, A. Loadable polymeric particles for enhanced imaging in clinical applications and methods of preparing and using the same United States Patent Application 20150258224 A1, 2015. Available in < http://patft.uspto.gov/netacgi/nph-Parser?d=PALL&p=1&u=%2Fnetahtml%2FPTO%2Fsrchnum.htm&r=1&f=G&l=50&s1=9114162.PN.&OS=PN/9114162&RS=PN/9114162>.

[71] Kaiho, T. Iodine Chemistry and applications United States of America: Wiley, 2015.

[72] Tang, C., Edelstein, J., Mikitsh, J. L., Xiao, E., Hemphill, A. H., Pagels, R. Chacko A-M., PrudHomme, R. Biodistribution and fate of core-labeled 125I polymeric nanocarriers prepared by Flash NanoPrecipitation (FNP). Jornal of Materials Chemistry B v.4, pp.2428 2434, 2016.

[73] Odian, G. Principles of Polymerization. 4th ed. United States of America: Wiley Interscience. 2004.

[74] Clayden, J., Greeves, N., Warren, S. Organic Chemistry England: Oxford, 2012.

[75] Tezuka, Y., Araki, A. Synthesis of poly (vinyl alcohol)-graft-polystyrene. Makromolecular Chemie v.194, pp.2827-2837, 1993.

[76] Kiran, Y. B., Konakahara, T., Sakai N. Green Reagent for the Iodination of Phenols. Synthesis, n.15, pp.2327–2332, 2008.

[77] Bovonsombat P., Leykajarakul J., Khan C., Pla-On K., Krause M. M., Khanthapura P., Ali R., Doowa N. Regioselective iodination of phenol and analogues using N-iodosuccinimide and p-toluenesulfonic acid Tetrahedron Letters v.50, pp.2664–2667, 2009.

[78] Tajik, H., Dadras, A., Hosseini, A. Green and Efficient Method for the Iodination of Phenols in Water. Synthesis and Reactivity in Inorganic, Metal-Organic, and Nano-Metal Chemistry, v.41, i.3, pp.258-261, 2011.

[79] Bird R. A., Russel K. E. The effect of phenols on the polymerization of vinyl acetate. Canadian Journal of Chemistry v.4, pp.2123-2125, 1965.

[80] Lartigue-Peyrou, F. The use of phenolic compounds as free-radical polymerization inhibitors. Industrial Chemistry Library v.8, pp.489-505, 1996.

[81] National Center for Biotechnology Information. PubChem Compound Database; CID=62453, Disponível em <https://pubchem.ncbi.nlm.nih.gov/compound/62453> Accesso em 19 ago. 2016.

[82] Food Component Database. Available in <http://foodb.ca/compounds/FDB010540> Acces in 18 jul 2017.

[83] Kato, M. A research on Polymerization of 0-, m-, and p-Vinylphenol. Journal of Photopolymer Science and Technology v.21, n.6, pp.711-717, 2008.

[84] Sovish, R. C. Preparation and Polymerization of p-Vinylphenol. The Journal of Organic Chemistry v.24, i.9, pp.1345-1347, 1959.

[85] Kaneko, M. S-K, Noguchi, T., Oka, N. Process for preparing vinylphenol polymers and stabilized composiions of vinylphenol containing polymerization raw material United States Patent US005959051, 1999.

[86] Canevarolo Jr., S. V. Ciência dos polímeros: um texto básico para tecnólogos e engenheiros. 2a ed., São Paulo: Artliber Editora, 2006.

[87] Yuan, H. G.; Kalfas, G.; Ray, W. R. Suspension polymerization. Journal of Macromolecular Science - Reviews in Macromolecular Chemistry and Physics, v.31, n.2-3, pp.215-299, 1991.

[88] Dowding, P. J.; Vicent, B. Suspension polymerisation to form polymer beads. Colloids and Surfaces A: Physicochemical and Engineering Aspects, v.161, n.2, pp.259-269, 2000.

[89] Santos, J.R., J. G. F., Peixoto, L. S., Nele, M., Melo, P. A., Pinto, J. C. Theoretical and Experimental Investigation of the Production of PMMA-Based Bone Cement, Macromolecular Symposia, v.243, n.1, pp.1-12, 2006.

[90] Lemos, L., Nele, M., Melo, P. A., Pinto, J. C. Modeling of Bone Cement Production, Macromolecular Symposia, v.243, n.1, pp.13-23, 2006.

[91] G. Moad, D.H. Solomon. The Chemistry of Radical Polymerization 2nd ed. Elsevier, 2006.

[92] Baldwin, R. M. Chemistry of radioiodine. International Journal of Radiation Applications and Instrumentation. Part A. Applied Radiation and Isotopes v.37, i.8, pp.817-821, 1986.

[93] Finn, R. Chemistry applied to iodine radionuclides. Handbook of Radiopharmaceuticals: Radiochemistry and Applications. United Kingdom: John Wiley & Sons 2003.

[94] Roig J. L., Gómez-Vallejo, V., Gibson, P. N. Isotopes in nanoparticles: Fundamentals and Applications. United States of America: Taylor & Francis, 2016.

[95] Seevers, R.; Counsell, E. Radioiodination techniques for small organic molecules. Chemical Reviews. v. 82, pp.575-590, 1982.

[96] Simone, E. A., Zern, B. J., Chacko, A-M., Mikitsh, J. L., Blankemeyer , E. R., Muro, S., Stan, R. V., Muzykantov, V. R. Endothelial targeting of polymeric nanoparticles stably labeled with the PET imaging radioisotope iodine-124. Biomaterials, v.33, pp.5406–5413, 2012.

[97] Lee, J., Lee, T. S., Ryu, J., Hong, S., Kang, M., Im, K., Kang J. H., Lim, S. M., Park, S., Song, R. RGD Peptide–Conjugated Multimodal NaGdF4:Yb3+/Er3+ Nanophosphors for Upconversion Luminescence, MR and PET Imaging of Tumor Angiogenesis. Journal of Nuclear Medicine, v.54, pp.96–103, 2013.

[98] Markwell, M. A. A new solid-state reagent to iodinate proteins. I. Conditions for the efficient labeling of antiserum. Analytical Biochemistry. v.125, i.2, pp.427-432, 1982.

[99] LEE, S. G., KIM, J. P., KWON, I. C., SHIN, D. S., HAN, S. S., & LYOO, W. S. Preparation of poly(vinyl acetate) microspheres with narrow particle size distributions by low temperature suspension polymerization of vinyl acetate. **Journal of Applied Polymer Science**, v.101, pp.4064-4070, 2006.

[100] Tsomides, T. J., H. N., EISEN, Stoichiometric labeling of peptides by iodination on tyrosyl or histydil residues. Analytical Biochemistry. v. 210, pp.129-135, 1993.

[101] Choi, J. S., Park, J. C., Nah, H., Woo, S., Oh, J., Kim, K. M., Cheon G. J., Chang, Y., Yoo, J., Cheon, J. A hybrid nanoparticle probe for dual-modality positron emission tomography and magnetic resonance imaging. Angewandte Chemie International Edition, v.47, i.33, pp.6259 6262, 2008.

[102] Chrastina, A., Schnitzer, J. E. Iodine-125 radiolabeling of silver nanoparticles for in vivo SPECT imaging. International Journal of Nanomedicine, v.5, pp.653-659, 2010.

[103] Omaditya Khanna, Monica L Moya, Emmanuel C Opara, Eric M Brey. Synthesis of multilayered alginate microcapsules for the sustained release of fibroblast growth factor-1. J Biomed Mater Res A. v.95, i.2, p.632-640, 2010.

[104] Blois, E., Chan, H. S., Breeman, W. A. P. Iodination and Stability of Somatostatin Analogues: Comparison of Iodination Techniques. A Practical Overview. Current Topics in Medicinal Chemistry. v. 12, p.2668-2676, 2012.

[105] Russell J., O'Donoghue J.A., Finn R., Koziorowski J., Ruan S., Humm J.L., Ling C.C. Iodination of annexin V for imaging apoptosis, J Nucl Med., v.43, i.5, p.671-677, 2002.

[106] Aurea Medic. Available on <http://www.aureamedic.com.br/anteparo-em-l.html>. Accessed May 2019.

[107] Tauhata, L., Salati, I., Di Prinzio, R., Di Prinzio, M. A. R. R. Radioproteção e Dosimetria: Fundamentos. Instituto de Radioproteção e Dosimetria. 9ª revisão. Rio de Janeiro:IRD/CNEN, 2013.

CHAPTER 3

BULK POLYMERIZATION

SPECT is an imaging technique used for diagnostic purposes in Nuclear Medicine. SPECT provides images of superior quality to X-rays imaging techniques that are normally used during vascular embolization procedures. Vascular embolization is a minimally invasive technique used to reduce the size of a tumor by applying polymeric microspheres. Therefore, radioiodinated polymeric microspheres can be used for SPECT imaging during vascular embolization to make this procedure more efficient and safer. As phenolic compounds allow radioiodination in high yields, these substances can be selected for both copolymerization and radioiodination. In this work, we evaluate the copolymerization between vinyl acetate and 4-vinylphenol for further radioiodination. Respectively, bulk polymerization tests and conversion study showed that the 4-vinylphenol must be used at 0.5 % w/w content and the copolymer maximum conversion is reached after 120 min. In addition, this phenolic comonomer affects the polymer mass distribution. Finally, FTIR, RMN, TGA and DSC results showed that the 4-vinylphenol is present in the polymer backbone. Therefore, these results indicate that the designed copolymer poly(vinyl acetate-co-4-vinylphenol) (P(VAc-co-4VPh)) was successfully obtained.

Keywords: copolymerization, microspheres, radioactive tracer, radioiodination, SPECT imaging.

3.1 Introduction

Copolymers may contain two or more monomers in the polymer chain, resulting in different composition and distribution of the monomers along the polymer backbone. Copolymerization can be used as a strategy to diversify the final polymer properties and end uses. Indeed, most of the commercial polymers are copolymers (1). Therefore, copolymerization allows the synthesis of a product with specifically

desired properties. Bearing this in mind, the insertion of a phenolic comonomer into poly(vinyl acetate) backbone can enhance a radioiodination reaction, for example. According to the literature, the phenol moiety enables the radioiodination of proteins containing phenolic residues of tyrosine or polymer nanoparticles containing phenol, in high yields (2,3). The 4-vinyl phenol naturally occurs in ciders, wines and berries, and is used as an additive or ingredient in the Food Industry (4-6). Besides, this substance exhibits both a free unsaturated hydrocarbon chain for the copolymerization and a phenol group for the radioiodination.

Single Photon Emission Computed Tomography (SPECT) technique is widely used in Nuclear Medicine for diagnostic purposes. SPECT uses gamma rays to provide higher resolution images when compared with X-rays techniques such as Computed Tomography, Angiography and Fluoroscopy (7,8). Normally, these X-ray techniques are used during vascular embolization procedures. Vascular embolization is a clinical procedure used to reduce the size of a tumor or to ease its removal during surgery. This procedure consists of injecting fine solid particles dispersed in an aqueous medium, with the aid of a catheter, into blood vessels near the tumor region. In this way, a blockade occurs, and the nutrient supply is interrupted. Over time, the tumor region shrinks and eventually die (9,10).

Polymeric biocompatible and nontoxic particles are used to promote the blood vessels obstruction. For example, poly(vinyl alcohol-co-vinyl acetate) microspheres can be used as an embolic agent. These copolymer particles are obtained through the suspension polymerization and hydrolysis processes where vinyl acetate is the monomer (11,12). Considering the SPECT high quality images, radioiodinated polymeric microspheres can lead to an innovative embolic agent for SPECT imaging. Consequently, the embolization procedure efficacy can be improved by allowing the track of particles distribution in the veins and tumor, the homogeneity of this distribution and the end of the embolization procedure for liver or uterus, for example. This work presents exploratory studies between vinyl acetate and 4-vinylphenol polymerization to form a copolymer for further radioiodination

reaction. Bulk polymerization tests, conversion study and polymer characterization regarding GPC, FTIR, RMN, TGA and DSC analysis were applied in this study.

3.2 Methodology

3.2.1 Chemicals

The initiator (benzoyl peroxide, BPO, 97 %, containing co-cristalized water 25 %) and the vinyl acetate (VAc) monomer (99.5 %) were supplied by Vetec Química Fina LTDA (Rio de Janeiro, Brazil). The comonomer 4-vinylphenol (4VPh) (10 % in propylene glycol) was supplied by Sigma Aldrich (Rio de Janeiro, Brazil). Tetrahydrofuran (THF, 99.9%) was supplied by Tedia Brasil (Rio de Janeiro, Brazil). Deuterated chloroform ($CDCl_3$, 99.8 atom % D, contains 0.1 % (v/v) TMS) was supplied by Cambridge Isotope Laboratories Inc. (Rio de Janeiro, Brazil). All reagents were used without further purification.

3.2.2 Comonomer load study

By using bulk polymerization tests, a range of 4VPh percentages (Table 3.1) was studied to define what content of this comonomer should be present in the final copolymer. To perform these tests, VAc and BPO were added in a test tube and mixed until complete homogenization. Then, 4VPh was added in this solution resulting in 4 g of the reaction mixture content. After, the test tubes were immersed in an ethylene glycol bath at 80 ^{o}C for 2 h. Visual inspection was used to evaluate viscosity variations.

Table 3.1: Batch of bulk polymerization tests.

Reaction	**Blank**	**R01**	**R02**	**R03**	**R04**	**R05**	**R06**	**R07**
BPO (% w/w)	1.00	1.00	1.00	1.00	1.00	1.00	1.00	1.00
VAc (% w/w)	99.00	98.90	98.85	98.80	98.75	98.50	98.00	94.00
4VPh (% w/w)	0.00	0.10	0.15	0.20	0.25	0.50	1.00	5.00

3.2.3 Conversion study

Once the content of 4VPh is defined, the reaction time in which the maximum polymerization conversion occurs must also be known. To achieve this parameter, a stock solution (44 ml) containing VAc (98.5 % w/w), BPO (1 % w/w) and 4VPh (0.5 % m/m) was prepared. Then, ten test tubes were weighed individually. A 4 mL aliquot of this solution was dispensed into each test tube, which was weighed again. Afterwards, the tubes were inserted into the ethylene glycol bath at 80 ^{o}C. At the desired time (0, 45, 60, 90, 120, 150, 180, 210, 240, and 270 min), each tube was removed from the bath, immersed in an ice bath, to interrupt the polymerization, and dried in a vacuum oven (60 ^{o}C and 400 mm Hg) up to constant weight. Finally, mass balance calculations were performed.

3.2.4 Characterization

Among all samples studied in the conversion, the one corresponding to 150 min of reaction (guarantee of maximum conversion) was characterized by different techniques. Such characterization allowed to determine the specifications of the polymer material and to confirm the occurrence of the desired copolymerization. The blank (PVAc) was also characterized under the same conditions, for comparison purposes. GPC analyses were performed at EngePol/UFRJ laboratory. NMR analysis was performed at IQ/UFRJ. TGA, DSC and FTIR analyses were performed at LAPIN/IMA/UFRJ.

The molar mass distribution of the obtained polymer was determined by the Viscotek gel permeation chromatography (GPC), model GPC Max, equipped with three Shodex columns (two KF 804L and one KF 805L) and a refractive index detector Viscotek VE3580. Calibrations were performed with polystyrene standards ranging from $8 \cdot 10^2$ to $1.8 \cdot 10^8$ Da. The samples were prepared solubilizing 6.00 mg of the material in 3 mL of tetrahydrofuran. This polymer solution was stirred for 24 h and filtered using a PTFE membrane with a 0.20 µm pore diameter. Then, about 200 µL of the solution were injected into the apparatus at 40 °C.

Infrared spectra (FTIR) were obtained in the transmission mode in a Varian 3100 Excalibur Series spectrometer to confirm the polymer chemical structure. The spectra were recorded between 4000 and 400 cm^{-1}, with 2 cm^{-1} of resolution and 64 scans per analysis using ATR geometry.

Nuclear Magnetic Resonance (NMR) analysis was used to confirm the formation of the copolymer. The sample (~250 mg) was solubilized in $CDCl_3$ (~0.6 mL) and stored in an appropriate test tube. ^{1}H-NMR resonance spectra were obtained using Bruker model AVIII-500 with a frequency of 400.1 MHz and a 5 mm probe at 24.5 °C.

Analyses of mass losses under heating were performed on TGA Q500 TA Instruments. The analyses were conducted in an inert atmosphere with a constant nitrogen flow at 40 $mL \cdot min^{-1}$ and a constant heating rate at 10 $^oC \cdot min^{-1}$. In addition, the examination of polymer thermal transitions was performed in a DSC equipment Q 1000 TA Instruments. Under nitrogen atmosphere, the thermograms were obtained in the second heating/cooling cycle using a constant heating/cooling rate of 10 $°C \cdot min^{-1}$. The first cycle was used for standardization of the samples thermal story.

3.3 Results and discussion

3.3.1 Comonomer load study

According to the viscosity macroscopic evaluation, an increase of viscosity occurred for the experiments from R01 to R05, showing that this range of 4VPh content allows copolymerization. In addition, the blank exhibited an increase of viscosity, as expected. Differently, the solution viscosity remained unchanged in the R06 and R07 experiments indicating that no polymerization occurs between VAc and 4VPh at these levels. Based on these results, any percentage ranging from 0.10 to 0.50 (% w/w) of 4VPh could be used for subsequent studies. However, small

amounts of 4VPh are more susceptible to errors and may hamper the obtained material characterization. Therefore, 0.50 (% w/w) of 4VPh was selected since it is the highest percentage that resulted in copolymerization.

3.3.2 Conversion study

Fig. 3.1 shows that the polymerization is slow in the first 90 min of reaction. However, an abrupt and significant increase occurs after this period. With 120 minutes of reaction, the conversion approaches its maximum (90 %) and varies gently around this level. Actually, the observed fluctuation is due to experimental error since the conversion reaches a constant value. Oliveira and coworkers showed a pure PVAc conversion curve obtained by bulk polymerization, in similar conditions, where the monomer conversion profile follows the usual S-shape trajectory, reaching 40 % after 60 min and 94 % after 120 min of reaction (13). The copolymerization conversion behavior shows that 4VPh acts as a polymerization reaction retarder what corroborates with the literature data (14,15). The comonomer 4VPh is a phenolic compound and this class of substances acts as a retarder because they react with the initiator. Moreover, this delay does not imply any impediment to obtaining the desired copolymer.

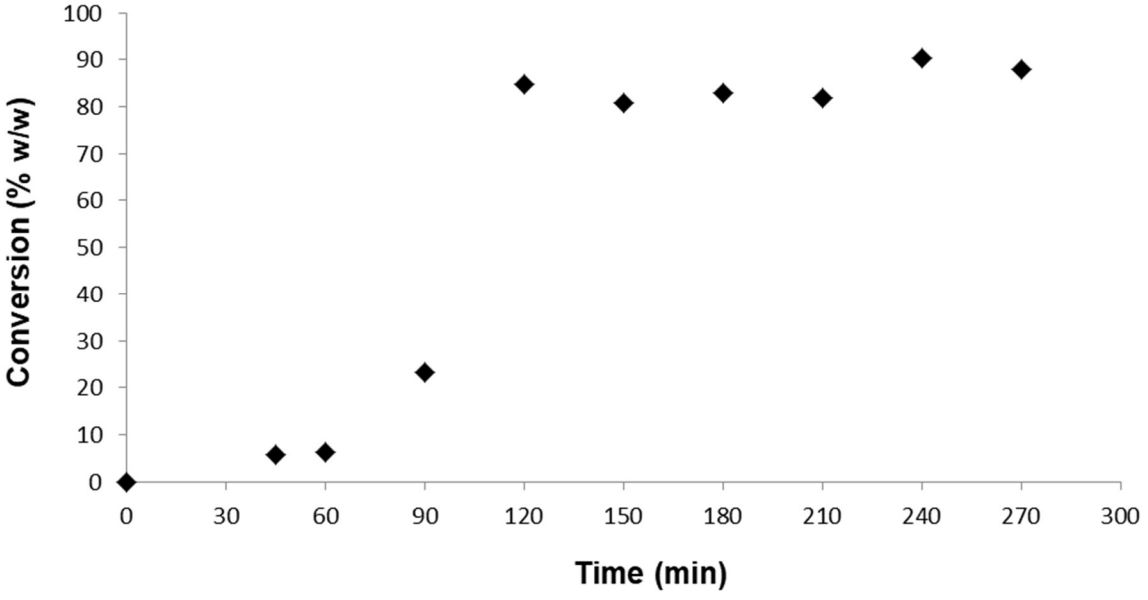

Figure 3.1. Conversion curve of the bulk polymerization between VAc (98.5 % w/w) and 4VPh (0.5 % w/w) performed with BPO (1 % w/w) at 80 ºC.

From now on, all the discussions related to the polymer characterization are referred to the likely obtained copolymer, the poly(vinyl acetate-co-4-vinylphenol) or P(VAc-co-4VPh), as shown in Fig. 3.2.

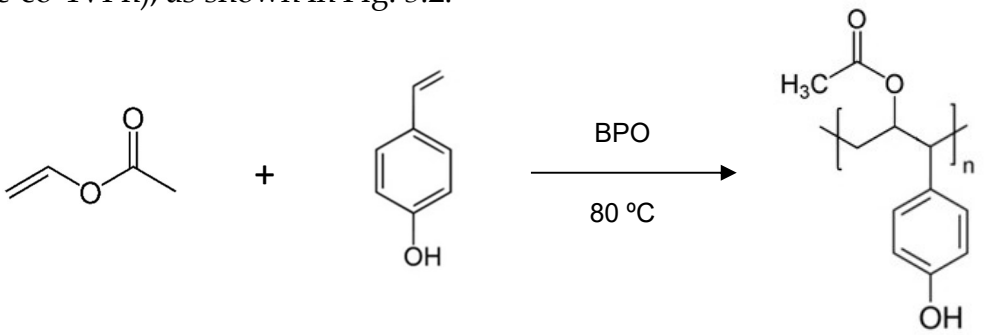

VAc 4VPh P(VAc-co-4VPh)

NOTE: weight ratio VAc/4VPh = 98.50/0.50

Figure 3.2. Polymerization reaction and the most likely chemical structure of the copolymer P(VAc-co-4VPh).

3.3.3 Molar mass distribution

GPC analysis results characterized the difference in the copolymer mass distribution related to the presence of 4VPh content (Table 3.2). The number average molecular weight (Mn), the weight average molecular weight (Mw) and the polydispersity index (PDI) were the measured parameters in this analysis. Due to the observed increasing of PDI (Table 3.2), considering that molar mass distribution is affected by the presence of the 4VPh comonomer in the polymer backbone seems reasonable. The PVAc obtained in this work has PDI values comparable to reactions that employ a chain transfer agent, while in the presence of 4VPh the PDI reaches values compatible with conventional polymerization (13).

Table 3.2. Mass distribution results and polydispersity index. PDI = Mw/Mn.

	P(VAc-co-4VPh)	PVAc
Mn (Da)	18,902	17,989
Mw(Da)	61,502	49,305
PDI	3.2	1.7

3.3.4 Infrared spectroscopy

Regarding to the infrared area (FTIR), Fig. 3.3 shows the absorption spectra of the pure PVAc and the copolymer P(VAc-co-4VPh) obtained by bulk polymerization. Both samples show similar spectra to the PVAc spectrum reported in the literature (16,17). These spectra show characteristic absorption bands at 1731 cm^{-1}, corresponding to the axial deformation C=O, and at 1227 cm^{-1}, corresponding to the axial deformation C–O, characterizing the presence of acetate originated from the VAc monomer. The copolymer spectra do not show an intense band at 1500 cm^{-1}, referents to vibrations of aromatic groups. This specific band should be an indicative of the 4VPh comonomer presence and its absence can be attributed to the low comonomer content (0.5 % w/w). However, the presence of a wide band at 3500 cm^{-1} refers to -OH stretching vibrations that suggest the 4VPh presence. This wide band is a characteristic of the association between hydroxyl (at 4VPh) and carbonyl (at VAc) groups by hydrogen bonding, resulting from the polymeric interaction. Nevertheless, this band can also be an indicative of humidity presence, since the amount of 4VPh used in the experiment is quite low. On the other hand, a wide band at 1600 cm^{-1} that corresponds to unsaturation of aromatic rings is present in the copolymer spectrum (17,18).

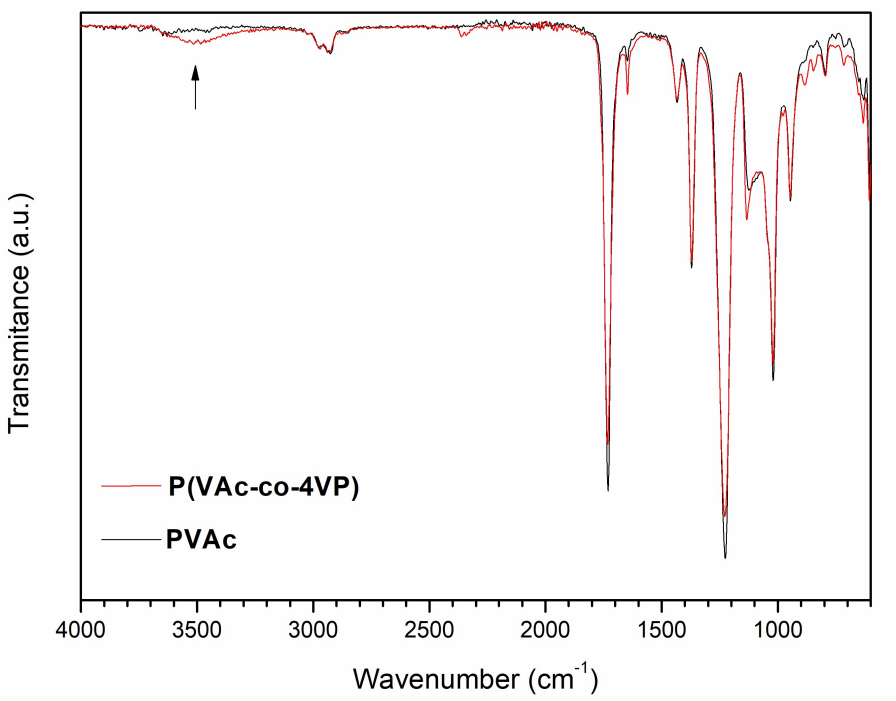

Figure 3.3. FTIR spectra of PVAc and P(VAc-co-4VPh) obtained by bulk polymerization.

3.3.5 ^{1}H-NMR analysis

The ^{1}H-NMR spectrum of PVAc (Fig. 3.4) is in good agreement with the literature reports (19,20). PVAc characteristic peaks are assigned in the Fig. 3.4a. The peaks at 1.6 and 2.2 ppm are, respectively, attributed to CH_2 and terminal CH_3 protons, while the peak of the methine proton is observed at 4.9 ppm. In addition, discrete peaks can be attributed to resulting structures from chain transfer reactions that are commonly observed in the VAc polymerization (19). The ^{1}H-NMR spectrum of the copolymer contains characteristic peaks of both VAc and PVAc monomers. As the 4VPh comonomer is present in low content, its new corresponding peaks exhibits a very low intensity in the spectrum. However, Figure

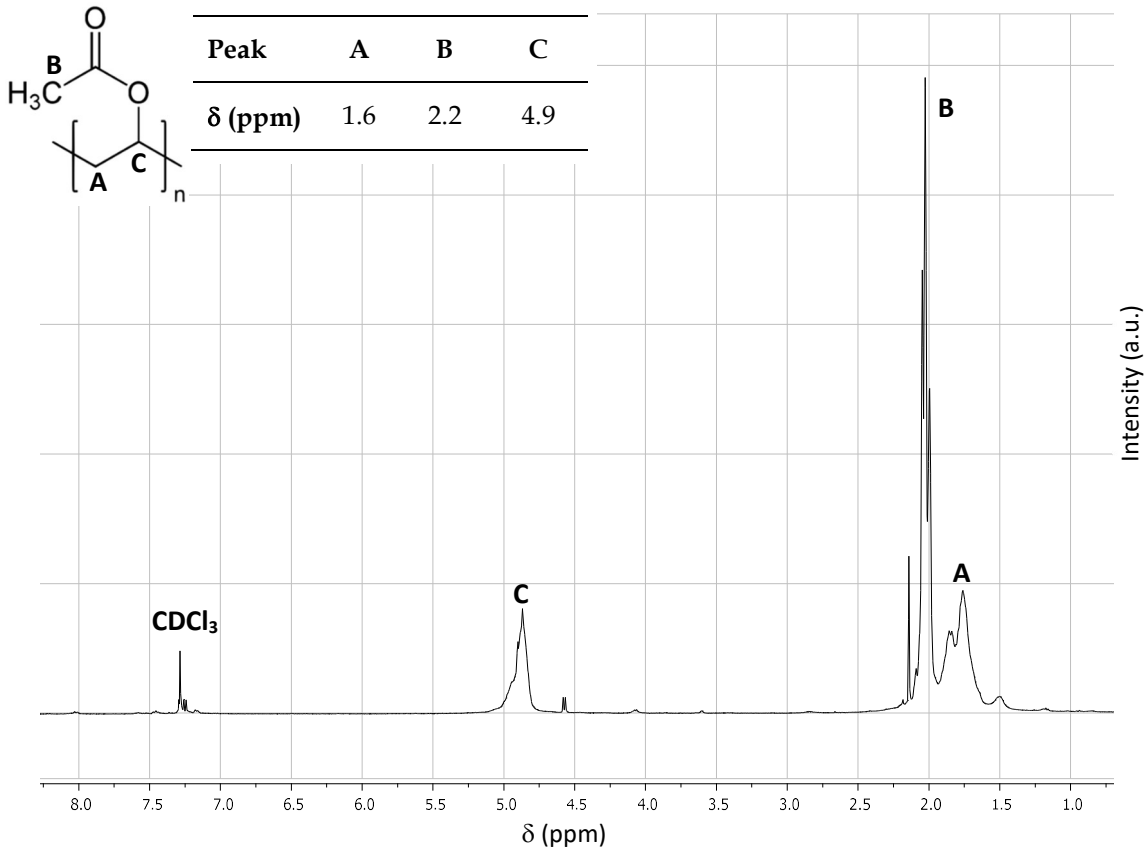
B
H3C
O
O
C
A
n
Peak A B C
δ (ppm) 1.6 2.2 4.9
B
A
C
CDCl3
Intensity (a.u.)
8.0 7.5 7.0 6.5 6.0 5.5 5.0 4.5 4.0 3.5 3.0 2.5 2.0 1.5 1.0
δ (ppm)

(a)

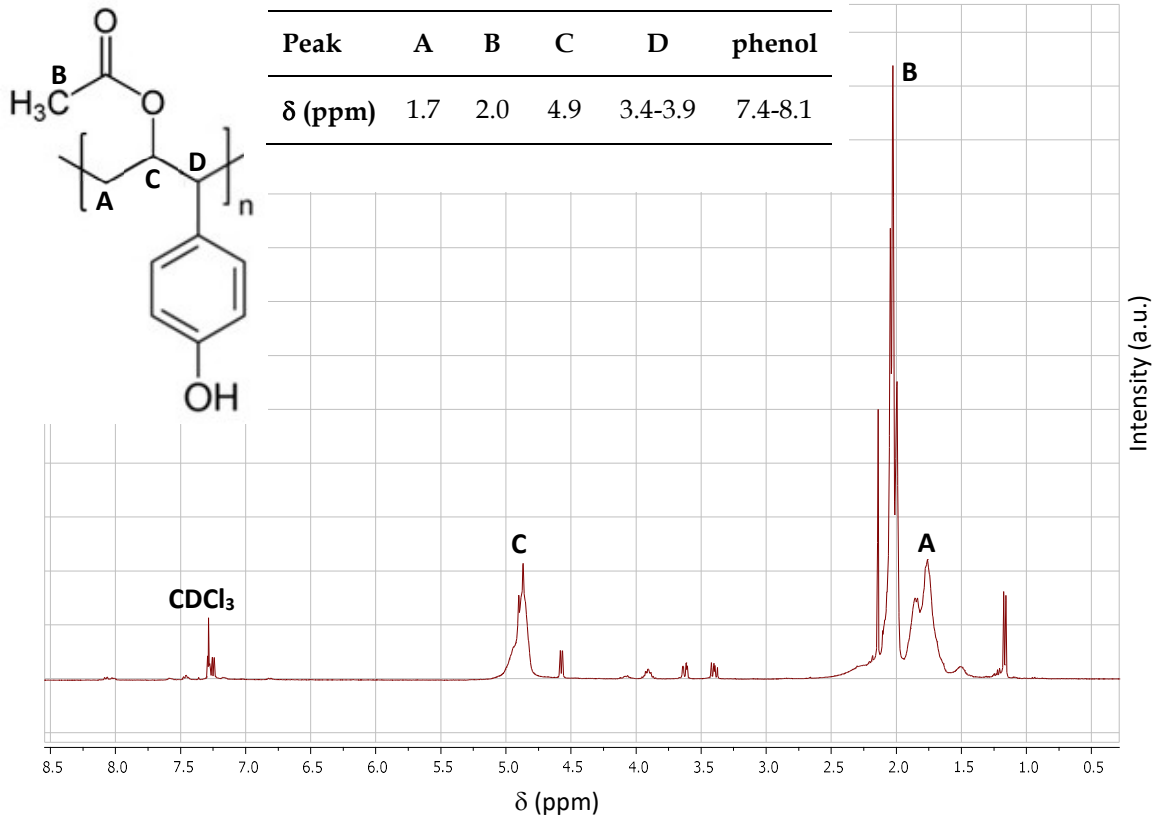
B
H3C
O
O
A
C
D
n
OH
Peak A B C D phenol
δ (ppm) 1.7 2.0 4.9 3.4-3.9 7.4-8.1
B
C
A
CDCl3
Intensity (a.u.)
8.5 8.0 7.5 7.0 6.5 6.0 5.5 5.0 4.5 4.0 3.5 3.0 2.5 2.0 1.5 1.0 0.5
δ (ppm)

(b)

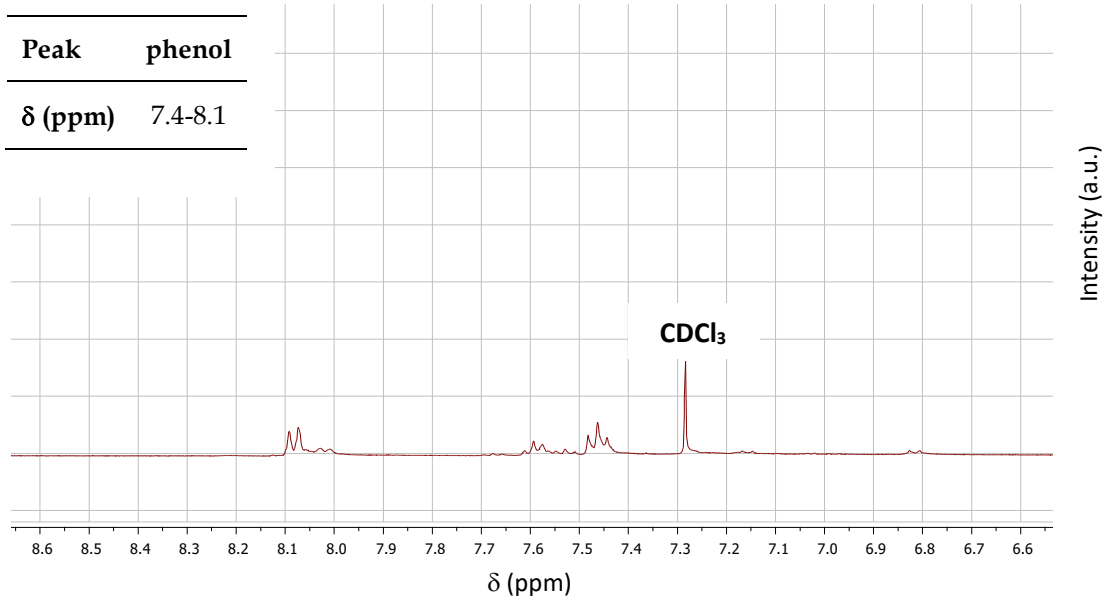

(c)

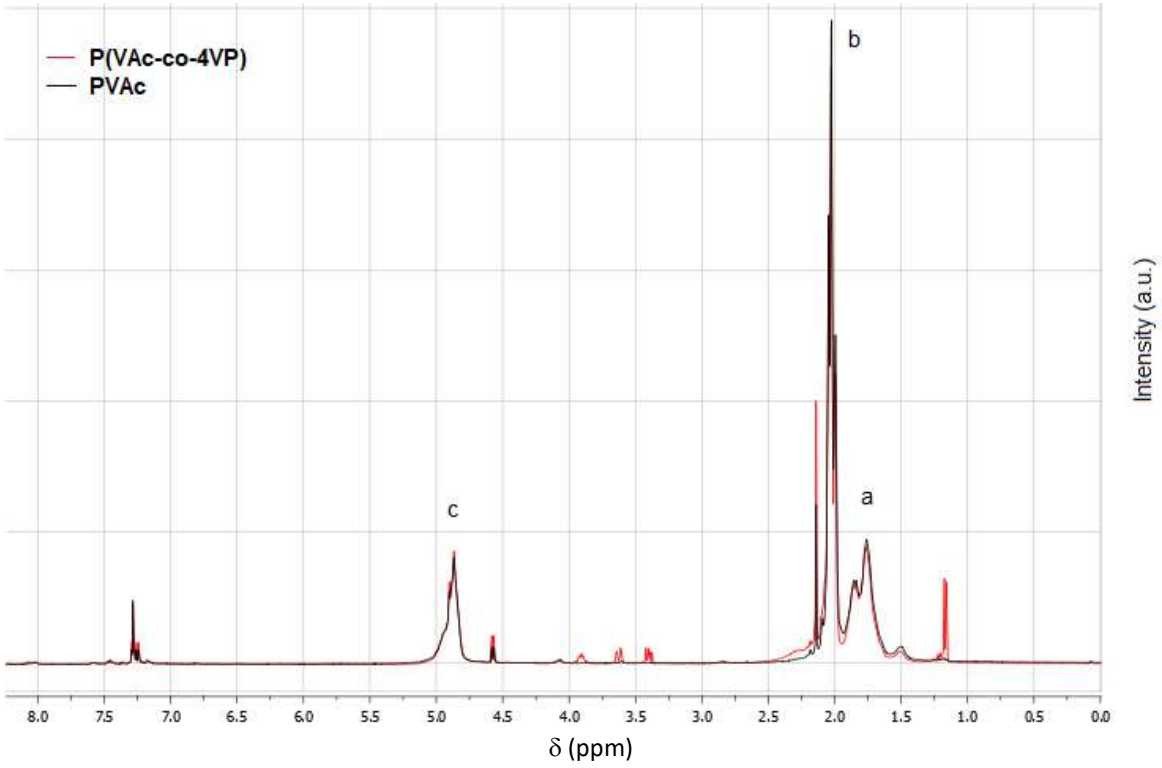

(d)

Figure 3.4. ^{1}H-NMR spectra (400.1 MHz, $CDCl_3$) of (a) PVAc and (b) P(VAc-co-4VPh) obtained by bulk polymerization, (c) a zoom of the phenolic peaks region, and (c) superposed spectra overview.

3.3.6 Thermal analysis

TGA and DTG curves of PVAc and the P(VAc-co-4VPh) modified polymer are shown in Fig. 3.5. In essence, both curves present the same behavior, i.e., two thermal degradation temperatures. At 328 ^{o}C, the first degradation step is the more intense and is identified as the deacetylation step. After the acetic acid elimination, the slighter degradation observed at a higher temperature (443 ^{o}C) is attributed to the decomposition of the remaining PVAc backbone (20, 21). Comparatively, the degradation of the 4VPh (maximum at 399 ^{o}C) is confounded with PVAc degradation (22). Moreover, up to 200 ^{o}C, a discrete mass loss indicates a lower thermal stability of the copolymer.

For the pure PVAc and its copolymer P(VAc-co-4VPh), DSC thermograms are displayed in Fig. 3.6. Only one glass transition temperature (Tg) is observed in both thermograms. The Tg value determined for PVAc (29.54 ^{o}C) is in good agreement with the value reported in the literature (20). The observation of a single Tg may be evidenced as an indicative of the effective copolymerization (18,23). Moreover, it can be seen that the copolymer Tg value deviated to the left regarding to the pure polymer one. Correspondingly, this is an expected effect since the insertion of phenol groups increase the mobility of the polymer chain (18,23).

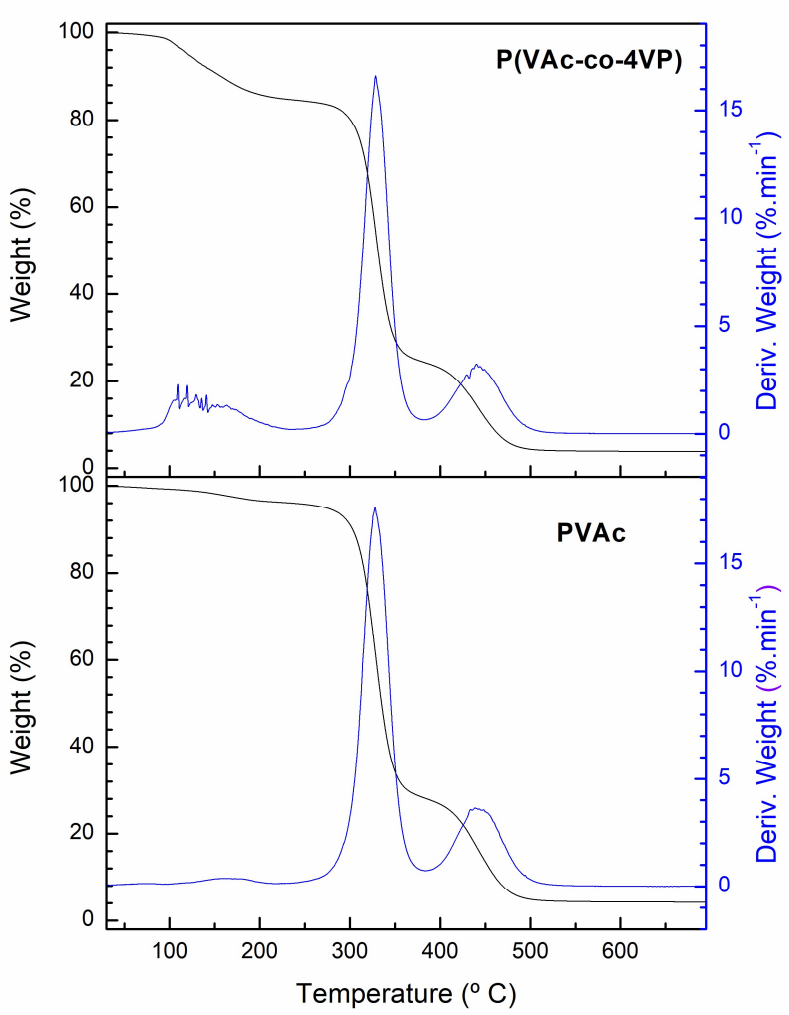

Figure 3.5. TGA and DTG curves of P(VAc-co-4VPh) (0.05 % w/w 4VPh) and PVAc.

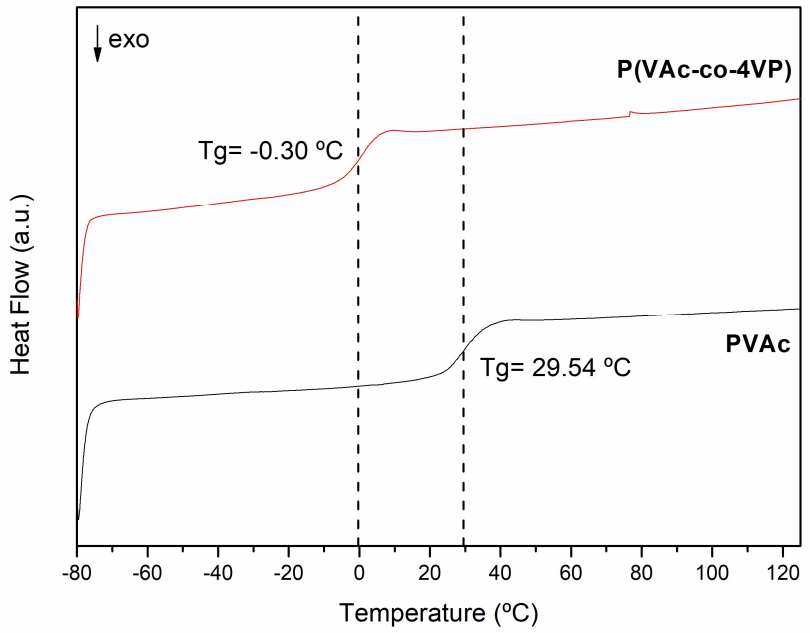

Figure 3.6. DSC thermograms of P(VAc-co-4VPh) (0.05 % w/w 4VPh) and PVAc.

3.4 Conclusions

A copolymer was designed to provide a new radioactive embolic agent for SPECT imaging purposes. When used in low content (0.5 % w/w), the 4VPh showed to be a suitable comonomer to form a polymer with VAc, as confirmed by the characterization results. The obtained copolymer, when compared with the PVAc homopolymer, lead to an increase of polydispersity in the molar mass distribution and a reduction in thermal stability. These effects are not a drawback for the obtained material. Overall, to preserve the phenol group in the polymer structure is important to allow further radioiodination. Therefore, the P(VAc-co-4VPh) microspheres can be obtained through the polymerization suspension reaction followed by radioiodination in future works.

3.5 Complementary remarks

Normally, values of 1 or 5 % (w/w) comonomer are sufficient to test copolymerization with the monomer present in higher concentration. However, as presented in this chapter, no appreciable polymerization occurred between VAc and 4VPh comonomer at this range. Even after one week, no change in the viscosity of the mixtures between these monomers was observed. On the other hand, when the content of 4VPh is in the range of 0.10 to 0.50 % (w/w), the polymerization occurs, as confirmed by the results of molar mass distribution (Table 3.3).

Table 3.3: Mass distribution results and polydispersity index. PDI = Mw/Mn.

Reaction	**Blank**	**R01**	**R02**	**R03**	**R04**	**R05**
Mn (Da)	17,989	18,945	28,410	17,373	17,950	18,902
Mw (Da)	49,305	36,206	70,433	51,535	40,064	61,502
PDI	1.7	1.9	2.5	3.0	2.2	3.2

Usually, the results obtained in the GPC analysis would characterize the difference in the copolymer molar mass distribution as a function of 4VPh percentages. However, as observed in Table 3.3, there was only one oscillation of values, - except for R02, whose analysis should be repeated. Based on Table 3.3, it seems reasonable to consider that molar mass distributions are little affected by the presence of the 4VPh comonomer.

In addition, according to the results displayed on Table 3.3, a 4VPh fraction ranging from 0.10 to 0.50 % (w/w) can be used for copolymer production. However, small amounts of 4VPh are more susceptible to aliquot errors and may difficult the characterization of the obtained material. For these reasons, as the 0.50 % (w/w) content of 4VPh is the highest fraction that resulted in appreciable copolymerization, this was the comonomer content selected for the study of kinetics and further characterizations. This percentage corresponds to 20 mg of the comonomer and is ten times greater than the amount of the routinely radioiodinated *meta*iodobenzylguanidine substrate (24). Therefore, this amount seemed acceptable for radioiodination.

Regarding conversion study, the curve should be replicate twice to improve results reliability. Moreover, according to Moad and Solomon (29) the difference between inhibitors and retarders depends on the substance concentration. When its concentration is high, it would be considered as an inhibitor; when used in very low concentration, a retarder. Indeed, this effect was observed when using 4VPh comonomer. At 1.0 and 5.0 % (w/w) concentrations, 4VPh did not allow polymerization, therefore acting as an inhibitor. From 0.10 to 0.50 % (w/w) concentrations, this comonomer acted as a retarder.

Due to the clear retarding effect of 4VPh, the use of an analogous compound containing other activations groups but phenol is a natural alternative. In this way, the simplest analogous is the 4-methoxy styrene (4-vinylanisole, 4VMS). Figure 3.8

presents its structure. Bulk polymerization tests were performed using 4VMS and VAc according to Table 3.4 and to the procedure described on section 3.2.2.

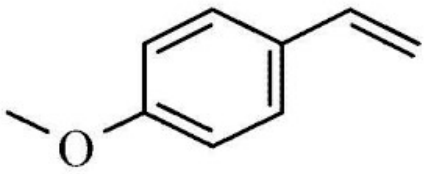

Figure 3.8. Chemical structure of 4-methoxy styrene (4VMh).

Table 3.4: Batch of bulk polymerization tests performed with 4-methoxy styrene (4VMS). 4VMS (99.5 % of purity) was supplied by CarboSynth (Berkshire, England).

Reaction	**Blank**	**R08**	**R09**	**R10**	**R11**
BPO (% w/w)	1.00	1.00	1.00	1.00	1.00
VAc (% w/w)	99.00	98.90	98.50	98.00	94.00
4VMS (% w/w)	0.00	0.10	0.50	1.00	5.00

According to visual inspection evaluation, no changes in viscosity occurred for the experiments from R08 to R11, indicating that this range of 4VMS content does not allow copolymerization with VAc in the reaction conditions studied herein. These results encouraged to move on with the goal of synthesizing the copolymer P(VAc-co-4VPh) in form of microspheres via suspension polymerization.

Kato (25) reports the successful synthesis of P4VPh (32-66 % of conversion and Mn equals to 22,000-37,000 Da) by using THF as solvent, at 50-70 ºC during 20-48 h. AIBN (0.5-1.0 % (w/w)) was used as initiator and the 4VPh concentration related to THF was 50.0-55.6 % (w/w). In this thesis, a similar experiment was performed using BPO 1 % (w/w) and 4VPh 99 % (w/w) at 80 °C for 48 h, based on the procedure described on section 3.2.2. Differently, the 4VPh was dissolved at 10 % (w/w) in propylene glycol solvent. However, this experiment did not result in significant viscosity change by means of visual inspection. The appreciable non-formation of

P4VPh homopolymer was evidenced by the GPC analysis result (Figure 3.7). Therefore, this experiment showed that the bulk polymerization of 4VPh did not seem to occur when performed with propylene glycol as solvent and BPO as initiator. Moreover, additional experiments could be performed replacing BPO by AIBN, and in the presence and absence of propylene glycol for evaluation and comparisons.

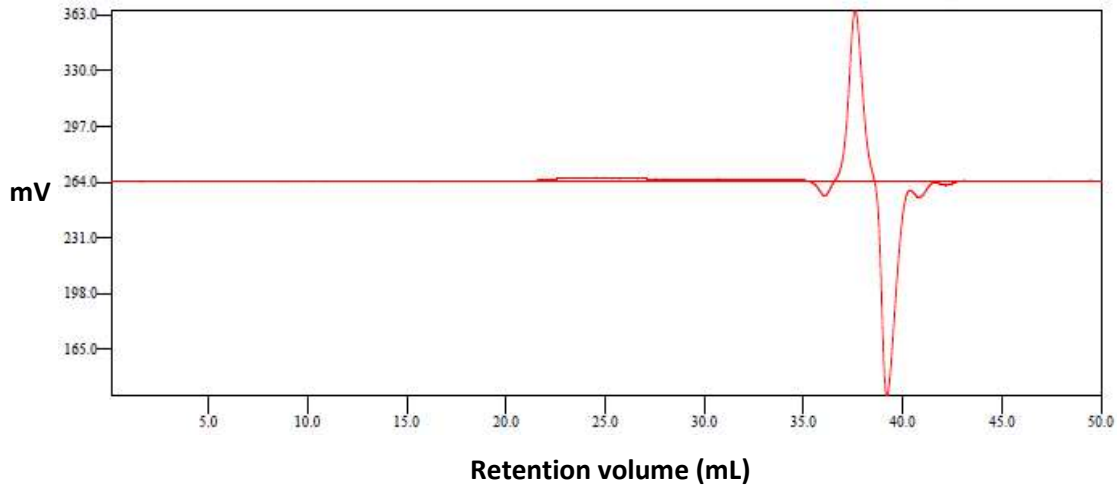

Figure 3.7. Refractive index curve for the homopolymerization of 4VPh. No signal is observed but noise at 35-40 mL, indicating no appreciable homopolymer formation. GPC assay was performed as described on section 3.2.4.

Additionally, an experiment was performed using BPO 1 % (w/w) and propylene glycol 99 % (w/w) at 80 °C for 48 h, based on the procedure described on section 3.2.2. No changes on viscosity were observed, indicating that the homopolymerization of propylene glycol seems to not occur at these reactional conditions. This result was also evidenced by the GPC analysis result (Figure 3.8). GPC assay was performed as described on section 3.2.4. Therefore, it seems that there is no influence of propylene glycol on the experiments performed in bulk polymerization study.

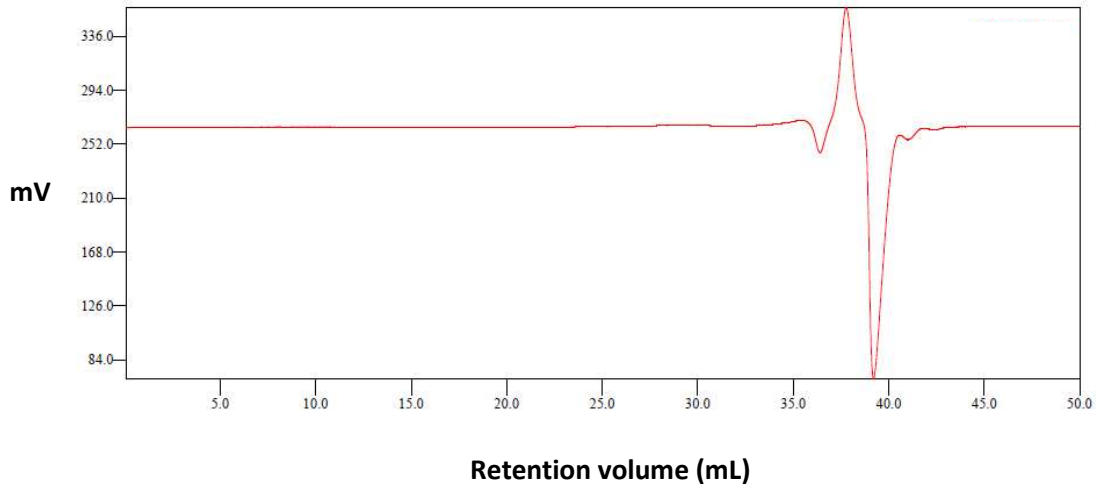

Figure 3.8. Refractive index curve for the homopolymerization of propylene glycol. No signal is observed but noise at 35-40 mL, indicating no appreciable homopolymer formation.

Considering the material characterization, with the exception of the TGA assay, GPC, FTIR, DSC and NMR assays showed that the presence of 4VPh in the polymeric matrix modified the corresponding PVAc results. Therefore, these results indicated that the P(VAc-co-4VPh) copolymer was successfully synthesized. To validate this statement, the quantitation of 4VPh in the polymeric matrix should be performed. To perform this determination using the direct measuring of the copolymer on a UV spectrometer is not allowed because PVAc and 4VPh absorb at the same wavelength region (230-260 nm) according to the literature (26,27). However, the adapted method of Water & Mole could be used, since this method is specific to phenol compounds (28). In this adapted method, samples of 5 mg of the copolymer would be dissolved in 1 mL of acetone and then diluted with 1 ml of sodium carbonate solution (0,5 $mol.L^{-1}$). Then, 0.25 ml of Folin-Ciocalteau reagent would be added. The Folin-Ciocalteau reagent is a mixture of phosphomolybdate and phosphotungstate used for the colorimetric assay of phenolic and polyphenolic compounds (28). After 60 min, the sample can be measured on a UV spectrophotomer at 760 nm. A calibration curve could be constructed at concentrations of 0.10, 0.20, 0.30, 0.40 and 0.50 % (m/m) of 4VPh dissolved in a solution of acetone and sodium carbonate.

Then, a quite good estimative of the 4VPh amount in the copolymer is expected to be obtained by using this adapted method.

References

[1] G. Odian, Principles of polymerization (Wiley, NJ: New York, 1991).

[2] E. A. Simone, B. J. Zern, A-M. Chacko, J. L. Mikitsh, E. R. Blankemeyer, S. Muro, R. V. Stan and V. R. Muzykantov, Endothelial targeting of polymeric nanoparticles stably labeled with the PET imaging radioisotope iodine-124, Biomaterials, 33, 5406 5413, 2012.

[3] C. Tang, J. Edelstein, J. L. Mikitsh, E. Xiao, A. H. Hemphill, R. Pagels, A-M. Chacko and R. Prud'homme, Biodistribution and fate of core-labeled 125I polymeric nanocarriers prepared by Flash NanoPrecipitation (FNP), Journal of Materials Chemistry B, 4, 2428-2434, 2016.

[4] M. Granvogl, and D. Langos, Studies on the Simultaneous Formation of Aromactive and Toxicologically Relevant Vinyl Aromatics from Free Phenolic Acids during Wheat Beer Brewing, Journal of Agricultural and Food Chemistry, 64(11), 2325-2332, 2016.

[5] R. Fujiwara, S. Noda, Y. Kawai, T. Tanaka and A. Kondo, 4-Vinylphenol production from glucose using recombinant Streptomyces mobaraense expressing a tyrosine ammonia lyase from Rhodobacter sphaeroides, Biotechnology Letters, 38(9), 1543-1549, 2016.

[6] L. Chen, W. Chai, W. Wang, T. Song, X-Y. Lian and Z. Zhang, Cytotoxic Bagremycins from Mangrove-Derived Streptomyces sp. Q22, Journal of Natural Products, 80, 1450-1456, 2017.

[7] R. A. Powsner and E. R. Powsner, Essential nuclear medicine physics (Blackwell Publishing, NJ: Massachusetts, 2006).

[8] S. R. Cherry, J. A. Sorenson and M. E. Phelps, Physics in nuclear medicine (Elsevier Saunders, NJ: Philadelphia, 2012).

[9] A. Laurent, Microspheres and nonspherical particles for embolization, Techniques in vascular and interventional radiology, 10, 248-256, 2007.

[10] R. J. T. Owen, Embolization of musculoskeletal tumors, Radiologic Clinics of North America, 46, 535-543, 2008.

[11] L. S. Peixoto, F. M. Silva, M. A. L. Niemeyer, G. Espinosa, P. A. Melo, M. Nele and J. C. Pinto, Synthesis of Poly(Vinyl Alcohol) and/or Poly(Vinyl Acetate)

Particles with Spherical Morphology and Core-Shell Structure and its Use in Vascular Embolization, Macromolecular Symposia, 243, 190–199, 2006.

[12] L.S. Peixoto, J. C. Pinto, M. Nele and A. P. Melo, Expanded core/shell (poly(vinyl acetate)/poly(vinyl alcohol) particles for embolization, Macromolecular Material and Engineering, 294, 463-471, 2009.

[13] M. Oliveira, B. S. Barbosa, M. Nele and J.C. Pinto, Reversible Addition–Fragmentation Chain Transfer Polymerization of Vinyl Acetate in Bulk and Suspension Systems, Macromolecular Reaction Engineering, 8, 493-502, 2014.

[14] R. A. Bird and K. E. Russel, The effect of phenols on the polymerization of vinyl acetate, Canadian Journal of Chemistry, 4, 2123-2125, 1965.

[15] F. Lartigue-Peyrou, The use of phenolic compounds as free-radical polymerization inhibitors, Industrial Chemistry Library, 8, 489-505, 1996.

[16] A. C. Mesquita, M. N. Mori and L. G. A. Silva, Polymerization of vinyl acetate in bulkand emulsion by gamma irradiation, Radiation Physics and Chemistry, 71, 251-254, 2004.

[17] L. R. Rubio, E. Lizundia, J. L. Vilas, L. M. León and M. Rodriguez, Influence of N-alkyl and rmalpha-substitutions on the termal behaviour of H-bonded interpolymer complexes based on polymers with acrylamide or lactame groups and poly(4-vinylphenol), Thermochimica Acta, 614, 191-198, 2015.

[18] H. Bourara, S. Hadjout, Z. Benabdelghani and A. Etxeberria, Miscibility and Hydrogen Bonding in Blends of Poly(4-vinylphenol)/Poly(vinyl methyl ketone), Polymers, 6, 2752-2763, 2014.

[19] J. Chen, X. Zhao, L. Zhang, Z. Cheng and X. Zhu, Reversible Addition-Fragmentation Chain Transfer Polymerization of Vinyl Acetate Under High Pressure, Journal of Polymer Science, Part A: Polymer Chemistry, 53, 1430–1436, 2015.

[20] M. Teodorescu, P. O. Stanescu, H. Iovu and C. Draghici, Free radical polymerization of vinyl acetate in the presence of liquid polysulfides, Reactive & Functional Polymers, 70, 419–425, 2010.

[21] B. Rimez, H. Rahier, G. Van Assche, T. Artoos, M. Biesemans and B. Van Mele, The thermal degradation of poly(vinyl acetate) and poly(ethylene-co-vinyl acetate), Part I: Experimental study of the degradation mechanism, Polymer Degradation and Stability, 93, 800-810, 2008.

[22] A. Lassoued and S. Djadoun, Thermal behavior of poly(styrene-co-methacrylic acid) with poly(4-vinylpyridine) or poly(N,N-dimethyl acrylamide) or poly(N,N-dimethyl acrylamide-co-4-vinylpyridine), J Therm Anal Calorim, 126, 541-552, 2016.

[23] Ch. Belabed, Z. Benabdelghani, A. Granado and A. Etxeberria, Miscibility and Specific Interactions in Blends of Poly(4-vinylphenol-co-methyl methacrylate)/Poly(styrene-co-4-vinylpyridine), Journal of Applied Polymer Science, 125, 3811-3819, 2012.

[24] L. Carvalheira, Desenvolvimento, otimização e validação parcial de método para determinação de pureza radioquímica da metaiodobenzilguanidina marcada com iodo 123 (123I MIBG). 2008. 157p. Dissertação (Mestrado em Química Analítica) – Instituto de Química, Universidade Federal do Rio de Janeiro, Rio de Janeiro, 2008.

[25] M. Kato, A research on Polymerization of 0-, m-, and p-Vinylphenol. Journal of Photopolymer Science and Technology v.21, n.6, pp.711-717, 2008.

[26] Bao, Qiaoliang; Zhang, Han; Ang, Priscilla; Wang, Shuai; Tang, Dingyuan; Jose, Rajan; Ramakrishna, Seeram; Lim, C.T.; Loh, Kian. Graphene–Polymer Nanofiber Membrane for Ultrafast Photonics. Advanced Functional Materials, v.20, p.782-791, 2010.

[27] Mingguang Zhu; Yunqian Cui. Determination of 4-vinylgaiacol and 4-vinylphenol in top-fermented wheat beers by isocratic high performance liquid chromatography with ultraviolet detector. Braz. arch. biol. technol. v.56, n.6, 2013.

[28] Jardel B. Silva, Kizzy M.F.M. Costa, Wesley A.C. Coelho, Kaliane A.R. Paiva, Geysa A.V. Costa, Antonio Salatino, Carlos I.A. Freitas, Jael S. Batista. Quantificação de fenóis, flavonoides totais e atividades farmacológicas de geoprópolis de Plebeia aff. flavocincta do Rio Grande do Norte. Pesq. Vet. Bras. v.36, i.9, p.874-880, 2016.

[29] G. Moad, D.H. Solomon. The Chemistry of Radical Polymerization 2nd ed. Elsevier, 2006.

CHAPTER 4

SUSPENSION POLYMERIZATION

The insertion of Iodine 123 on poly(vinyl acetate) backbone by means of copolymerization with 4-vinyl phenol was investigated. This phenolic compound allows both copolymerization and radioiodination reactions. This work presents an investigation on kinetic of suspension copolymerization between 4 vinyl phenol and vinyl acetate, and detailed information about molecular properties and morphology of the polymeric microspheres. Moreover, the results of suspension polymerization obtained herein were compared to previous ones obtained with bulk polymerization regarding this phenolic comonomer at 0.50 % w/w. The evaluation of both conversion curves and characterization results led to the selection of 4-vinylphenol at 0.10 % w/w for the radioiodination studies. Labeling results indicated that the microparticles labeling occurred to some extent with low stability, and that the labeling reaction should be carried out on the comonomer prior to copolymerization.

Keywords: 4-vinylphenol, PVAc microspheres, embolization, iodine 123, SPECT.

4.1 Introduction

Vascular embolization is a clinical procedure that promotes blood vessels obstruction by using biocompatible and nontoxic microspherical particles. This blockade interrupts the nutrient supply and, consequently, the tumour shrinks or even dies. During this clinical procedure, a catheter is used to conduct an aqueous dispersion of solid particles to the tumour neighbouring blood vessels. Vascular embolization can be used to reduce tumour size, to facilitate tumour removal during surgery or to define a tumour malformation treatment (1,2). The uterine artery embolization (UAE) is an example. In comparison with the hysterectomy surgery, the UAE is a less invasive alternative for uterine fibroids treatment, plus preserving woman uteri (3).

Polymeric microspheres ranging from 40 to 1,200 μm have been used as embolization agents since 1945. Poly(vinyl alcohol) (PVA), gelatinous sponges and trisacrylate gelatin are the embolization agents commonly used, being PVA the most important due to its advantageous properties such as good biocompatibility and elasticity, high compressibility, good chemical resistance to acids, bases and detergents, for example (4-5). Suspension polymerization followed by hydrolysis is the most used process to synthesize PVA microspheres from poly(vinyl pivalate) or poly(vinyl acetate) (PVAc) particles (6-8). As this process results in particles with no regular spherical morphology that can lead to aggregation, poly(vinyl alcohol co vinyl acetate) (P(VA co Vac)) particles of core-shell structure with controlled spherical morphology were synthesized (9). In addition, P(VA co VAc) microspheres containing iron (III) oxide nanoparticles were studied for the simultaneous use of embolization and hyperthermia (10). PVAc copolymers can also be used for chemoembolization procedures, i.e., the use of embolization agents loaded with drugs. In this procedure, the embolization agent promotes both physical occlusion and the controlled release of drugs (11). For example, the drug amoxicillin was incorporated into poly(vinyl acetate co methyl methacrylate) microspheres via suspension polymerization for chemoembolization procedures (12).

Computed Tomography (CT), Angiography and Fluoroscopy are the X-ray techniques used during vascular embolization procedures. However, only pathological exams can show the exact location of blockade and microspheres (13). Conversely, Single Photon Emission Computed Tomography (SPECT) technique provides higher resolution images than these X-ray ones. In Nuclear Medicine, SPECT is a diagnostic imaging technique for the study of biochemical dysfunctions present in the early stages of diseases, their mechanisms, and associations with pathological states. In addition, the combined SPECT and CT imaging results in simultaneous metabolic and morphological information (14,15).

The SPECT technique uses gamma ionizing radiation (100 to 300 keV) emitted from radioisotopes whose decay, preferably, do not release ionizing particles. The gamma

radiation is detected by scintillation detectors that form the γ-camera. This device provides cross-sectional images of the radioisotope distribution in the target organ, displaying tumors sized in the centimetric scale (16). An advantage for SPECT is that numerous research institutions, medical centers, regional and local hospitals possess the γ-camera and the required radioisotope to implement this technique (17). Several labelled particles can be used in the SPECT diagnostic. For instance, cobalt 57 polystyrene microspheres for blood flow measurements, indium 111 polymeric micelles for the diagnostic of lymphatic ducts and sentinel lymph nodes, technetium 99m monoclonal antibodies to detect infections and inflammation (18,19).

Indeed, the iodine 123 (^{123}I) exhibits the most suitable nuclear characteristics for the SPECT technique. The ^{123}I emits gamma rays of 159 keV with 83 % of abundance, has a physical half-life of 13.2 h and decay without releasing ionizing particles. Equally important, the product formed is the stable element tellurium 123 whose negligible quantity (between 10^{-18} and 10^{-14} g) is safely below its lethal dose of 20 $mg \cdot kg^{-1}$ (20,21). Moreover, radioiodinated compounds are of medical and biological interest. Molecules such as radioiodinated peptides, proteins, and antibodies have been used in a wide range of applications, for many years. Finally, the chemical versatility of radioiodination is remarkable due to labeling can occur by electrophilic or nucleophilic substitution in lipophilic or hydrophilic substances. However, only iodinated substances such as aromatic and vinyl compounds show the greatest *in vivo* stability, since iodine binds irreversibly to these compounds (22).

The iodination of a molecule is mainly governed by the oxidized form of iodine as iodonium (I^+). Normally, radioiodine is commercially available as sodium radioiodide, and radioiodide is oxidized to I^+ by various oxidizing agents (22-25). For example, iodo-beads is an oxidizing agent formed of immobilized *N*-chlorobenzenesulfonamide (chloramine-T) in non-porous polystyrene spheres with 2-8 mm diameter. Iodo-beads are known as a suitable oxidant for the radioiodination of proteins and peptides in high yields. These biomolecules contain phenolic residues that are aromatic compounds ready to iodine attachment by

aromatic electrophilic substitution (26,27). Also, iodo-beads were used in the successful radioiodination of polymeric matrices containing the phenol group (28,29).

To the best of our knowledge, the study of radioiodinated PVAc microspheres has not been reported in the literature. Our previous study reports the synthesis of poly(vinyl acetate-co-4-vinylphenol) (P(VAc-co-4VPh)) by bulk polymerization and suggests that this copolymer can be obtained and further radioiodinated (30). In this study, P(VAc-co-4VPh) microspheres were produced using suspension polymerization with different contents of 4VPh. The final characteristics of the obtained products were evaluated and drove the selection of a comonomer content for further ^{123}I labelling using iodo-beads in order to produce particles potentially useful for SPECT.

4.2 Methodology

4.2.1 Chemicals

Both the vinyl acetate (VAc) monomer (99.5 %), the benzoyl peroxide (BPO, 97 %, containing co-crystalized water 25 %) initiator, and chloroform ($CHCl_3$) were supplied by Vetec Química Fina. Poly(vinyl alcohol) (PVA) suspending agent with a hydrolysis degree of 86.5-89.5 % and viscosity range of 40–48 mPas was also supplied by this company. The 4-vinylphenol (4VPh) comonomer (10 % in propylene glycol), azobisisobutyronitrile (AIBN, 98 %), deuterated chloroform ($CDCl_3$) (99.8 atom % D, contains 0.1 % (v/v) TMS) and dimethyl sulfoxide (DMSO-d6) were purchased from Sigma Aldrich. Tetrahydrofuran (THF, 99.9%) and hydroquinone (> 99 %) were supplied by Tedia Brasil. Iodo-beads (97 %) were supplied by Thermo Fisher Scientific. NaCl (> 98 %), KH_2PO_4 (> 98 %), and Na_2HPO_4 (> 98 %) were purchased from Merck. $Na^{123}I$ in NaOH 0.02 mol/L was provided by the Nuclear Engineering Institute. Deionized water was obtained from the Gehaka Master WFI MS2000 system. All chemicals were used with no prior purification.

4.2.2 Suspension polymerization

Polymeric microspheres were synthesized (31-33) using an automated and miniaturized reactor system (Mettler Toledo, Easy Max 102, 100 mL of total capacity). Table 1 shows the reagents weight fraction used in this synthesis. The reactor was fed in with 54.16 mL of a PVA solution (0.47 $g \cdot L^{-1}$) under stirring (900 rpm). After heating the system to 65 °C, 27.60 mL of a freshly prepared mixture containing the desired monomers and the initiator was added. From this moment on, the reaction was started. Immediately, the system temperature was set to 85 °C. Finally, the reaction was interrupted after 300 min and the obtained product was washed with deionized water. This entire procedure was replicated twice for each suspension polymerization test. An additional experiment was performed using the same conditions of R01 experiment (Table 4.1), replacing BPO by AIBN 2 % w/w.

Table 4.1. A batch of suspension polymerization tests performed with PVA (0.1 % w/w), BPO (2 % w/w) and water (67.7 g). Monomers ratio (VAc:4VPh) expressed by weight fraction.

Reaction	**R00**	**R01**	**R02**	**R03**
VAc:4VPh	98.00:0.00	97.90:0.10	97.75:0.25	97.50:0.50

4.2.3 Conversion study with different contents of 4VPh

As 4VPh is a phenolic compound that is used commonly as a retarder, its influence in the polymerization reaction conversion was studied using a gravimetric technique described in the literature (29,31). First, an aluminum capsule was weighed both empty and containing 0.30 mL of 1 % hydroquinone solution prior to receiving an aliquot (1 mL) of the reaction medium. Afterward, the capsule was quickly weighed again. Fourteen aliquots were taken from the reaction system, at the desired time (0, 5, 10, 15, 20, 30, 60, 90, 120, 150, 180, 210, 240, 270, and 300 min), while suspension polymerization tests were carried out. The capsule set was dried in a vacuum oven

(70 ºC and 400 mm Hg) up to constant weight to allow mass balance calculations. This procedure was applied in the tests performed according to Table 4.1.

4.2.4 Polymers characterization

Different techniques were employed to characterize the polymeric material obtained in the set of suspension polymerization tests. GPC and PSD analyses were performed at EngePol/UFRJ laboratory. NMR analysis was performed at IQ/UFRJ. TGA, DSC and FTIR analyses were performed at LAPIN/IMA/UFRJ.

Molar mass measurements were performed on a Viscotek gel permeation chromatography (GPC), model GPC Max, equipped with three Shodex columns (two KF-804L and one KF-805L) and a refractive index detector Viscotek VE3580. Calibrations were performed with polystyrene standards in the range from $8 \cdot 10^2$ to $1.8 \cdot 10^8$ Da. The samples (6.00 mg of the material in 3 mL of tetrahydrofuran) were stirred for 24 h and filtered before being injected (200 µL) into the apparatus at 40 °C.

Thermogravimetric analysis (TGA) was carried out on a TGA Q500 TA Instruments under a constant nitrogen flow of 40 $mL.min^{-1}$ and a constant heating rate of $10\ °C \cdot min^{-1}$. The investigation of thermal transitions occurred by means of differential scanning calorimetry (DSC) under nitrogen atmosphere in a Q1000 TA Instruments equipment. The first cycle of heating/cooling at a constant rate of $10\ °C \cdot min^{-1}$ was used for standardization of the samples thermal story. Then, the second cycle provided the thermograms.

The morphology of polymeric particles was observed by optical microscopy in an Axiovert 40MAT Carl Zeiss equipment, using the dark field technique and a 5x objective. Particle size distribution (PSD) was determined in a Mastersizer 2000 Hydro 2000S Malvern Instruments equipment. Small amounts of wet particles were directly added to the equipment until reaching a minimum level of light scattering.

Infrared (IR) spectroscopy analysis was carried out on a Varian 3100 Excalibur Series in the transmission mode using ATR cell, in a range of 4000-400 cm^{-1}, with 2 cm^{-1} of resolution and 64 scans per analysis. Nuclear magnetic resonance (NMR) analysis was performed on a Bruker AVIII-500 at a frequency of 400.1 MHz with a 5 mm probe at 24.5 °C containing 25 mg of the sample solubilized in 0.6 mL of $CDCl_3$. Prior to NMR analysis, P(VAc-co-4VPh) particles were purified by dissolving the material in $CHCl_3$ and filtering using a Millipore filter unit. After drying at room temperature, the polymeric film was then weighed.

4.2.5 Radioiodination

Counting measurements (number of disintegrations per second, CPS) were performed on a NaI(Tl) radiation detector (Canberra Industries, model 2007P) accoupled to a spectrometer (Nuclear Engineering Institute, model 4031) after 1 hour of warming and using capped vials. Each counting measurement lasted 60 s. These measurements were made in duplicate. Calculations of decay correction were performed. Counting measurements were conducted at room temperature.

Labeling of polymeric microparticles with ^{123}I was performed as follows: 50 µL of $Na^{123}I$ in NaOH 0.02 mol $\cdot L^{-1}$ (1.85 x 10^7 Bq) were added to a glass vial containing 5 mL of phosphate buffer solution (pH = 5-6). After the counting measurement of this solution, two pearls of iodo-beads were added to this vial that was capped and kept under magnetic stirring for 5 min. Afterward, 50 mg of the desired polymeric microparticles were added, and the reaction proceeded for 60 min under agitation in the capped vial. Next, both the supernatant and the particles were separated and transferred to individual vials for counting measurements. Before measurements, particles were washed 5-6 times with a solution of sodium chloride (NaCl) 0,9 %. This procedure was repeated twice for each labeling reaction. These experiments were conducted at room temperature. This procedure was adapted from the literature (27). Before labeling, fresh-prepared microparticles were filtered, washed with deionized water, and dried at room temperature for 24 h.

In order to follow the stability of radioiodinated microparticles with time, counting measurements were performed for the washed particles. In sequence, 5 mL of NaCl 0.9 % solution were added to these particles that stayed under magnetic stirring for 15 min. Then, the supernatant was completely removed, and a new aliquot of 5 mL from a NaCl 0.9 % solution was added. The stirring was again conducted for 15 min. This procedure was replicated seven times. After 120 min, the supernatant was again removed, and counting measurements for the radioiodinated microparticles were performed. This study was conducted at room temperature.

In this study, previous experiments considering non-radioactive iodine were not performed since small quantities of radioiodine were convenient and necessary to improve the reliability of labeling results, as the detection of incorporated radioiodine in the particles is far more sensitive than conventional analytical techniques used in the non-radioactive iodine quantification.

4.3 Results and discussion

4.3.1 Reaction kinetics

Figure 4.1 displays the conversion curves obtained from batch suspension polymerization tests performed according to Table 4.1. As it can be observed in this Figure, the conversion reaches 100 % near 120 min for the VAc suspension polymerization (R00) as observed in similar conditions (31,32). The presence of 4VPh, even at its minimum content (0.10 % w/w), decreased the maximum conversion to 40-60 % and retarded the reaction extinction to 150 min (R01), furthermore a clear inhibition behavior is observed. Unexpectedly, with a higher content of 4VPh (0.25 % w/w) the maximum conversion slightly increased to 50-70 % but it was delayed to 180 min (R02). As expected, the highest content of 4VPh (0.50 % w/w) resulted in the lowest conversion (R03) with a maximum conversion of about 30 % reached near 280 min of reaction. Comparatively, in the bulk polymerization between VAc (98.5 % w/w) and 4VPh (0.50 % w/w) performed with BPO (1 % w/w)

at 80 ºC, the polymerization is delayed in the first 90 min and reaches a final conversion of about 90 % after 120 min (30). Therefore, the presence of 4VPh in the system difficult the polymerization.

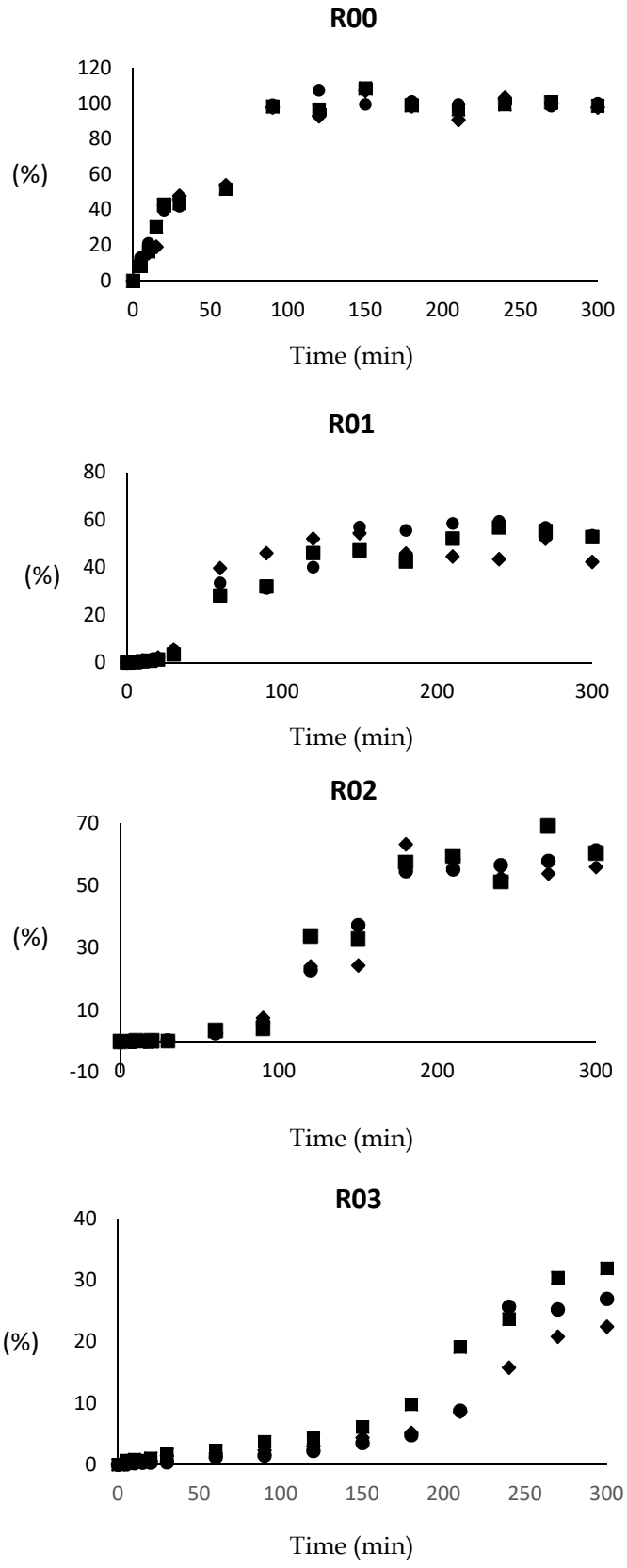

Figure 4.1: Evolution of conversion with reaction time for VAc when varying the contents of 4VPh. The % indicates the data of weighed mass balance.

In general, due to reaction inhibition due to 4VPh, as its content increases both the final conversion is reduced and the polymerization reaction is delayed (Figure 4.1). Similar reduction was observed in the conversion of VAc suspension polymerization in the presence of amoxicillin at 3.00 % w/w that also contains a phenol group on its structure, as displayed on Figure 4.2 (33,34).

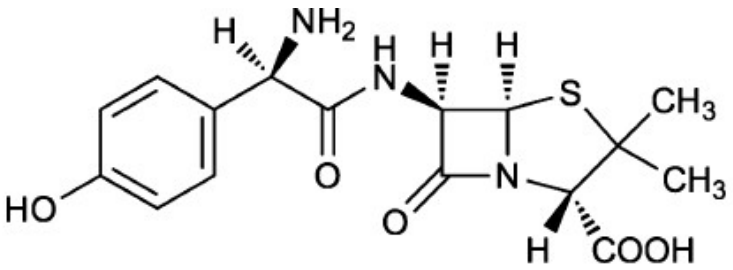

Figure 4.2: Molecular structure of amoxicillin.

The initiator AIBN, that is another commonly used initiator in free radical polymerization, was used as an attempt to overcome the retarding effect of phenol. Indeed, the use of AIBN improved the conversion (Figure 4.3) as more free radicals were generated (BPO:AIBN molar ratio is 1:4) and the use of 4VPh was not a limitation for conversion. Besides, the observed fluctuation in Figures 4.1 and 4.3 is inherent to the gravimetric methodology used where sampling needs reaction system opening and therefore may favor monomers scape.

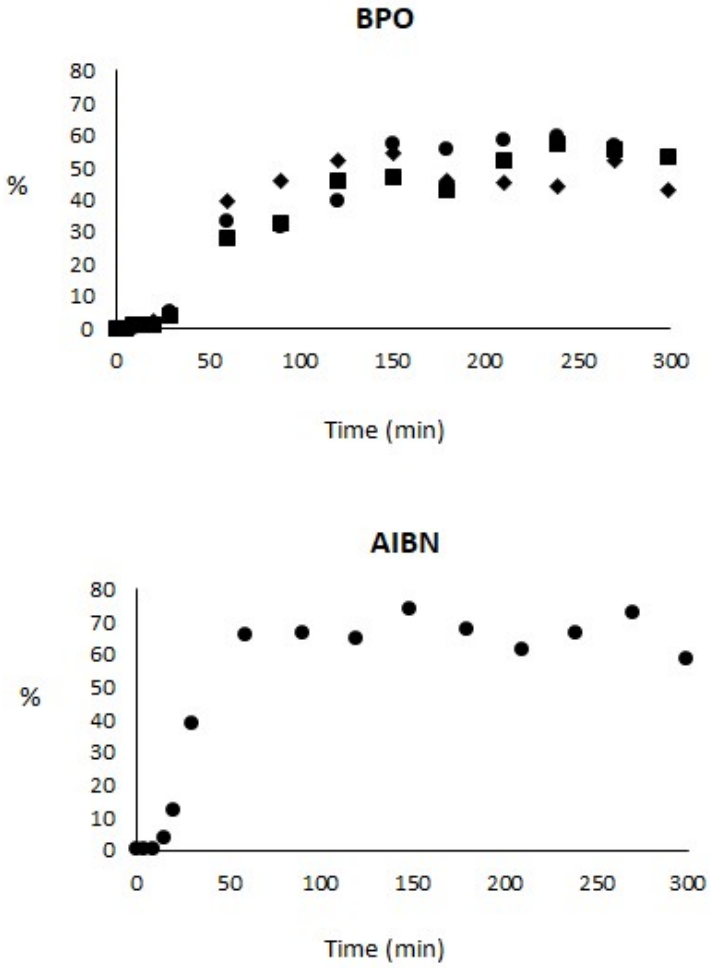

Figure 4.3: Comparison of conversion curves using BPO and AIBN (2 % w/w, molar ratio BPO:AIBN equals to 1:4) as initiator. The % indicates the data of weighed mass balance.

Based on these conversion results, retarding effect and molecular mass distribution, it is possible to propose a kinetic scheme for VAc (M) and 4VPh (V) copolymerization:

$$I_2 \rightarrow 2I* \qquad (1)$$

$$I* + M \rightarrow P_1 \quad (2)$$

The initiator (I_2) decomposes and attack a monomer species (1), (2), but it can also attack a 4VPh (V) molecule by its hydroxy group and be consumed (3), this reaction

accounts for the inhibition behavior observed. The new species ($V^{=}$) is still able to participate in the polymerization reaction.

$$I* + V \rightarrow V^{=} \quad (3)$$

These reactive species (M and $V^{=}$) can be inserted into the polymer chain (P_n) ((4), (5)) and the formed living polymer chains are still able to grow, albeit with different velocities. However, if V (4VPh) is inserted in the polymer chain (6), a polymer specie carrying a hydroxyl group (P^{OH}_{n+1}), that is able to attach the iodine group, is formed.

$$Pn + V^{=} \rightarrow P^{v}_{n+1} \quad (4)$$

$$Pn + M \rightarrow P_{n+1} \quad (5)$$

$$Pn + V \rightarrow P^{OH}_{n+1} \quad (6)$$

The living polymer species also can react with 4VPh by its hydroxyl group and form a dead polymer that capable of being inserted into another chain since it has a double-bound (7). Furthermore, the standard mechanisms of free radical polymerization termination are also in operation ((8),(9)).

$$Pn + V \rightarrow Q^{=}_{n+1} \quad (7)$$

$$Pn + Pm \rightarrow P_{n+m} \quad (8)$$

$$Pn + Pm \rightarrow Q_n + Q_m \quad (9)$$

4.3.2 PVAc and P(VAc-co-4VPh) characterization

Table 2.2 shows the number-average molecular weight (Mn), weight average molecular weight (Mw) and the polydispersity index (PDI) for PVAc microspheres, theses correspond to those ones obtained in bulk (31). In comparison with PVAc (R00), the presence of 4VPh in the polymer backbone significantly decreased the molar mass values, as observed at the low content of 4VPh (R01). In fact, this reduction highlights a retarding effect of the phenolic comonomer on the PVAc

chains growth (34). At higher concentrations of 4VPh (R02 and R03), the values became smaller but unexpectedly close. When comparing with R01 reaction, Mn and Mw values practically doubled due to the higher efficiency of AIBN on polymerization conversion. In addition, these values were higher than the R00 reaction ones. The PDI was not affected, as expected. Therefore, these macromolecular properties (Mw, Mn and PDI) are affected by the content of 4VPh and the initiator used.

Table 2.2 Molar mass distribution results. PDI = Mw/Mn.

Reaction	**R00**	**R01**	**R02**	**R03**	**AIBN**
Mn (Da)	31,300	21,600	14,900	12,900	43,100
Mw (Da)	116,100	76,500	49,700	48,300	157,300
PDI	3.7	3.5	3.3	3.7	3.7

TGA and DTA curves for the polymeric materials are shown in Figure 4.4. The complete degradation of the polymeric materials occurs from 250 to 550 °C, indicating that their thermal stability is suitable for vascular embolization. Similarly, from 325 to 329 °C, the first peak is more expressive and represents more than 90 % of the degradation of the materials. Subsequently, from 432 to 446 °C, the complete polymeric matrix disappears. These results agree with, respectively, deacetylation and decomposition of PVAc backbone steps reported in the literature (31). Overall, these results show that the presence of the comonomer in different contents has not significantly affected the polymer thermal degradation behaviour. Moreover, bulk copolymerization performed with 4VPh at 0.50 % w/w resulted in similar results (30).

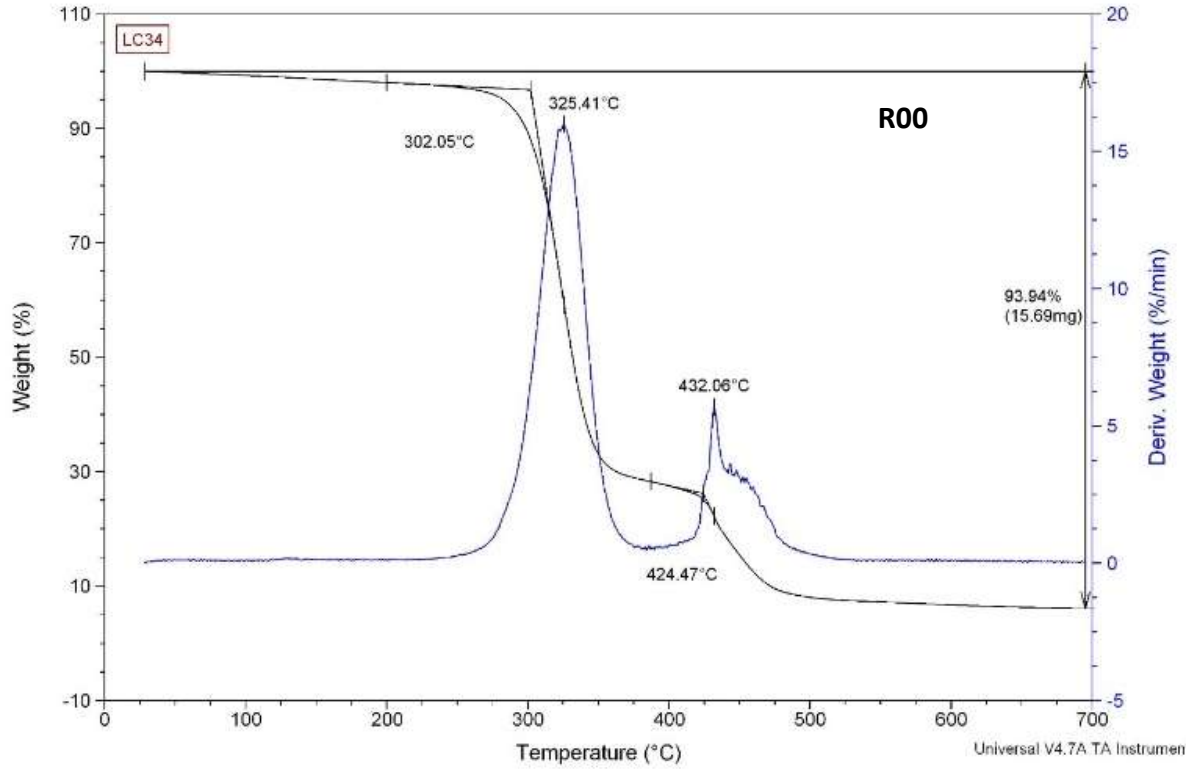
LC34
R00
325.41°C
302.05°C
432.06°C
424.47°C
93.94%
(15.69mg)
Weight (%)
Deriv. Weight (%/min)
Temperature (°C)
Universal V4.7A TA Instrumen

(a)

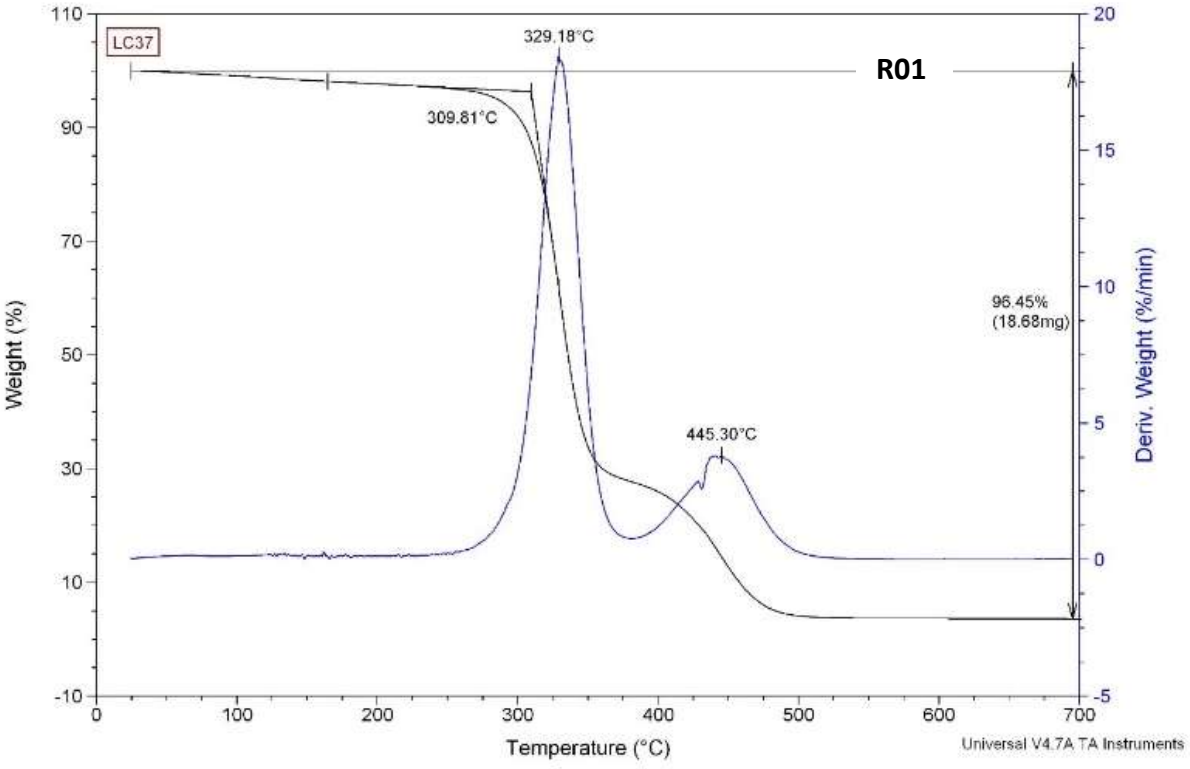
LC37
R01
329.18°C
309.81°C
445.30°C
96.45%
(18.68mg)
Weight (%)
Deriv. Weight (%/min)
Temperature (°C)
Universal V4.7A TA Instruments

(b)

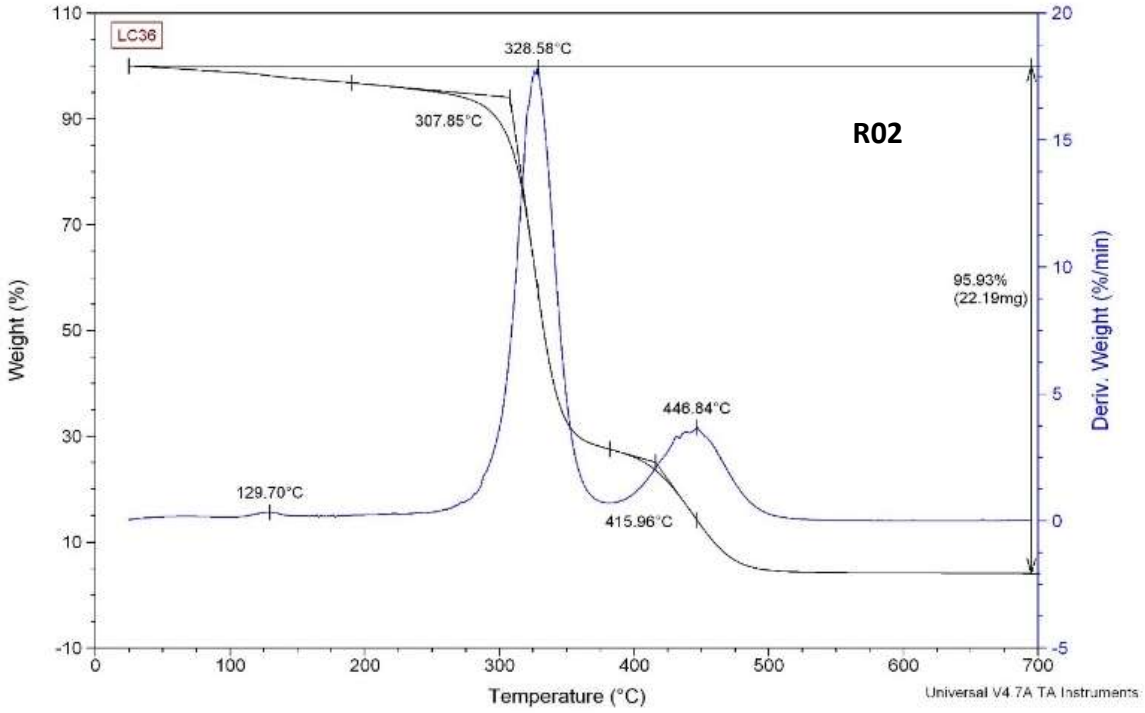

(c)

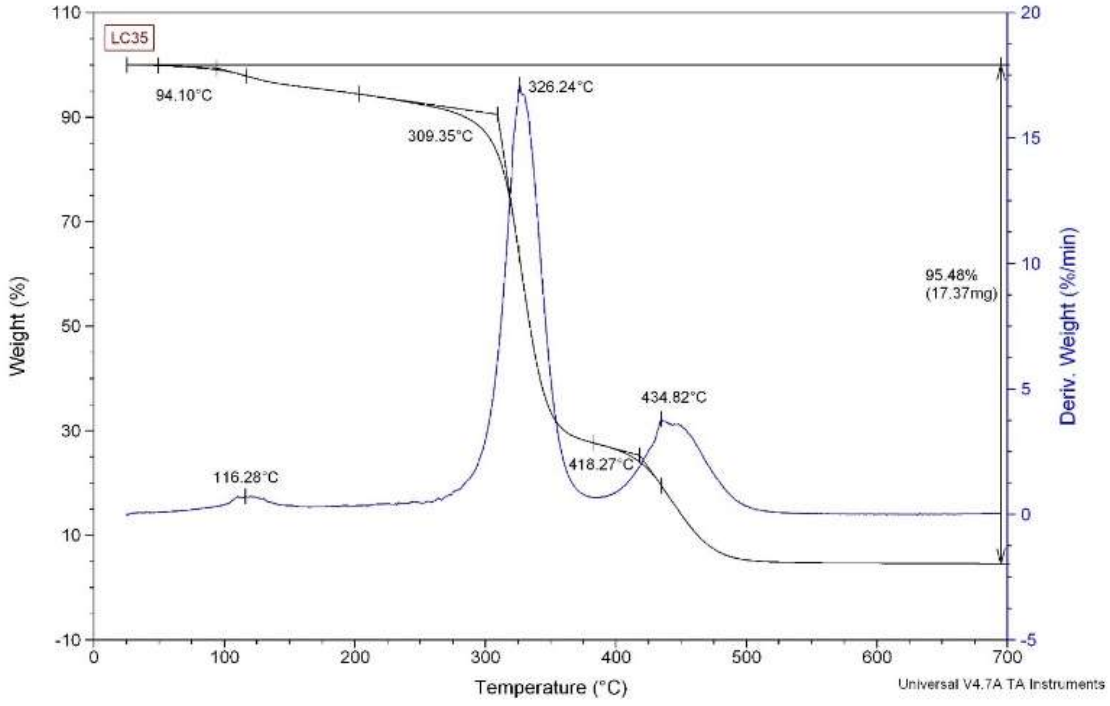

(d)

Figure 4.4: Thermal degradation of (a) PVAc and (b to d) P(VAc-co-4VPh) polymers by means of TGA and DTA analyses.

Figure 4.5 shows the glass transition temperatures (Tg) for the polymeric materials studied. Regarding the other copolymers (R01 to R03), the single Tg value observed

indicates the presence of one type of thermoplastic material. Table 3 displays the Tg values extracted from Figure 4.3. The obtained Tg for the PVAc microspheres is similar to reported ones (8,27). As a matter of fact, the presence of phenol groups in the PVAc backbone reduces the Tg of the material (30). Accordingly, the highest content of 4VPh resulted in the lowest Tg. However, this effect was not observed with 4VPh at 0.25 % w/w content that exhibited higher than expected probably due to experimental errors. The literature presents Tg measurements for the poly(4-vinylphenol) homopolymer (P4VPh) that falls in the range of 150-180 °C (35-37). Surprisingly, bulk polymerization performed with 4VPh at 0.50 % w/w resulted in a Tg value of - 0.3 °C (30). This Tg value is likely to be a result of an aleatory 4VPh incorporation in the polymeric matrix or molar mass reduction. As the temperature of the human body is approximately 37 °C, PVAc and P(VAc-co-4VPh) particles may be deformed, what helps to occlude blood vessels during embolization procedures.

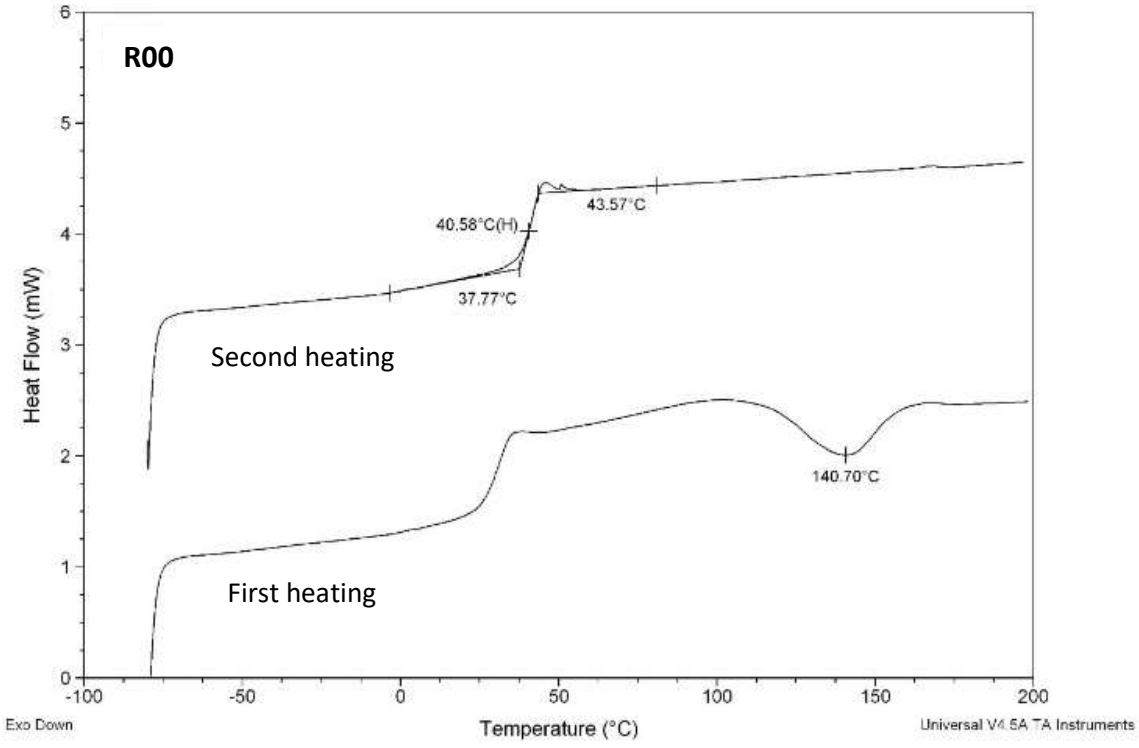

(a)

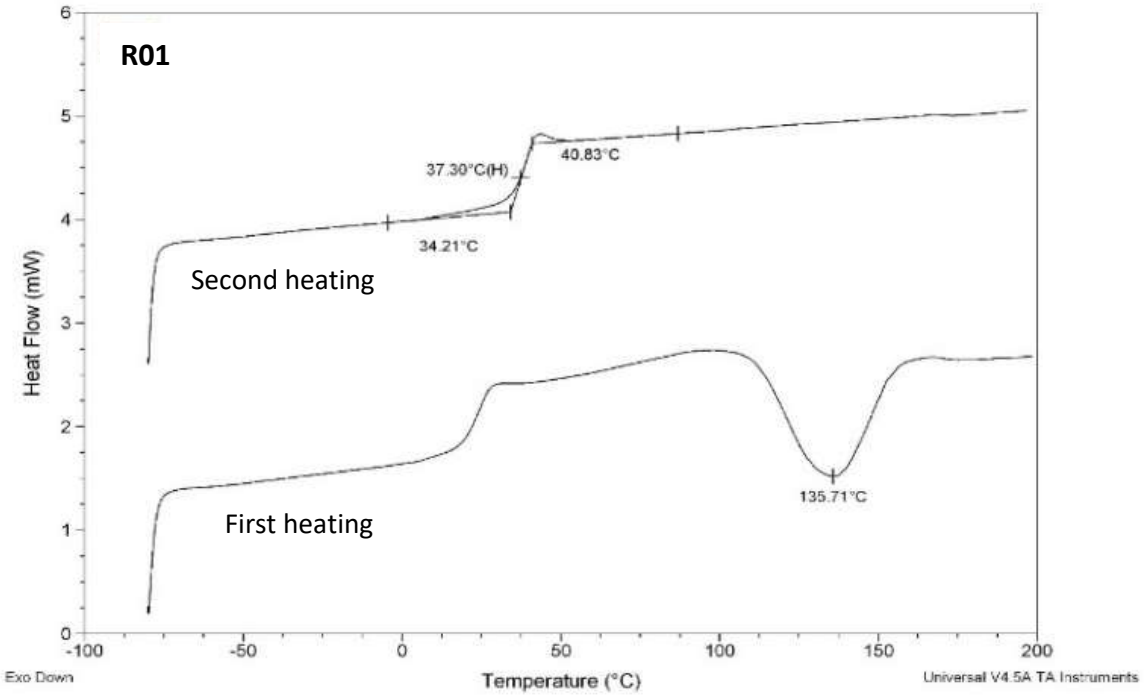
R01
37.30°C(H)
40.83°C
34.21°C
Second heating
First heating
135.71°C
Heat Flow (mW)
Temperature (°C)
Exo Down
Universal V4.5A TA Instruments

(b)

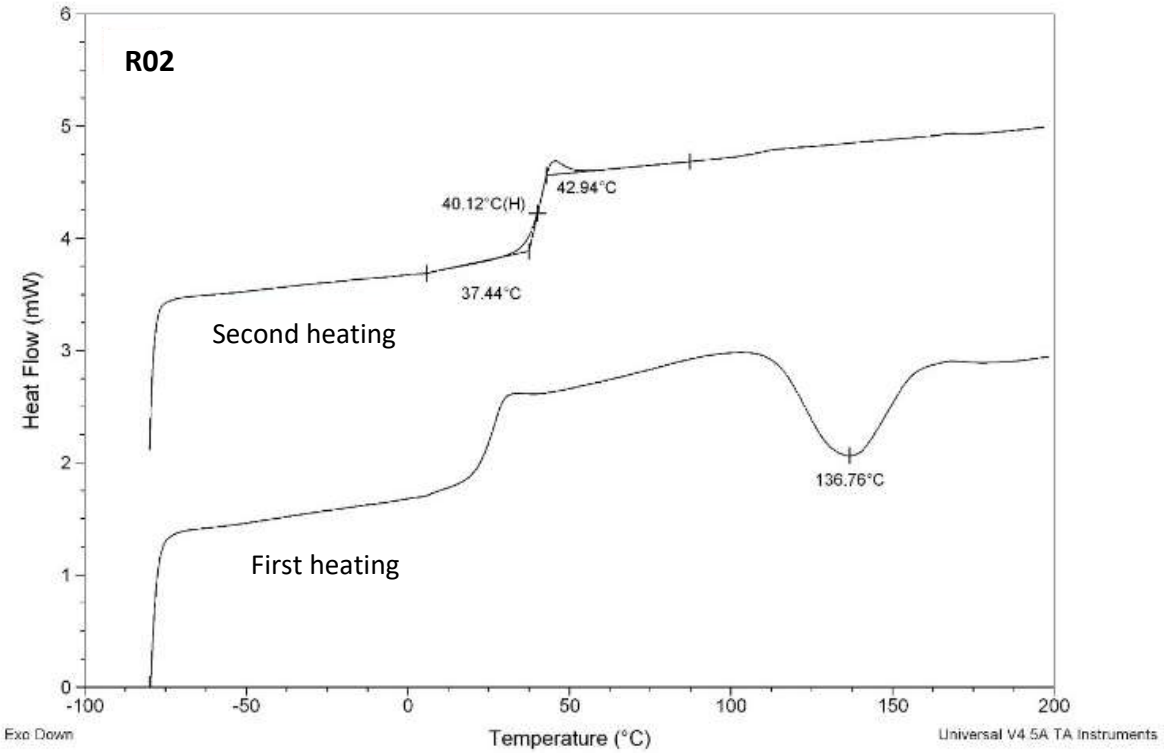
R02
40.12°C(H)
42.94°C
37.44°C
Second heating
First heating
136.76°C
Heat Flow (mW)
Temperature (°C)
Exo Down
Universal V4.5A TA Instruments

(c)

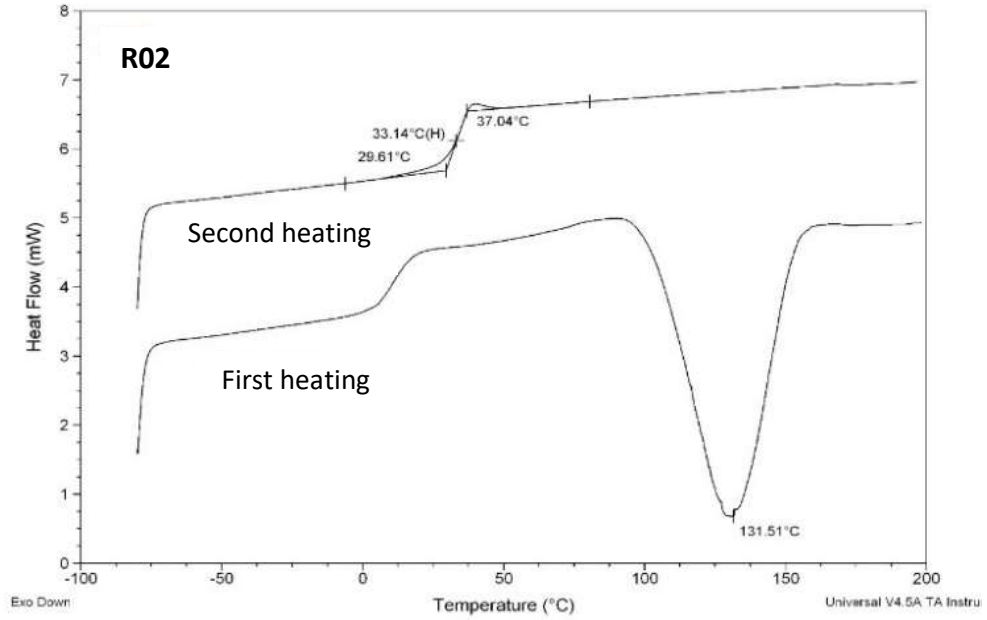

(d)

Figure 4.5: Thermal transitions for the (a) PVAc and (b to d) P(VAc-co-4VPh) polymers by means of DSC measurements.

Table 4.3. Glass transition temperatures (Tg) for the polymeric material studied.

Reaction	**R00**	**R01**	**R02**	**R03**
4VPh (% w/w)	0.00	0.10	0.25	0.50
Tg (°C)	40.58	37.30	40.12	33.14

Figure 4.6 displays PSD curves where the synthesized microparticles present a volume average diameter of 150-600 µm size is in the range of 100-1000 µm. The insertion of 4VPh at 0.10 and 0.25 % w/w improved the PSD homogeneity for PVAc. In addition, the use of AIBN resulted in the narrowest PSD curve (Figure 4.7). In embolization procedures, particles with narrow PSD curve are preferred since they can occlude, selectively, the target blood vessel. Particles with larger or smaller size may obstruct neighboring vessels and cause side effects (1-5). On the other hand, for embolization procedures, particles size is also desirable to be in the range of 350-500 µm (31). Therefore, the particles synthesized herein needs further sieving and size classification steps.

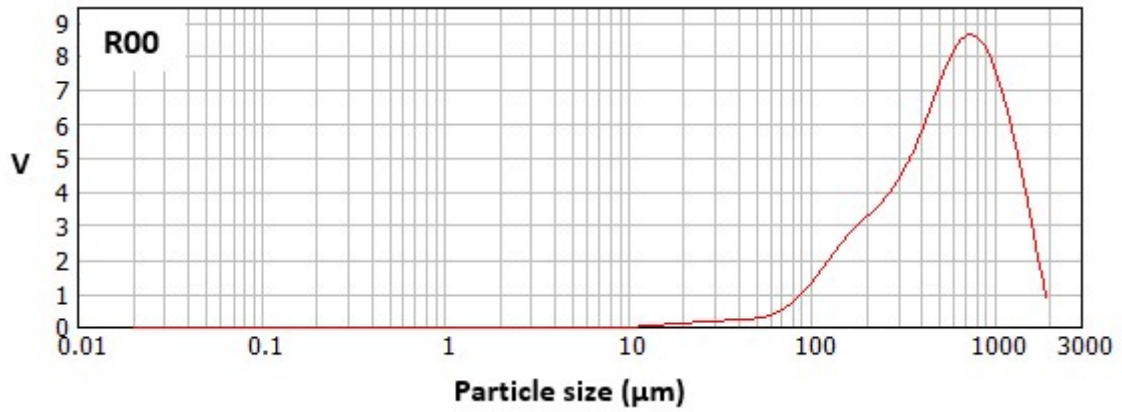
R00
V
0
1
2
3
4
5
6
7
8
9
0.01
0.1
1
10
100
1000
3000
Particle size (µm)

(a)

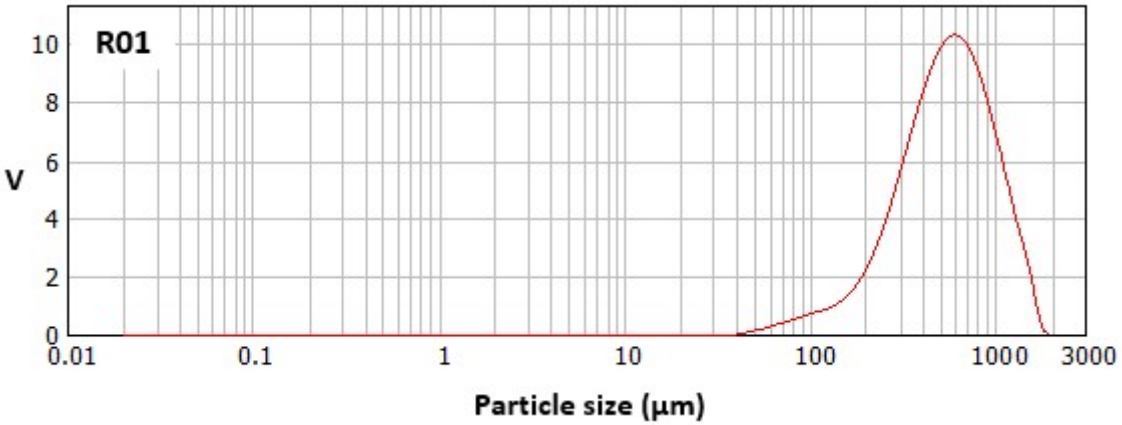
R01
V
0
2
4
6
8
10
0.01
0.1
1
10
100
1000
3000
Particle size (µm)

(b)

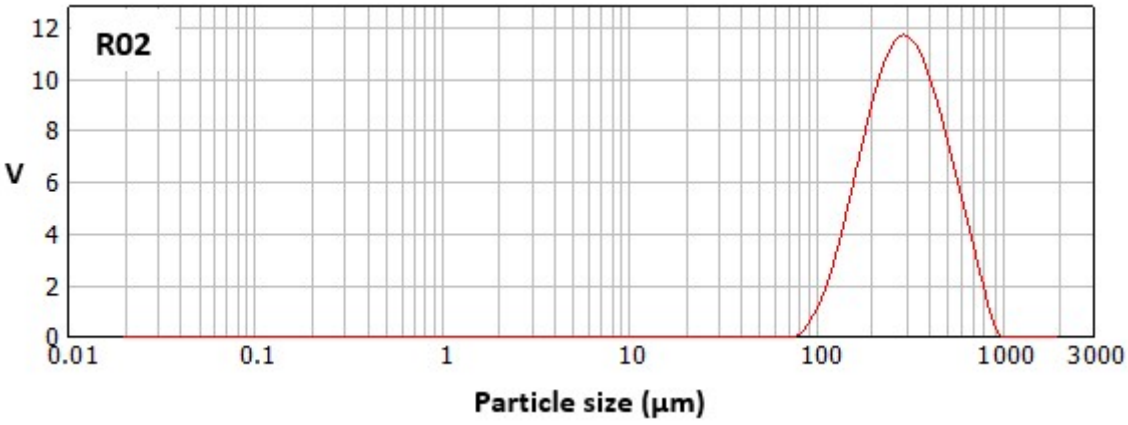
R02
V
0
2
4
6
8
10
12
0.01
0.1
1
10
100
1000
3000
Particle size (µm)

(c)

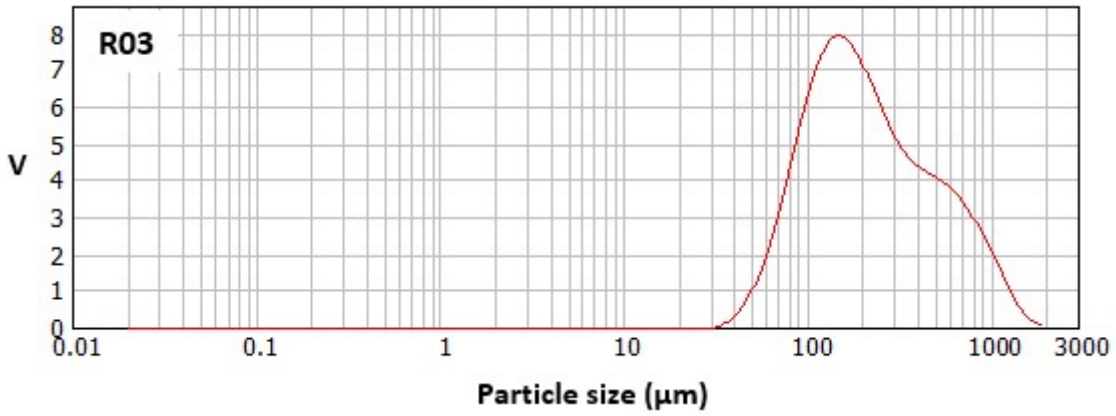

(d)

Figure 4.6: PSD curves of (a) PVAc and (b to d) P(VAc-co-4VPh) particles. V = volume expressed in %.

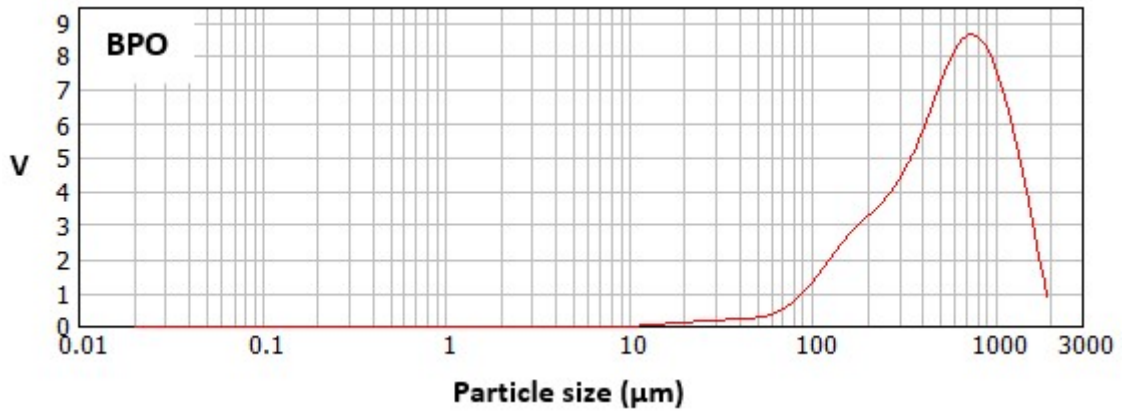

(a)

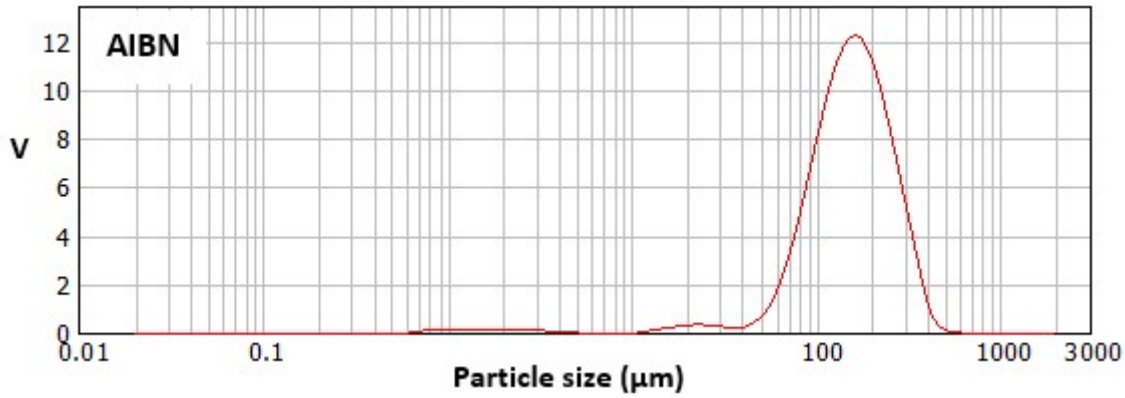

(b)

Figure 4.7: PSD curves of P(VAc-co-4VPh) particles using (a) BPO and (b) AIBN initiators. V = volume expressed in %.

For embolization procedures purpose, a highly spherical morphology is preferred and needed to avoid aggregate formation during clinical intervention procedures. With respect to particles morphology (Figure 4.8), PVAc microspheres are typically spherical as reported in the literature (32). However, the loss of this spherical shape is evident as the content of 4VPh rises, resulting in aggregates with rubbery aspect. This rubbery aspect can be related to the reduction of molar masses, glass transition temperature and conversion caused by the incorporation of 4VPh in the reaction system. Moreover, as observed on the R01 reaction with BPO, particles obtained using AIBN also resulted in a more spherical morphology (Figure 4.9).

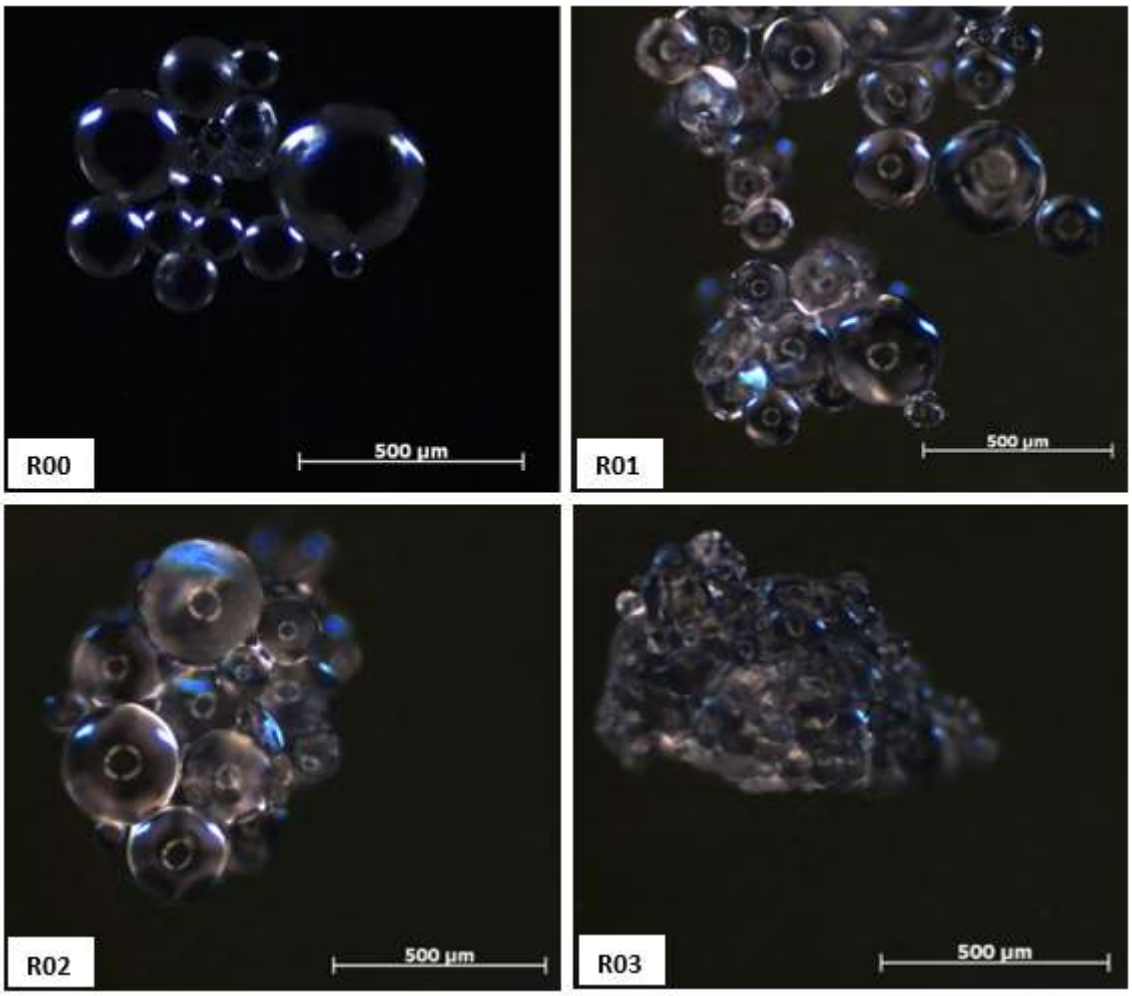

Figure 4.8: Morphology of PVAc and P(VAc-co-4VPh) particles.

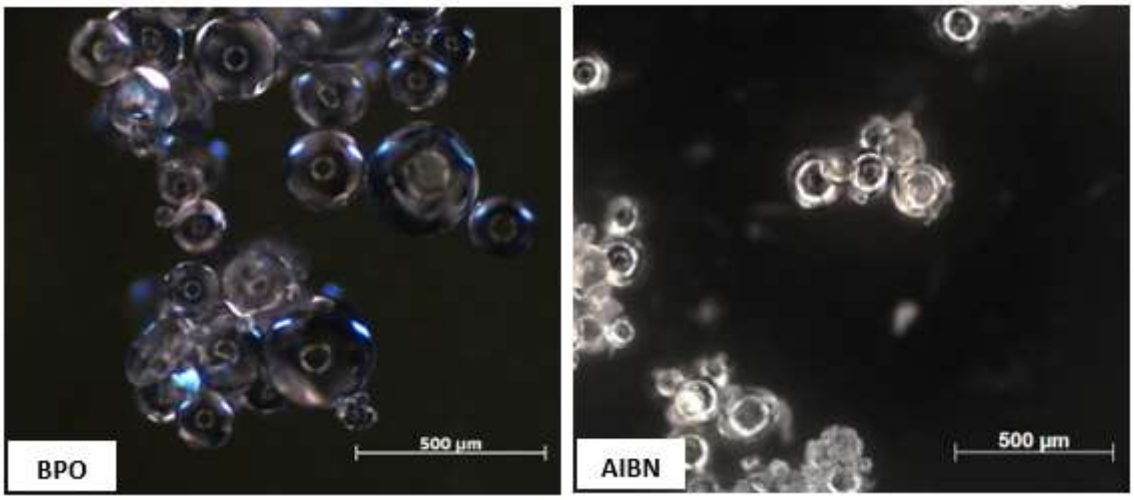

Figure 4.9: Morphology of P(VAc-co-4VPh) particles obtained with different initiators at 2 % w/w, VAc 97.90 % w/w, and 4VPh 0.10 % w/w.

IR spectra of PVAc and P(VAc-co-4VPh) polymers are quite equivalent (Figure 4.10). In each spectrum is possible to identify the characteristics peaks of PVAc backbone, related to the presence of the acetate group at 1750-1700 cm^{-1} and 1200-1300 cm^{-1} regions (32,33). Similar features were reported for bulk copolymerization with 4VPh at 0.50 % (w/w) (30). These spectra show that the polymerization occurred, but observing from R01 to R03 spectra, no significative variation in the band intensity related to phenol moiety (3500-3000 cm^{-1}) was observed. In the literature, this band is clearly observed in the IR spectrum of 4VPh homopolymer and its copolymers (36-38). Possibly, the quite low amount of 4VPh used in this work can be under the detection limit of the IR technique.

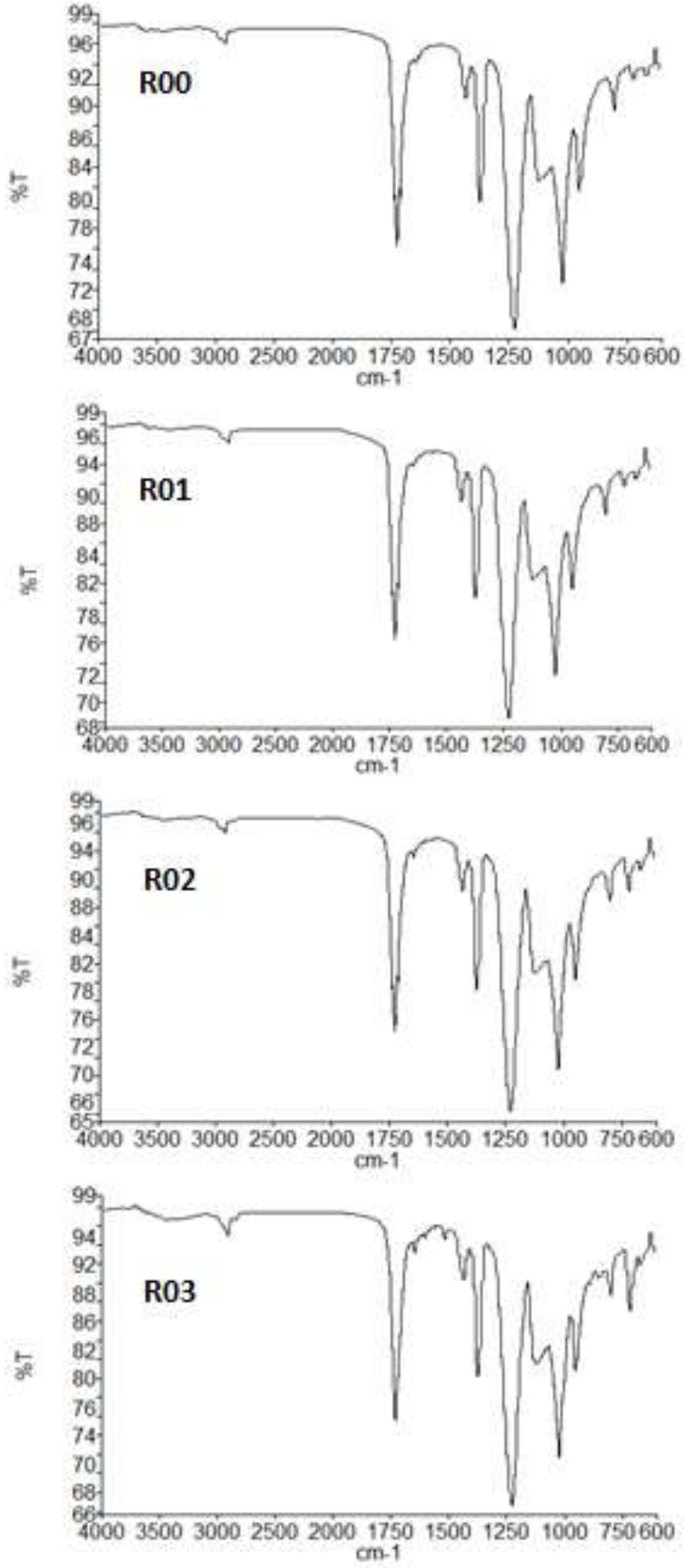

Figure 4.10: Infrared spectra of PVAc and P(VAc-co-4VPh) copolymers.

In our previous work (30), no peak for 4VPh was observed in the ^{1}H-NMR spectra. This was attributed to the low 4VPh content of the copolymer produced (0.50 % (w/w)). In order to confirm this hypothesis, a new ^{1}H-NMR analysis was performed for microparticles of P(VAc-co-4VPh) with 4VPh at 0.5 % (w/w) (Figure 4.11). Figure 4.11 displays the main resonance segments of the PVAc main polymer: CH_2 and terminal CH_3 protons correspond to the peaks at 1.7 and 2.0 ppm, respectively, and the peak of the methine proton is observed at 4.9 ppm. In Figure 4.10, the absence of impurities such as BPO and PVA due to the purification step, reveals a significative signal related to the phenol moiety (7.4-8.1 ppm), which indicates that this activating group is present in the polymer backbone.

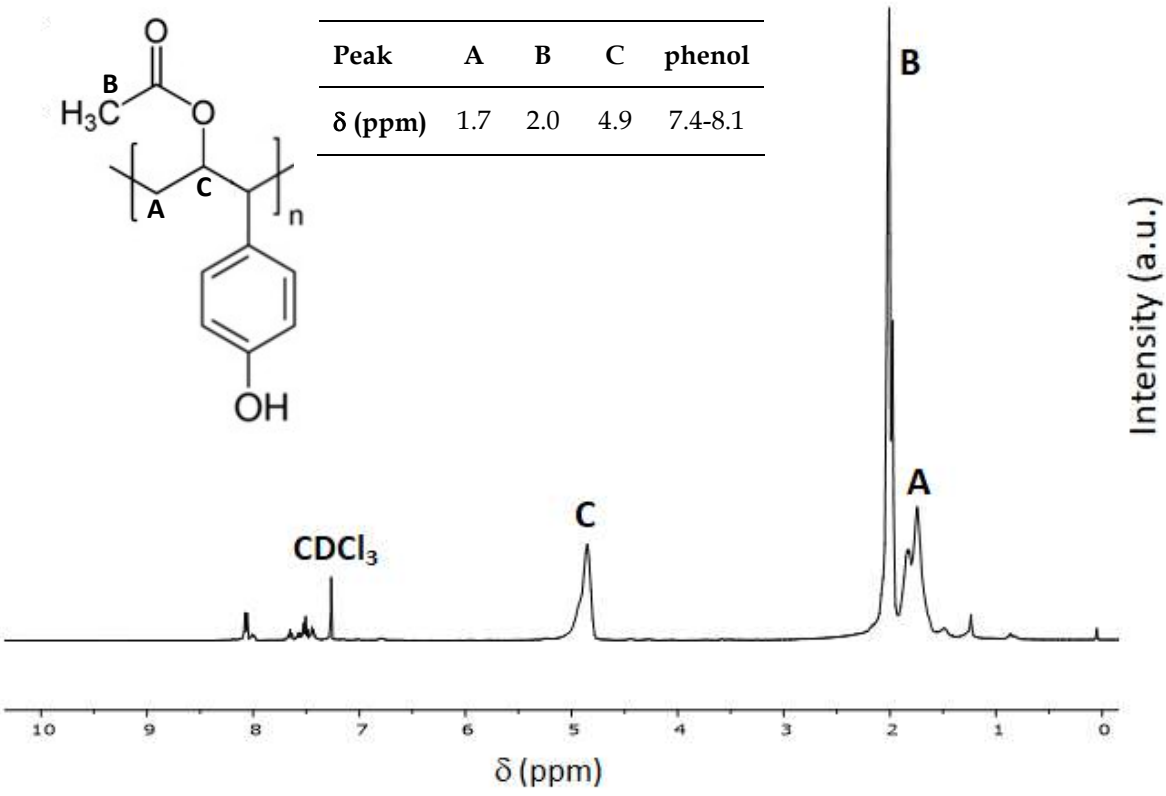

Figure 4.11: ^{1}H-NMR spectrum of P(VAc-co-4VPh) microparticles containing 4VPh 0.50 % (w/w) after purification.

Considering all the results, we selected the 0.10 % (w/w) comonomer content to develop further radioiodination studies since this system displayed the following results: the shortest time to reach equilibrium in conversion using BPO, the highest

molar mass distribution, satisfactory thermal stability, satisfactory Tg value, and the most spherical shape.

4.3.3 Microparticles labeling

The systems used in counting measurements are sensitive to the sample geometry, i.e., to the solid angle of the sample (39). The higher is the solid angle, the higher is the detection efficiency. In this way, the systems used in counting measurements must respect sample geometry for measurements comparisons (39). When comparing the geometry of supernatant and microparticles, the latter exhibit the highest solid angle and consequently, also the higher detection efficiency. Besides, microparticles do not form a homogeneous dispersion in a NaCl solution. Therefore, the comparison of counting measurements between microparticles and the supernatant is not allowed.

Counting measurements were performed for both supernatants and microparticles before and after labelling with ^{123}I using a NaI(Tl) detection system. According to Figure 4.12, both initial and final counting for supernatants are statistically equivalent, i.e., no labeling occurred. If very low changes occurred in the counting measurements of the supernatant, the NaI(Tl) detection system cannot measure such changes due to its high detection limit and high statistical fluctuation (39). In this case, counting measurements should be performed on a Germanium hyper pure (HPGe) detection system that reaches very low detection limits with low statistical fluctuation (39).

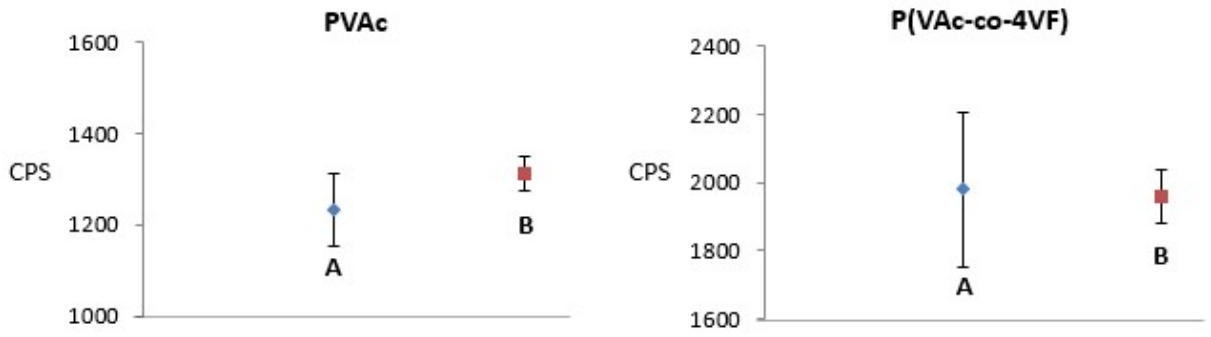

Figure 4.12: Statistical comparison between counting measurements of supernatants before (A) and after (B) labelling with ^{123}I. The calculation included the Student's t-test (α = 99 %). CPS = disintegrations per second.

On the other hand, Table 4.4 displays a significative change when comparing counting measurements for microparticles before and after labeling, indicating that the labeling occurred to high extent. In this case, the high solid angle of the microparticles improved the efficiency of counting measurements. In this system, the phenomenon to be observed is the migration of ^{123}I from the supernatant to the microparticles. Definitely, labeling results show that this migration occurred. However, this migration cannot be quantified since supernatant and microparticles exhibit different geometries.

Table 4.4. Counting measurements for the microparticles before and after labelling with ^{123}I. The calculation included the Student's t-test (α = 99 %). CPS = disintegrations per second.

Microparticles	**PVAc**	**P(VAc-co-4VPh)**
Counting before labelling (CPS)	1.5 ± 0.30	1.7 ± 0.50
Counting after labelling (CPS)	3,647 ± 88.72	3,708 ± 105.31

As observed in Table 4.4, both PVAc and P(VAc-co-4VPh) particles were radioiodinated. This result indicates that iodine can be added to the PVAc backbone. Valuable to note this phenomenon was studied earlier (40,41). In these literature

reports, IR spectra reveal the complex formation of PVAc-I_2 after reacting iodide (I_2) dissolved in an aqueous solution of potassium iodine and a methanolic solution of PVAc at 15 °C. PVAc-I_2 is formed by the chemical bond of I_2 with the unpaired electrons of oxygen atom from the carbonyl group present in the PVAc structure. This complex exhibits an equilibrium constant of 10^5 at 15 °C (40,41). In the radioiodination procedure performed herein, radioactive I^+ stems from the oxidation of radioiodine and was expected to be attached to the aromatic ring through aromatic electrophilic substitution mechanism.

Since both PVAc and P(VAc-co-4VPh) particles were labeled with ^{123}I, probably, a competition between the aromatic ring iodination and the complex formation occurred. As the aromatic ring is present in a smaller amount, the formation of radioactive PVAc-I_2 prevailed. To perform the counting measurement related to the phenol ring radioiodination, after labeling, the particles could be washed with a solution of sodium citrate or tartrate (0.1 $mol.L^{-1}$) to form a complex with the remaining radioiodine and to withdraw the radioiodine from the PVAc-I_2 complex.

4.3.4 Stability of labelled microparticles

At first sight, the formation of PVAc-I_2 sounds like a simple and suitable methodology for the radioiodination of PVAc microparticles. Indeed, the results obtained herein ratify this statement. As observed in Table 4.4, the presence of 4VPh in the polymeric matrix is not an indispensable requirement to attach radioiodine to PVAc polymeric microspheres. The radioiodination of PVAc simplifies the process and the logistic of preparing an embolization agent labeled with ^{123}I. For example, a batch of PVAc microspheres can be prepared and stored in a defined amount ready to be labeled in a SPECT center, for example. Besides, the loss of significative amounts of radioiodine after successive washings (Table 4.5) does not mean that the radioiodinated material is not useful for embolization procedures. This loss indicates that this radioiodine attachment seems to follow an adsorption mechanism with subsequent desorption, after exhaustive washings.

Table 4.5. Stability of microparticles labelled with ^{123}I after 120 min. CPS = disintegrations per second.

Microparticles	**PVAc**	**P(VAc-co-4VPh)**
Initial counting (CPS)	3,647 ± 88.72	3,708 ± 105.31
Final counting (CPS)	723 ± 19.20	809 ± 25.73
Radioiodine loss (%)	80.2	78.2

Therefore, the strategy used in this work for the radioiodination of PVAc backbone was successful. To improve the chemical attachment of radioiodine on the polymer backbone, an alternative is to perform the protection of 4VPh unsaturation prior to its iodination. After unsaturation deprotection, the iodinated 4VPh is expected to undergo suspension polymerization with VAc using AIBN as initiator.

4.4 Conclusions

The copolymerization of 4VPh and VAc was confirmed by molar mass, thermal transitions, microspheres morphology and NMR spectrum analysis. In general, the higher the amount of comonomer, the larger is the observed effect 4VPh on the polymer properties. It was observed that the presence of 4VPh on the VAc suspension polymerization retards the reaction and decrease the conversion. Furthermore, changes in the molecular weight distributions in the final polymer were observed. Regarding thermal properties, thermal stability was practically not dependent on the 4VPh content while glass transition temperatures were. Results of microscopic analyses indicated that a rubbery aspect is observed and aggregates are formed as the content of 4VPh is increased. Moreover, AIBN initiator showed to improve the conversion and the PSD, besides increasing the copolymer chain size without affecting particles morphology. Therefore, the use of AIBN as initiator is recommended to decrease the retarding effect of 4VPh. According to the obtained results, the copolymer containing 0.10 % w/w of 4VPh exhibited the best thermal characteristics, spherical morphology, and conversion performance. This comonomer

content was selected to perform radioiodination experiments. Labeling results indicated a significant insertion of radioiodine in both PVAc and P(VAc-co-4VPh) backbone.

4.5 Complementary remarks

Further investigation about the P(VAc-co-4VPh) copolymer synthesis was performed by means of a ^{13}C-NMR analysis (Figure 4.12). In this spectrum, specific chemical shifting related to 4VPh unsaturation (111 ppm) is absent. In addition, signals near 130 ppm that are related to the 4VPh aromatic ring are present in this spectrum. The literature reports chemical shifting (δ) for PVAc polymer, as shown in Figure 4.12 (43). These chemical shifting are present on Figure 4.13. Therefore, it seems reasonable to affirm that 4VPh is chemically attached to the PVAc matrix, forming the P(VAc-co-4VPh) copolymer. Unfortunately, as ^{13}C-NMR is less sensitive than ^{1}H-NMR analysis, the signal referred to phenol group (146 ppm) was not observed. Probably, as 4VPh amount was too small, its phenol signal should be confounded with noise.

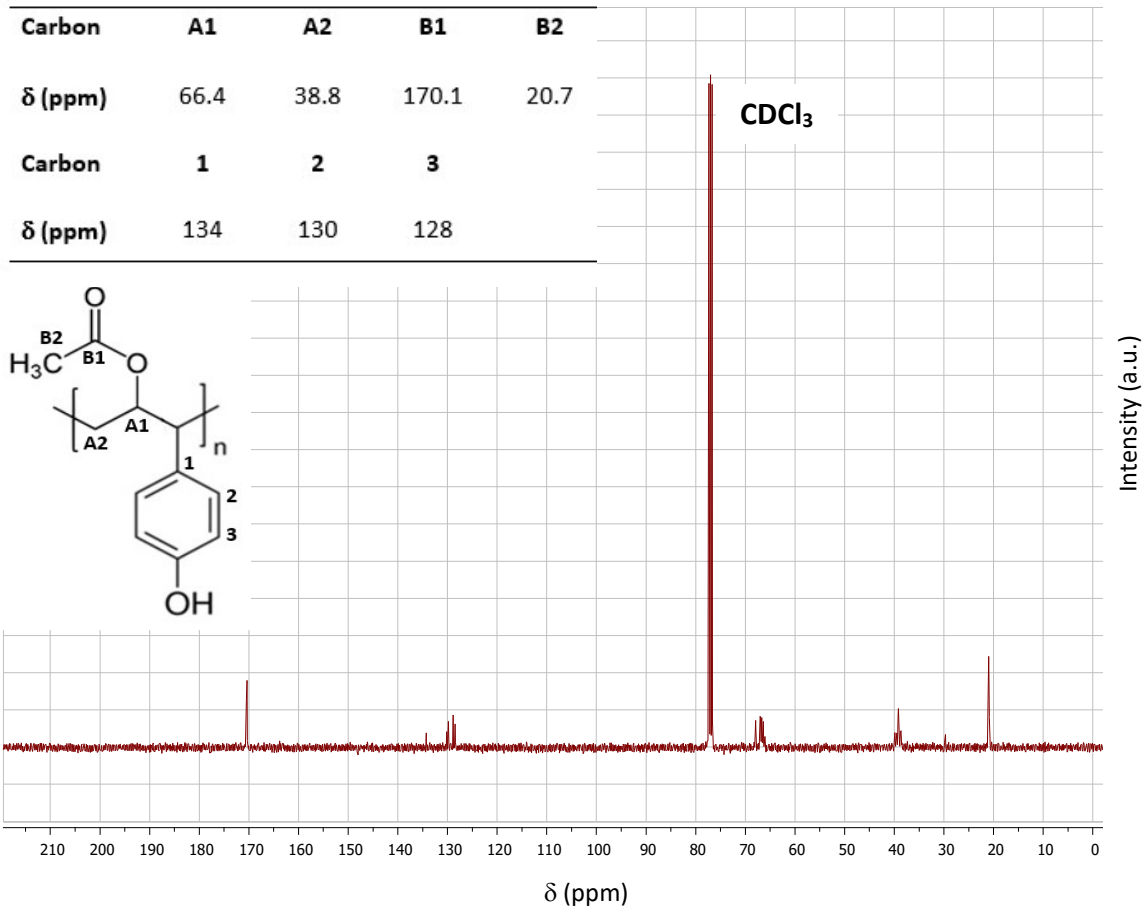

Figure 4.13. ^{13}C-NMR spectrum of P(VAc-co-4VPh) copolymer. This analysis was performed in the same conditions described in section 4.2.4.

Among the instrumental analysis techniques used in the copolymer characterization, NMR qualitatively confirmed the copolymerization of 4VPh and VAc. The NMR technique can be used quantitatively to define the composition of a polymeric sample. In summary, this quantitation is performed by calculating the area of the carbon peaks and proportionality correlations. In this thesis, the signal related to phenol peaks is too near noise, what compromises quantitation. Alternatively, spectrophotometric measurements of 4VPh in the ultraviolet region could be performed in the aqueous phase, before and after suspension polymerization reaction. To perform this comonomer quantitation, a calibration curve could be constructed at concentrations of 4VPh 0.10, 0.20, 0.30, 0.40 and 0.50 % (m/m) dissolved in a solution of PVA 0.47 g · L^{-1}. According to the literature, PVA poorly absorbs in the 200-800 nm UV region (44) while 4VPh absorbs at 230-260 nm (45).

Therefore, it seems reasonable that the 4VPh quantitation can be performed in the presence of PVA by UV spectrophotometry. With this analysis result, the difference of 4VPh amount before and after polymerization can be estimated. Therefore, this difference directly corresponds to the amount of 4VPh present in the P(VAc-co-4VPh) matrix.

The retarding effect of 4VPh is overcame by alternative strategies of polymerization. For example, the literature presents several methods to prepare high molecular weight PVPh through polymerization with the phenolic hydroxyl group protected, and subsequently performing deprotection. The usually employed protective groups are *t*-butoxycarbonyl, trialkylsilyl, and acetyl groups (46). Despite interesting, this methodology clearly needs more steps and toxic reactants usage. As this thesis intended to provide a polymeric material with potential to be used as an embolization agent for SPECT imaging, pharmacological guidelines were considered along its design and planning, as well. An example of pharmacological guideline is to perform toxicological studies of the developed embolization agent. If the use of toxic reactants is avoided, toxicological testing is simplified. For this reason, methodologies that employ the use of protective groups were not considered.

The ^{123}I solution is supplied in 0.02 mol.L^{-1} NaOH solution, which does not meet the appropriate radioiodination pH, which should be in the range of 5-7. Therefore, it was necessary to define a buffer volume for the pH adjustment. The literature (47) indicates the use of PBS buffer (buffer containing phosphate and chloride), however, for the volumes of 0.02 mol.L^{-1} NaOH solution shown in Table 4.6, the pH remained in the range of 7-8. As an alternative, another phosphate buffer solution (885 mg of KH_2PO_4 and 30 mg of $Na_2HPO_4.7H_2O$ in 100 mL, supplied by Vetec Química Fina) was tested.

Table 4.6: Values of pH obtained for the mixing of different volumes of phosphate buffer and 0.02 mol.L^{-1} NaOH solutions. The pH indicator strips used (range 0 to 14) were supplied by Merck.

NaOH 0.02 mol.L^{-1} (mL)	0.5	0.8	1.0	2.0
Buffer solution (mL)	1	2	5	10
pH	5-6	5-6	5-6	5-6

As observed in Table 4.6, the pH value remained in the range of 5-6 for the different volumes of NaOH and phosphate buffer solutions studied. Therefore, 5 mL of buffer solution was the chosen volume to ensure the pH required for the radioiodination reaction.

In the radioiodination studies, sample measurements were made in terms of counting measurements. As the sample measurements would be comparative, it was not necessary to know the activity of the samples. To express counting measurements in terms of activity, one would need to know the absolute efficiency of the detection system. Counting and activity are related as presented in the following Equation:

$$A = \frac{N}{\varepsilon \, . P_{\gamma} . t}$$

Where *N* is the number of photons of the energy of interest recorded by the detector, ε corresponds to the absolute efficiency of the detection system, P_{γ} corresponds to the gamma emission probability, and *t* is the counting time.

For comparison purposes, the decay correction with the measurement time was performed according to the Equation below (48). The counting measurement value after the reaction or washing was divided by the factor D and the value obtained, compared to the counting measurement value before the reaction or washing.

$$D = e^{-\lambda t}$$

Where D is the sample decay factor, λ corresponds to the radioactive decay constant, and t is the time interval between the sample counting measurement before and after the reaction or washing.

Moreover, as the strategy used in this work favored the radioiodination of the PVAc backbone, the radioiodination of the other copolymers compositions synthesized herein was aborted, since the expected result would be quite similar. Regarding macromolecules radioiodination methodologies that could be performed for comparisons with iodo-beads methodology, the following evaluation was performed: As isotopic exchange needs heating in the range of 150-170 °C, this methodology cannot be used since this heating could damage the polymeric microspheres. The Bolton-Hunter reagent attaches to the amines group present in the substrate. Therefore, this methodology could not be used either since no amines are present in the P(VAC-co-4VPh) microparticles structure. Radioiodinations experiments using Chloramine-T (49) and Iodogen® (50) methodologies could be performed. However, this study was also interrupted for the same reason above mentioned.

References

[1] Brassel F., Meila D. Evolution of Embolic Agents in Interventional Neuroradiology. Clin Neuroradiol., v. 25, i.2, p. 333–339, 2015.

[2] Medsinge A., Zajko A., Orons P., Amesur N., Santos E. A Case-Based Approach to Common Embolization Agents Used in Vascular Interventional Radiology. Am J Roentgenol. v.203, pp.699-708, 2014.

[3] de Bruijn A.M., Ankum W.M., Reekers J.A., Birnie E., van der Kooij S.M., Volkers N.A., Hehenkamp W.J. Uterine artery embolization vs hysterectomy in the treatment of symptomatic uterine fibroids: 10-year outcomes from the randomized EMMY trial. Am J Obstet Gynecol. v.215, i.6, p.745.e1-745.e12, 2016.

[4] Berenstein, A., Russel, E. Gelation Sponge in Therapeutic Neuroradiology: A Subject Review. Radiol. v. 141, p.105-112, 1981.

[5] Vaidya S., Tozer K. R., Chen J. An Overview of Embolic Agents. Semin Intervent Radiol. v. 25, p.204-215, 2008.

[6] Sandler S. R., Karo W., Bonesteel J-A., Pearce E. M. Polymer Synthesis and Characterization. United States of America: Academic Press 1998.

[7] Nguyen, V. H.; Haldorai, Y.; Pham, Q. L.; Noh, S. K.; Lyoo, W. S.; Shim, Jae-Jin. Preparation of poly(vinyl pivalate) microspheres by dispersion polymerization in an ionic liquid and saponification for the preparation of poly(vinyl alcohol) with high syndiotacticity. Europ. Polym. J v.46, p.2190–2198, 2010.

[8] Lyoo, W; Lee, H. Synthesis of high-molecular-weight poly(vinyl alcohol) with high yield by novel one-batch suspension polymerization of vinyl acetate and saponification. Colloid Polym. Scienc. v.280, i.9, p.835–840, 2002.

[9] L. S. Peixoto, F. M. Silva, M. A. L. Niemeyer, G. Espinosa, P. A. Melo, M. Nele and J. C. Pinto, Synthesis of Poly(Vinyl Alcohol) and/or Poly(Vinyl Acetate) Particles with Spherical Morphology and Core-Shell Structure and its Use in Vascular Embolization. Macromol Symp. v.243, p.190–199, 2006.

[10] Ferreira G. R., Segura T., Jr Souza F. G., Umpierre A. P., Machado F. Synthesis of poly(vinyl acetate)-based magnetic polymer microparticles Europ Polym Journal v.48, p.2050-2069, 2012.

[11] Sung W. S. The Current Practice of Transarterial Chemoembolization for the Treatment of Hepatocellular Carcinoma Korean. J Radiol. v.10, i.5, p.425–434, 2009.

[12] Oliveira M. A., Jr. Melo P. A., Nele M., Pinto, J. C. In-Situ Incorporation of Amoxicillin in PVA/PVAc-co-PMMA Particles during Suspension Polymerizations, Macromol Symp., v. 299-300, p.34–40, 2011.

[13] A. Laurent, Microspheres and nonspherical particles for embolization. Techn Vasc Intervent Radiol. v.10, p.248-256, 2007.

[14] Imam S. K. Molecular Nuclear Imaging: The Radiopharmaceuticals (Review). Canc Biother Radiopharmac., v. 20, n. 2, p. 163-172, 2005.

[15] Jamous M., Haberkorn U., Mier W. Synthesis of Peptide Radiopharmaceuticals for the Therapy and Diagnosis of Tumor Diseases. Molec. v.18, p. 3379-3409, 2013.

[16] S. R. Cherry, J. A. Sorenson and M. E. Phelps, Physics in nuclear medicine. Elsevier Saunders, NJ: Philadelphia, 2012.

[17] Gomes C. M., Abrunhosa A. J., Ramos P., Pauwels E. K. J. Molecular imaging with SPECT as a tool for drug development. Adv Drug Deliv Reviews, n. 63, p.547–554, 2011.

[18] Shanti C. N., Gupta R., Mahato A. K. Traditional and emerging applications of microspheres: A Review. Internat J Pharm Tech Research. v. 2, i.1, p.675-681, 2010.

[19] Grallert S. R. M., Rangel-Yagui C. D., Pasqualoto K. F. M., Tavares L. C. Polymeric micelles and molecular modeling applied to the development of radiopharmaceuticals. Braz J Pharm Sciences, v.48, n.1, p.1-16, 2012.

[20] Eckerman K. F., Endo A. MIRD: Radionuclide data and decay schemes. 2nd ed. Reston: The Society of Nuclear Medicine, 2007.

[21] Martel B. Chemical Risk Analysis: A practical Handbook. United Kingdom: Kogan Page Science, 2004.

[22] Saha G. B. Fundamentals of Nuclear Pharmacy. 5th ed. United States of America: Springer. 2004.

[23] Welch M. J., Redvanly C. S. Handbook of Radiopharmaceuticals: Radiochemistry and Applications. United Kingdom: John Wiley & Sons, 2003.

[24] Mock B. Radiopharmaceutical chemistry: Iodination techniques. In book Nuclear Medicine, 2ed, Chapter 28, Elsevier, Robert E. Henkin, p.397-405, 2006.

[25] Coenen H. H., Mertens J., Mazière B. Radioiodination reactions for pharmaceuticals: Compendium for effective synthesis strategies United States of America: Springer, 2006.

[26] Wager K. M., Jones G. B. Radio-Iodination Methods for the Production of SPECT Imaging Agents. Curr Radiopharm. v.3, p.37-45, 2010.

[27] Pierce Iodination beads. Description. < https://www.thermofisher.com/order/catalog/product/28665>

[28] Lee J., Lee T. S., Ryu J., Hong S., Kang M., Im K., Kang J. H., Lim S. M., Park S., Song R. RGD Peptide–Conjugated Multimodal NaGdF4:Yb3+/Er3+ Nanophosphors for Upconversion Luminescence, MR and PET Imaging of Tumor Angiogenesis. J Nuc Medic. v.54, p.96–103, 2013.

[29] Simone E. A., Zern B. J., Chacko A-M., Mikitsh J. L., Blankemeyer E. R., Muro S., Stan R. V., Muzykantov V. R. Endothelial targeting of polymeric nanoparticles stably labeled with the PET imaging radioisotope iodine-124. Biomat., v.33, p.5406–5413, 2012.

[30] Carvalheira, L. Synthesis of the copolymer P(VAc-Co-4VP) for developing a new SPECT radioactive tracer. IOSR J Appl Chem, v. 11, i. 2, p. 45-51, 2018.

[31] Azevedo G. D., Pinto, J. C. C. da Silva. Particle size distributions of P(VAc-co-MMA) beads produced through nonconventional suspension copolymerizations, Powder Technology, v.355, p.727–737, 2019.

[32] Santos, D. P., Alves, T. L. M., Pinto, J. C. Adsorption of BSA (Bovine Serum Albuminum) and lysozyme on poly(vinyl acetate) particles. Polímeros, v. 26, i.4, p.282-290, 2016.

[33] M. Oliveira, B. S. Barbosa, M. Nele and J.C. Pinto, Reversible Addition–Fragmentation Chain Transfer Polymerization of Vinyl Acetate in Bulk and Suspension Systems, Macromol React Engineer., v.8, p.493-502, 2014.

[34] Oliveira M. A., Jr. Melo P. A., Nele M., Pinto, J. C. Suspension Copolymerization of Vinyl Acetate and Methyl Methacrylate in the Presence of Amoxicillin. Macromol React Engineer., v.6, p.280–292, 2012.

[35] R. A. Bird and K. E. Russel, The effect of phenols on the polymerization of vinyl acetate, Canadian Journal of Chemistry, 4, 1965, 2123-2125.

[36] Sovish, R. C. Preparation and Polymerization of p-Vinylphenol. Journal of Organic Chemistry, v.24, i.9, p.1345–1347, 1959.

[37] Hernandez-Montero N., Meaurio E., Elmiloudi K., Sarasua J-R. Novel miscible blends of poly(p-dioxanone) with poly(vinyl phenol), Europ Polym J., v.48, p.1455–1465, 2012.

[38] Xu Y., Painter P., Coleman M. M. Synthesis and infra-red spectroscopic characterization of random copolymers of 4-vinylphenol with n-alkyl methacrilates, Polym., v.34, n.14, p.3010-3018, 1993.

[39] Knoll G. F. Radiation detection and measurement. New York: John Wiley & Sons, 1979.

[40] Hayashi S., Kaneko I., Hojo N. Reaction of Iodine into Poly(vinyl acetate) Particles Suspended in Aqueous Solution in the Presence of Potassium Iodide. Polym J., v.6, p.33–38, 1974.

[41] Yamada H., Kozima K. The Molecular Complexes between Iodine and Various Oxygen-Containing Organic Compounds. J. Am. Chem. Soc., v.82, i.7, p.1543–1547, 1960.

[42] Dewanjee M. K. Radioiodination: Theory, Practice and Biomedical Applications United States of America: Springer Science + Business Media LLC, 1992.

[43] Oliveira, M. A. M. Produção de micropartículas e nanopartículas poliméricas para aplicações biomédicas em sistemas heterogêneos de polimerização. 2011. 277p. Tese (Doutorado em Engenharia Química) – COPPE, Universidade Federal do Rio de Janeiro, Rio de Janeiro, 2011.

[44] Shadpour Mallakpoura, Ahmadreza Nezamzadeh Ezhieh. Preparation and Characterization of Chitosan-Poly(vinyl alcohol) Nanocomposite Films Embedded with Functionalized Multi-Walled Carbon Nanotube. Carbohydrate Polymers, v.166, p. 377–386, 2017.

[45] Mingguang Zhu; Yunqian Cui. Determination of 4-vinylgaiacol and 4-vinylphenol in top-fermented wheat beers by isocratic high performance liquid

chromatography with ultraviolet detector. Braz. arch. biol. technol. v.56, n.6, 2013.

[46] Yun Xu, Paul C. Painter, Michael M. Coleman. Random copolymers of 4-vinylphenol with n-alkyl methacrylates Polymer, v. 34, i.14, p.3010-3018, 1993.

[47] Pierce Iodination beads. Description. < https://www.thermofisher.com/order/catalog/product/28665>.

[48] Da Costa, L. A. Análise por ativação neutrônica: estudo de interferências primárias nas determinações de alumínio, magnésio, manganês e sódio. 2007. Dissertação (Mestrado em Ciência e Tecnologia das Radiações, Minerais e Materiais) - Centro de Desenvolvimento da Tecnologia Nuclear, Belo Horizonte, Minas Gerais, 2007.

[49] David S. C. Lee, Bertram W. Griffiths. Comparative studies of iodo-bead and chloramine-T methods for the radioiodination of human alpha-fetoprotein. Journal of Immunological Methods, v.74, i.1, p.181-189, 1984.

[50] W. T. Millar, J. F.B. Smith. Protein iodination using Iodogen®. The International Journal of Applied Radiation and Isotopes. v.34, i.3, p.639-641, 1983.

CHAPTER 5

FINAL REMARKS

Bulk polymerization experiments showed that it is possible to perform copolymerization between VAc and 4VPh in percentages of the latter below 0.5 % (w/w). The characterization of the material obtained with these experiments showed that the copolymer P(VAc-co-4VPh) was successfully obtained. Bulk polymerization of 4VPh indicated that its homopolymer is not formed in the presence of propylene glycol solvent and BPO initiator.

Suspension polymerization of VAc and 4VPh resulted in different microspheres where the particles containing 0.10 % (w/w) of 4VPh resulted in the material whose characteristics fulfills embolization agent requirements such as most spherical shape. Radioiodination and stability studies of this polymeric material indicated that the labeling of these microspheres occurred for both PVA and P(VAC-co-4VPh) microspheres, preferentially in the carbonyl group present in the polymeric matrix.

With respect to the inhibition effect of phenol group on polymerization, the replacement of this group by methoxy unexpectedly did not resulted in polymerization. Besides, this work showed that the AIBN initiator provided the best conversion results on suspension polymerization, therefore being highly recommended to be used in further polymerization studies involving 4VPh.

In conclusion, this work accomplished its specific objectives and indicated other pathways that should be explored in the development of the proposal launched in this thesis that is to provide a radioiodinated embolization agent to improve SPECT imaging during embolization procedures.

FUTURE WORKS

The results obtained in the bulk and suspension polymerization, and radioiodination experiments indicated other study possibilities. For instance, the bulk polymerization involving 4VPh and 4VMS (4-methoxy styrene) can be studied using AIBN as initiator, since this initiator showed better results when comparing with BPO in suspension polymerization.

To perform the 4VPh iodination prior to its suspension polymerization with VAc using AIBN as initiator is also an alternative. Subsequently, the removal of any remaining iodine must be performed using SPE (solid-phase extraction) technique to avoid the iodination of PVAc backbone. In this synthesis route, the iodine can be added to the 4VPh unsaturation and, instead of undergoing copolymerization, the encapsulation of the iodinated 4VPh in PVAc can occur. After developing this study with non-radioactive iodine, the next step is to repeat it using the radioiodine. A successful microspheres radioiodination is achieved when labeling yield is expected to be, at least, 90%, as described in the literature about radioiodination using iodo-beads methodology. Specially, radioiodine release studies from the polymeric microparticles must be performed, since the presence of radioiodine in the blood stream can compromise the quality of SPECT imaging. As this synthesis route needs more steps than the proposed in this thesis, attention must be paid to cares with radioactivity manipulation. Concerning radioactivity measurements, the use of a HPGe radiation detection system is highly recommended, especially in the studies of radioiodine release, where the expected activity to be measured is too low. In addition, it is worthwhile to perform the characterization of the radioiodinated material after decay to assess possible damage of its integrity. Similarly, this entire synthesis route can be performed replacing 4VPh by 4VMS, since 4VMS does not undergo successful copolymerization with VAc in the conditions studied herein.

Moreover, among these two proposals, the one which exhibited the best results can be modeled to better understanding the thermodynamics of this new polymerization system. By developing a mathematical model for this system is possible to optimize it

and to predict the quality of the polymeric microspheres in terms of the operational conditions of suspension polymerization. In suspension polymerizations, the correct prediction of droplet sizes, of mixing effects, and of polymer sedimentation may require particular attention. Also, this mathematical development is of great importance when the study changes from the laboratorial to the industrial scale.

Equally important is these two proposals undergo radiolysis study. Many labeled compounds are decomposed by the radiation emitted by the radionuclides present in their structures. This kind of decomposition is called radiolysis. Radiolysis increases the amount and types of radiochemical impurities present in the obtained product. The stability of radioiodinated microspheres is expected to be consistent with the duration of the embolization procedure to avoid patient exposure to an unnecessary dose of released radioiodide. As it is difficult to predict the stability of a radiolabeled substance, this parameter must be determined experimentally. Another parameter that must be considered is the *in vivo* deiodination of the labeled microspheres. The level of deiodination must be compatible with embolization procedures duration that lasts a maximum of, approximately, 3 h for the therapy of uterine fibroids, for example. Therefore, for uterus fibroids embolization, is desirable that no losses of radioiodine or radiolysis occur for about 3 h.

Another remaining question is to determine the minimum activity of ^{123}I present in the particles to provide both the minimum dose for the patient and the best imaging during embolization procedures. Parameters such as the energy fraction of the ionizing radiation that is absorbed by the target blood vessel and the dose constant of equilibrium must be studied. This latter represents the average energy released per unit of radioiodinated microparticles activity and is obtained by the Monte Carlo mathematical method. In this case, MCNP that is a general-purpose Monte Carlo N-Particle code used for neutron, photon, electron, or coupled neutron/photon/electron transport can be used.